THE FLOW OF GASES AND VAPOURS
THROUGH
ADSORBING POROUS MEDIA

TOMLINSON

THE FLOW OF GASES AND VAPOURS
THROUGH
ADSORBING POROUS MEDIA

A Thesis

by

Richard Howden Tomlinson, B.Sc.

Submitted to the Faculty of Graduate
Studies and Research in partial fulfilment of the requirements for the
degree of Doctor of Philosophy

McGill University

April 1948

ACKNOWLEDGEMENTS

The author wishes to express his sincere
gratitude to his director of research

Dr. O. Maass

whose interest and encouragement were a
source of inspiration,
and to

Dr. E.A. Flood
of the National Research Council,
Ottawa,

whose valuable suggestions greatly influenced the course of this research.

LIST OF FIGURES

page

page

LIST OF TABLES

page

GENERAL INTRODUCTION

Fluid flow has been measured through almost every type of porous material. A considerable portion of these permeability studies has been directed towards the flow of gases through a bed of charcoal grains. The interest in gas flow through charcoal arises from the ability of charcoal to separate one gas from another, and this property has been widely applied both in chemical warfare and industry.

It is of fundamental importance to the knowledge of gas flow through a bed of charcoal grains to understand the process by which the sorbable gas is carried into the interior of the charcoal grain. It is usually conceded that a grain of charcoal, which has no visible cracks or fissures, is permeated by a network of micropores in which the adsorption occurs. The object of this research has been to determine the effect of adsorption on the flow of gases and vapours through the micropores of a solid charcoal rod.

Although the importance of gas flow in solid charcoal has long been realized, it is only in recent years that suitable forms of charcoal have been available for determining the flow through the ultimate charcoal particle. The theory of flow phenomena associated with the fine grained structure of the charcoal is therefore very limited. One might expect that, in the case of a porous material having micropores capable of being filled with adsorbable vapours, the permeability of the material to sorbable gas would be much less than its permeability to non-sorbable gas. This theory, however, has not previously been checked by experiment.

The lack of information on the flow of gases through charcoal has made it necessary to resort to fundamental theory applicable to porous systems where the effect of adsorption is negligible. The theory of flow through porous diaphragms is very complicated, and the complications are accentuated by the inexact knowledge of the shape, size and structure of the pores. Equations relating to the flow through porous materials must of necessity be empirical and involve many assumptions. Many of these equations have been collected and correlated in the Historical Introduction.

At the outset it was difficult to estimate which flow mechanism, in the absence of strong adsorption, would determine the gas flow through a charcoal rod. However, early in the experimental work it was found that the flow through charcoal exhibits certain characteristics which definitely preclude certain types of flow. For this reason flow of gases through metals, zeolites etc., as well as turbulent flow, have been dealt with in a very superficial manner in the Historical Introduction.

It was anticipated that when a gas flows into a porous medium on which it is strongly adsorbed, a time interval would be required between the instant the experimental conditions of temperature and pressure are fixed, and the time when the steady state of flow is established. At the outset this time lag was considered only as an experimental obstacle to the determination of the steady state flow, but it became apparent that a knowledge of conditions obtained during the non-stationary flow would supplement and give further proof of the conclusions drawn from the steady state flow measurements. Theoretical analysis of the non-stationary flow has been possible only for very special experimental conditions and the data obtained are not complete. Conclusions based solely on the non-stationary flow would therefore be subject to criticism, but in conjunction with more complete data on stationary flow, tend to confirm the theories necessary to explain the phenomena involved.

The theory of non-stationary diffusion has been largely obtained by a mathematical analogy with heat flow. There are however, systems where the analogy is not apparent. Except where specifically useful equations dealing exclusively with diffusion have already been developed, the mathematics of the non-stationary state flow has been reserved for discussion with the experimental results. With these mathematical derivations reference has been made where possible to similar solutions that have been obtained in connection with other problems.

The experimental difficulties in measuring flow through the charcoal rods are not only complicated by the very low flow rates, but also by two other factors:

(1) The difficulty of attainment of a steady state of flow due to adsorption phenomena.

(2) The necessity of providing a flexible type of gas-tight seal to the wall of the charcoal rod.

It is a criterion of steady state flow, that the quantity of gas flowing in and out of every element of length in the path of the flow be identical. From this it is apparent that no pressure decay-rate apparatus can be used to measure the flow rate, since it involves continuously changing adsorption - desorption conditions within the charcoal. The necessity of the flexible seal for holding the charcoal rod is accounted for by the volume changes in the charcoal rod that accompany adsorption and desorption.

If the flow rate is to be in any sense characteristic of the fine structure of a porous material, it is, of course, essential that this material be free from adventitious cracks, holes and other mechanical faults not characteristic of the porous substance. It is obvious that any relatively large hole or crack would make such a large contribution to the total flow rate, that it would completely mask the flow phenomena associated with the inherent structure. Many types of charcoal activation cause the formation of visible faults, and it is therefore difficult to obtain a suitable material for the present investigation. It is possible, however, to obtain a very uniform type of charcoal from wood meal that has been carbonized with zinc chloride. Most of the experimental work in this research has been conducted on a commercial zinc chloride charcoal.

It was desirable to know as much as possible about the physical characteristics of the charcoal in order to understand and interpret the flow data. For this reason the adsorption isotherms of the strongly adsorbed gases, the helium and mercury densities, and the nitrogen surface area have been determined for the zinc chloride charcoal.

A charcoal of even more uniform appearance than the zinc chloride charcoal has been prepared from Saran plastic. Activated Saran charcoal may be prepared in any size or shape without introducing any apparent defects in its structure. Only preliminary experiments have been conducted with the Saran charcoal, but it offers interesting possibilities for future investigation.

HISTORICAL INTRODUCTION

A. Steady State Flow Through Systems Other Than Charcoal

(a) Capillary flow (single capillary)

The mechanism of the flow through porous systems is more clearly understood with a thorough knowledge of gas flow phenomena in a single capillary. The first significant work on the flow of fluids through a single capillary was conducted by Poiseuille (1) who established the empirical relation that

$$V = \frac{K' \Delta P R^4}{L} \qquad \ldots\ldots \quad (1)$$

where V is the flow per unit time,

ΔP is the hydraulic head,

L is the length of capillary,

K' is a constant

and R is the radius of capillary.

This empirical relation was placed on a theoretical basis by Wiedermann (2) who considered the forces acting on a unit cylindrical element of fluid within the capillary. Subsequent integration of the forces acting on this element necessitated assumptions regarding the boundary conditions. When it is assumed that the velocity of the gas in contact with the wall is zero, the Poiseuille relation is obtained in the form:

$$V = \frac{\pi R^4 \Delta P}{8L \eta} \quad \cdots\cdots\cdots \quad (2)$$

where η is a constant for any fluid at a given temperature and is known as the viscosity coefficient.

Other terms as previously defined. [#]

More accurate determinations showed that the Poiseuille relation did not exactly describe the flow rate of gases, and it was assumed that the discrepancies were due to "slippage" at the wall of the capillary. Maxwell (3) has shown on a purely theoretical basis that if there is slip at the wall of the capillary, the Poiseuille equation can be stated more accurately in the form:

$$V = \frac{\pi R^4 \Delta P \bar{P}}{8L \eta P} + \left(\frac{\pi}{2}\right)^{3/2} \frac{R^3 \Delta P}{L P} \sqrt{\frac{R_0 T}{M}} \left(\frac{2 - f}{f}\right) \quad \cdots\cdots \quad (3)$$

where V is the volume per unit time measured at pressure P,

M is the molecular weight of the gas,

R_0 is the gas constant,

T is the absolute temperature,

f is the fraction of molecules giving non-specular reflections from the surface of the capillary,

---

[#] Uniform symbols are used throughout regardless of form shown in original literature reference. A glossary of symbols appears immediately preceding the Bibliography.

$\bar{P}$ is the gas mean pressure defined by $\frac{P_1 + P_2}{2}$,

P_1 is the influent gas pressure,

and P_2 is the effluent gas pressure.

All factors in equation (3) are easily measurable except the quantity f. Direct measurements of f have been made by Taylor (4) by impinging beams of lithium, potassium and caesium atoms on the cleavage plane of sodium chloride crystals. Taylor records that under these conditions f equals 1.000. Blankenstein (5) has determined f by the rotating cylinder viscometer. This method is indirect, as f is evaluated by the solution of equation (3). Blankenstein found that air and oxygen gave only 2% and 1% specular reflections respectively from a surface of burnished silver oxide (i.e. f equals 0.98 and 0.99 respectively); helium and hydrogen on the other hand gave no measurable specular reflections at all. Other measurements of f indicate larger variations in its value. Millikan (6) calculated values of f equals 0.9 in connection with his oil drop experiments.

Examination of equation (3) indicates that only under very special conditions can both parts of the equation contribute significantly to the total flow rate. It may be seen that if R (the radius) is large, then, in order that the term due to "slip" contribute to the flow rate, $\bar{P}$ must be small. It may also be inferred from equation (3) that if

R is very small, the term due to "slip" might become an important function even at relatively high pressures. That is, when R or $\bar{P}$ are sufficiently small, the Maxwell "slip term" governs the significant contribution to the total flow rate.

Knudsen (7) has derived an equation to describe the flow rate when the mean free path of the gas molecule is of the same order of magnitude as the diameter of the capillary. This regime of flow should therefore correspond to the flow governed by the Maxwell "slip term" of equation (3). Knudsen developed his equation by consideration of the mathematical chance of a molecule passing through a capillary. Knudsen's equation may be expressed in the form:

$$V = \frac{4}{3} \sqrt{2\Pi} \sqrt{\frac{R_o T}{M}} \frac{R^3 \Delta P}{L P} \quad \ldots\ldots \quad (\underline{4})$$

It is notable that equation (3) when only the "slip term" is effective, and equation (4), which describes the flow for similar conditions, are identical in form although they were derived by completely different considerations.

Knudsen (8) found experimentally that equation (4) described the flow rate accurately only under the limiting condition that the mean free path of the molecule was greatly in excess of the pore radius. Semi-empirically, Knudsen obtained an equation which best fits the experimental results for all possible values of given variables, provided that the capillary has sufficient length that the kinetic energy correction introduced by Brillouin (9) may be neglected, and that the linear flow rate does not exceed the value that would cause the flow to become turbulent.# The complete Knudsen empirical equation for the flow through a capillary may be stated in the form:

$$V = \frac{\pi R^4 \Delta P \bar{P}}{8L \eta P} + \frac{4}{3}\sqrt{2\pi}\sqrt{\frac{R_0 T}{M}} \cdot \frac{R^3 \Delta P}{L P}\left(\frac{1 + .81\,^{5R}/\lambda}{1 + \,^{5R}/\lambda}\right) \quad \ldots\ldots \quad (5)$$

where λ is the mean free path of the gas molecules.

Equation (5) is often expressed in other forms. Knudsen (8), and Adzumi (11), use the form:

$$T = K = \frac{V P}{\Delta P} = \frac{\pi R^4 \bar{P}}{8L \eta} + \frac{4}{3}\sqrt{2\pi}\sqrt{\frac{R_0 T}{M}} \cdot \frac{R^3}{L}\left(\frac{1 + .81\ 5R/\lambda}{1 + \,^{5R}/\lambda}\right) \quad \ldots\ldots \quad (6)$$

where T is used by Knudsen, and K by Adzumi.

Turbulence occurs when:

$$R_e = \frac{m W \rho}{\eta} \quad 580 \text{ (c.g.s. units)}$$

where R_e is Reynold's number (10),
m is the hydraulic radius defined by the ratio of pore cross sectional area to periphery,
ρ is the density of the fluid,
η is the viscosity coefficient,
and W is the limiting mass velocity.

Both the T and K functions are expressed in units of volume times pressure per unit pressure gradient per unit time. The utility of this form of the flow equation is apparent from the fact that a plot of T or K vs. $\bar{P}$ will give a straight line over a wide pressure range for a given gas and capillary, if the temperature is maintained constant.

Another common form of equation (5) for the flow rate of gases is:

$$G = V\rho_g = \frac{VPM}{R_o\,T} = \frac{\pi\,R^4 \Delta\,P\bar{P}M}{8L\eta R_o\,T} + \frac{4}{3}\sqrt{2\pi}\sqrt{\frac{M}{R_o\,T}}\cdot\frac{R^3\Delta\,P}{L}\left(\frac{1 + .81\;5R/\lambda}{1 + 5R/\lambda}\right) \qquad \ldots\ldots\ldots \quad (7)$$

where G is the mass flow per unit time,

ρ_g is the density of the gas at the pressure at which the volume was measured; ρ_g is defined by the gas law,

$$= \frac{PM}{R_o\,T} \text{ for an ideal gas.}$$

(b) Capillary flow in porous solids.

Corresponding to the Poiseuille equation (2) for the flow rate in a single capillary, Kozeny (12) has derived an equation for the flow through a porous diaphragm. Kozeny assumed that a porous system could be considered as an agglomeration of uniformly packed particles with a uniform net work of pores between them. If there are n" similar channels in which Poiseuille type flow occurs, the total flow of gas through a porous system will be given by the equation:

$$V' = \frac{2\,n''\pi\,m^4\,\Delta P}{L\,z\,\eta}$$

where V' is the volume per unit time measured at the pressure $\bar{P}$,

L is the thickness of the porous material,

z is the tortuosity factor such that Lz equals pore length,

and m is the hydraulic radius which is defined by the relation

$$\frac{\text{capillary cross section}}{\text{capillary periphery}} \, .$$

That is for circular capillaries m equals $R/2$.

But $n''\pi\,m^2K$ is the total cross section area of the capillaries if K is a shape factor which depends on the shape of the capillaries.

Also, $A_o\varepsilon$ is the total cross sectional area of the capillaries if A_o is the cross sectional area of porous material, and ε is the fraction of voids

$$= \frac{\text{volume of voids}}{\text{volume of voids and solids}} \, .$$

That is $$V' = \frac{2\,A_o\,\varepsilon\,m^2\,\Delta P}{K\,Lz\,\eta}$$

But $$m = \frac{\text{pore cross section}}{\text{pore periphery}} = \frac{\text{pore volume}}{\text{pore surface}} = \frac{\varepsilon}{S_v\,(1 - \varepsilon)}$$

if S_v is the surface area per unit volume of porous material.

Hence

$$V' = \frac{A_o \Delta P}{K_o L \eta S_v^2} \left(\frac{\varepsilon^3}{(1 - \varepsilon)^2} \right) \quad \ldots\ldots (\underline{7})$$

where K_o is a factor including both the shape factor and the tortuosity factor. Carman (13) has shown that for a wide range of porosities and particle shapes K_o equals 5.

The Kozeny equation (7) is based on the assumption that Poiseuille type flow occurs in the pores, and therefore it can only apply to systems where the pores are sufficiently large that surface slippage may be neglected.

By the same methods as were used by Kozeny, Holmes (14) has developed an equation for the flow through porous systems which corresponds to the Knudsen equation (4) for a single capillary.

$$V = \frac{8}{3} \sqrt{\frac{2}{\pi}} \sqrt{\frac{R_o T}{M}} \; \frac{A_o \Delta P}{PLS_v} \left(\frac{\varepsilon^2}{(1 - \varepsilon)} \right) \quad \ldots\ldots (\underline{8})$$

Since equation (8) was derived from the Knudsen equation (4) it can be valid only if the radii of the pores are less than the mean free path of the gas molecules. Unlike the Kozeny equation (7), the Holmes equation makes no allowance for the shape or tortuosity of the pores, although it appears to this reviewer that at least a tortuosity factor must be required.

During the course of this investigation, several equations have been developed which correspond to the "general" flow equation (5) of Knudsen. Such equations are:

1) the Rigden equation (15),
2) the Arnell equation (16),
3) the Lea and Nurse equation (17).

It has recently been shown by Arnell (18) that these equations are essentially equivalent in form but differ slightly in numerical constants. These differences are accounted for by the various assumptions regarding shape factors and effective porosity that the authors included in their derivations. At this point it will therefore be sufficient to consider the equation of Arnell:

$$V' = \frac{A_0 \Delta P \varepsilon^3}{5 L \eta S_v^2 (1-\varepsilon)^2} + \delta \frac{8}{3} \sqrt{\frac{2 R_0 T}{\pi M}} \frac{\Delta P}{\bar{P} L} \frac{A_0 \phi \varepsilon}{S_v (1-\varepsilon)} \qquad \ldots\ldots (9)$$

where ϕ is the effective fraction of void area,
δ is a factor depending on the coefficient of slip and is approximately equal 0.9.

It may be seen that equation (9) reduces to the Kozeny equation (7) when the surface area is small and the pressure large. When the surface area is large and the pressure small the Arnell equation reduces to the Holmes equation (8). Intermediate between these conditions, both terms of the Arnell equation must be considered.

Previously Adzumi (11) had shown that the flow through a number of capillaries in series and in parallel is approximately given by the equation:

$$K = \frac{\pi \bar{P}}{8 \eta} \sum^{n''} \left[\frac{1}{\sum^{m''} l'/r^4} \right] + \delta \frac{4}{3} \sqrt{2 \pi} \sqrt{\frac{R_0 T}{M}} \sum^{n''} \left[\frac{1}{\sum^{m''} l'/r^3} \right] \quad \ldots\ldots\ldots \ (10)$$

where l' is the length of individual pore,

r is the radius of individual pore,

n'' is the number of capillaries in parallel

and m'' is the number of capillaries in series.

For a porous system the solution of equation (10) is only possible if all the n'' paths in parallel are identical, and may be considered as having a radius $\bar{r}$ and length L, where L is the thickness of the porous sample. With these approximations equation (10) takes the form:

$$K = \frac{\pi \bar{P}}{8 \eta} \frac{n'' \bar{r}^4}{L} + \delta \frac{4}{3} \sqrt{2 \pi} \sqrt{\frac{R_0 T}{M}} \cdot \frac{n'' \bar{r}^3}{L} \quad \ldots\ldots \ (11)$$

The Adzumi equation in the form of equation (11) is directly comparable to the flow equation (6) for a single capillary.

Arnell (19) has shown that equations (9) and (11) are essentially similar, but the differences in their form give each equation a specific use. From the Arnell equation (9) it is possible to calculate the surface area per unit volume of porous material, whereas from the Adzumi equation (11) it is possible to calculate both the number and mean radius of the channels through the porous material. The surface areas calculated with the aid of equation (9) have been shown to compare well with the values obtained by other methods (19). The pore radius calculated from the Adzumi equation (11) is not a fundamental constant of the porous system. Inspection of equation (11) reveals that $\bar{r}$ represents the radius of a capillary in an idealized system of straight and uniform pores that would give the same flow rate as the porous material.

Both Adzumi (11) and Arnell (16) suggest the use of a constant equal 0.9 for the term δ which is dependent on the coefficient of slip, whereas it is apparent from Knudsen's equation (6) that this quantity has a pressure variable value. It is therefore not to be expected that either equation (9) or equation (11) can exactly fit experimental results over a wide range of pressures.

The Adzumi equation (11) may be expressed in the form:

$$K = \frac{V\,P}{\Delta\,P} = A\,\bar{P} + B \qquad \ldots\ldots\ldots \qquad (12)$$

where

$$A = \frac{\pi \bar{r}^4}{8 \eta L} = \frac{A'}{\eta} \quad \ldots\ldots \quad (\underline{13})$$

$$B = \delta \frac{4}{3} \sqrt{2\pi} \sqrt{\frac{R_0 T}{M}} = B' \sqrt{\frac{T}{M}} \quad \ldots\ldots \quad (\underline{14})$$

where A' and B' are constants of the porous system.

Equation (12) indicates that if the experimental flow rates for a given porous system are expressed in K units, a plot of K vs. the mean pressure $\bar{P}$ will give a straight line. The slope of this straight line plot represents A (as defined above) and the intercept on the K axis represents B. The constants A and B may therefore be evaluated if the flow rate of any gas through a given porous system has been measured at two or more mean pressures.

From equations (13) and (14) it may be seen that for a given porous system the value of A varies inversely as the viscosity of the gas, and the value of B directly as the square root of the temperature and inversely as the square root of the molecular weight of the gas. If the values of A and B have been determined experimentally for a given gas it is therefore possible to evaluate A and B for any other gas, provided that the molecular weight and viscosity of the gas are known at the required temperature. The flow rate of any gas through a capillary system may therefore be calculated with the aid of the Adzumi equation for any conditions of temperature and pressure, if the flow rate of one gas through the system is first established as a function of the mean pressure.

B. Gas Flow Through Metals and Zeolites

When the holes in a porous system are of molecular dimensions, only gas molecules of exceptional energy are capable of forcing an entry into the pores. From Kinetic Theory it was known (20) that the fraction of gas molecules having energies exceeding a given value increases rapidly with temperature, and it is therefore to be expected that the rate of diffusion of gas molecules into solids permeated by very small pores will be highly temperature-dependent.

Hey (21) has shown that the diffusion constant for the diffusion of water vapour into heulandite contains a term e^{-E/R_0T}, where E is considered to be the energy that a molecule must attain in order to diffuse between two points of equilibrium in the heulandite lattice. Richardson, Nicol and Parnell (22) have shown that the gas flow into metals is governed by a similar exponential law. Such diffusion processes are known as activated diffusions and are easily recognized experimentally by their high temperature coefficients.

C. The Steady State of Flow Through Charcoal

(a) Damköhler's theory of diffusion in a small capillary

The first theoretical discussion of gas flow through porous solids in which significance is attached to the effect of adsorption has been given by Damköhler (23). Damköhler predicts that in small pores diffusion will be controlled not only by Knudsen molecular streaming (equation (4)) but also by surface diffusion, providing the adsorption is large.

The first indication of the phenomenon known as surface diffusion was provided by Volmer and Estermann (24), who observed a remarkably rapid growth of mercury crystals, when the crystals were formed at -63° C. from mercury vapour at -10° C. The rate of growth under these conditions was over 1000 times greater than could be explained by the Kinetic Theory. Volmer and Adhikari (25) have observed the diffusion of benzophenone on the surface of glass and found as might be expected, that its rate of transfer was proportional to the concentration gradient. This surface diffusion was found to be quite analogous to the volume diffusion which occurs in gases and solutions with the exception that it is restricted to two dimensions. This experiment of Volmer and Adhikari has provided the first experimental proof of surface diffusion.

Bangham and Fakoury (26) provide indirect evidence of the mobility of adsorbed gases on charcoal. They have shown that the adsorbed films investigated behave as two-dimensional gases whose expansive pressure is directly proportional to the linear expansion of the charcoal block. Evans (27) has extended the treatment of Bangham to show that the adsorbed layer does not behave as an ideal gas. The deviation from ideality is attributed to the mutual cohesion between the adsorbed molecules, which becomes significant at high surface concentrations.

Assuming that a surface diffusion as well as a volume diffusion occurs in the pore of an adsorbent, Damköhler considers the diffusion into a pore would be governed by the differential equation:

$$\frac{\partial}{\partial t}(N_g + N_a) = D_g \frac{\partial^2 N_g}{\partial x^2} + D_a \frac{\partial^2 N_a}{\partial x^2} \qquad \ldots\ldots. \qquad (15)$$

where N_g is the number of molecules in the gas phase per cm. pore length,

N_a is the number of molecules in the adsorbed phase per cm. of pore length,

$D_g = 2/3\, R\, \bar{\omega}$ is the volume diffusion constant,

$D_a = 1/2\, \Lambda_a\, \bar{\omega}$ is the surface diffusion constant,

R is the pore radius,

$\bar{\omega}$ is the root mean square velocity

and Λ_a is the mean free path of adsorbed molecule.

Damköhler has also shown that equation (15) may be represented in the form:

$$\frac{\partial}{\partial t} N_g = D \frac{\partial^2 N_g}{\partial x^2} \qquad \ldots\ldots \quad (16)$$

where

$$D = \frac{D_g + A''D_a}{1 + A''} \qquad \ldots\ldots \quad (17)$$

and

$$A'' = \frac{N_a}{N_g} = \frac{s}{q}.a.e^{Q/RT}$$

s is the pore circumference,

q is the pore cross sectional area,

Q is the adsorption potential

and a is a constant.

Damköhler assumes that where a high degree adsorption occurs, the ratio of the number of molecules in the adsorbed phase to the number in the gas phase equals 10^{+3} equals A''. From this value of A'' together with equation (17) and the definitions of D_g and D_a, Damköhler has shown that, as the value of the pore radius approaches 10^{-6} cm., D equals D_a and the rate of diffusion becomes largely dependent on the surface diffusion. Unfortunately, Damköhler did not check his theories with experiment.

(b) Gas flow through respirator charcoal

The flow of gases through a bed of charcoal grains has received considerable attention in connection with gas separation by devices such as the respirator. Outstanding among the more recent publications on this subject are the papers of Wicke (29) (30) (31). Wicke (30) developed both theoretical and empirical equations relating to the dynamic sorption of an adsorbable gas from a carrier gas. Development of the theory of the flow through a bed of charcoal grains required a knowledge of the rate of diffusion of the adsorbed gas into the interior of the charcoal grain. The importance of this diffusion process is pointed out by Wicke (32), who states that in a dynamic gas separation, where an adsorbable gas is carried into a bed of charcoal grains by a gas that is not adsorbed, the diffusion of the gas from the surface of the charcoal grain into the fine structure of the charcoal is the rate-determining process.

(c) Gas diffusion in a charcoal pellet

The rate of diffusion in a grain of charcoal has been measured by Wicke (32). Wicke expected that the surface diffusion predicted by Damköhler would play an important part in this experiment. The theory of Damköhler considered only the diffusion in a single pore, so that it was necessary for Wicke to make further assumptions regarding the pore structure. Wicke observed that the "medicinal charcoal" which he used had a foamlike nature with microscopically visible pores of a magnitude of 10^{-4} cm. From capillary condensation theory Wicke concluded that there were also numerous pores of the order of 10^{-7} cm. To fulfill these conditions Wicke made the following assumptions:

1) The charcoal is composed of ball-like particles. Between these particles there is a continuous network of macropores whose radii are of the order of 10^{-4} cm.

2) The individual ball-like particles are permeated with fine pores in a "fjord-like manner". These micropores have radii of the order of 10^{-7} cm. It is in these pores that most of the adsorption takes place.

3) The diffusion rate into the micropores is rapid compared to the volume diffusion in the macropores.

From these assumptions Wicke developed an equation for the rate of diffusion into a round charcoal pellet sufficiently large that it would be made up of a large number of the ball-like particles.

$$\gamma(t) = 1 - \frac{6}{\pi^2} \sum_{n=1}^{\infty} \frac{1}{n^2} e^{-\frac{n^2 \pi^2 D t}{R_1^2 A}} \qquad \ldots\ldots (\underline{18})$$

where $\gamma(t) = \frac{n(t)}{n(\infty)}$ for adsorption,

$\gamma(t) = \frac{n(0) - n(t)}{n(0)}$ for desorption,

$\gamma(t)$ is the ratio of flow at time t to flow at t_∞,

A is the fraction of void space in a charcoal grain occupied by the adsorbed gas,

R_1 is the radius of the charcoal pellet, and D is the effective diffusion constant of gas into the grain.

Wicke exposed evacuated pellets of charcoal to a 1 mm. pressure of carbon dioxide and observed the rate of pressure drop. This rate of pressure drop was in accordance with the rate expected from equation (18) and therefore Wicke was able to calculate the effective diffusion constant. The normal diffusion constant of the charcoal was obtained by observing the half life for the decay of pressure of a known volume of gas through a single grain of charcoal glued into a glass tube. The values of the two diffusion constants were found to be identical within the experimental error of the methods, and therefore Wicke was led to the following conclusions:

1) The rate of transport of gas through the charcoal is determined solely by the macropores, and the surface diffusion does not contribute significantly to the total flow.
2) The assumptions regarding the structure of the charcoal are consistent with the data obtained, for the effective diffusion constant calculated from these assumptions compared favourably with the diffusion constant measured in the normal manner.

Wicke explains that the fast diffusion process that might have been expected on the basis of Damköhler's theory was not observable in the system used by him because:

1) the macropores were so large that the volume diffusion through them was large compared to the surface diffusion occurring in the micropores,

2) the fine structure was not continuous but separated by the surfaces of the macropores.

These experiments of Wicke were all conducted with carbon dioxide at a pressure of 1 mm., so that there was no attempt to give a Kinetic Theory interpretation of the results, or to show how the diffusion constant would vary with temperature, pressure or the properties of the gas. The lack of reproducibility of the results suggests the necessity of experimental refinements.

(d) Experimental proof of surface diffusion on charcoal

By a different approach Wicke (33) has demonstrated that surface diffusion does take place on activated charcoal. Experimentally he observed this phenomenon by sweeping one end of a charcoal plug with a mixture of carbon dioxide and nitrogen at constant partial pressures. The other end of the charcoal plug was swept at the same total pressure with nitrogen, and the carbon dioxide diffusing into the pure nitrogen stream was quantitatively analysed by means of a sensitive heat conductivity apparatus. Wicke has shown that at 0^{o}C. and 760 mm. pressure, half of the total carbon dioxide is transported through German technical charcoal by a surface diffusion process. The total transport of the carbon dioxide is made up of three components:

1) Normal diffusion of the adsorbable gas through the carrier gas occurring in pores whose diameter is large relative to the mean free path of the molecules.
2) Knudsen molecular streaming in pores whose diameters are small compared to the mean free path.
3) Surface diffusion of the adsorbed molecules on the pore walls.

Wicke conducted these experiments at partial pressures varying from 0 to 760 mm. and temperatures from 0^{o} C. to 300^{o}C., but it was not possible to differentiate between the temperature - pressure dependence of each of the three types of diffusion. With sintered glass plugs it was found that volume diffusion predominates except at low pressures. With clay plugs, on the other hand, Knudsen flow prevails. Medicinal charcoal is intermediate in behaviour, showing predominant volume diffusion at a pressure of one atmosphere, but allowing increasing proportions of Knudsen flow at low pressures. With the technical charcoals of the German Activated Charcoal Company, referred to as "KA" and "KS", surface diffusion accounts for an appreciable part of the total transport. The surface diffusion was shown to be partly continuous, i.e., moving parallel to, but independently of, the volume diffusion, and partly discontinuous, i.e., at constrictions in the pores, gas molecules being transported by volume diffusion may condense on the surface and move by surface diffusion.

The glues that Wicke found to be most suitable for sealing the charcoal to the diffusion cell were Bakelite paste "P", a resorcinol formaldehyde resin of the Bakelite Company for low temperatures, and magnesia cement for higher temperatures. Wicke found however that the unequal expansion of the glue and charcoal caused the formation of cracks. This difficulty was not overcome# and Wicke found it impossible to obtain reproducible results. For example, if the rate of diffusion were measured at a low temperature and the sample subsequently heated, Wicke found that a repeated diffusion at the low temperature gave a larger rate than that previously observed. This lack of reproducibility made the analysis of the data extremely difficult.

D. The Non-Stationary State of Flow

The non-stationary state of flow has been treated frequently as a diffusion problem. The fundamental law of

---

Whereas resorcinol formaldehyde resins were found to be only partially successful by Wicke for sealing charcoal into glass tubing for flow measurements, it is of interest to note that the candidate has found that this bakelite type plastic makes an excellent base wax for skis.

diffusion was established by Fick (34) and may be stated in the mathematical form

$$\frac{\partial c}{\partial t} = D\left(\frac{\partial^2 c}{\partial x^2} + \frac{\partial^2 c}{\partial y^2} + \frac{\partial^2 c}{\partial z^2}\right)$$

where C is the concentration at time t at a point x, y, z,

D is the diffusion constant, whose dimensions are

$$l^2\ t^{-1}\ .$$

For linear or one-dimensional diffusion Fick's law reduces to the form:

$$\frac{\partial c}{\partial t} = D\frac{\partial^2 c}{\partial x^2} \qquad \ldots\ldots\ (\underline{19})$$

In the case of gas flow into solids the diffusion constant is intimately connected with the solubility or adsorbability of the gas in the solid, as well as the kinetics of the gas in the system. Some of the numerous interpretations of the diffusion constant have been summarized by Barrer (35).

The diffusion equation (19) is similar in mathematical form to the differential equation for the flow of heat. Solutions to the non-stationary heat flow equation have been compiled by Carslaw (36) for a large number of the possible boundary conditions. As long as the diffusion constant remains independent of the concentration, the solutions to Fick's law should correspond to the solutions of the heat flow equation.

In many diffusion systems, the diffusion constant has been found to be strongly dependent on the concentration. Boltzman (37) has shown that, when the diffusion constant is dependent on the concentration, general solutions to the diffusion equation are not possible unless the concentration can be expressed by a function of $x/\sqrt{t}$.

Barrer (38) has collected numerous useful solutions to Fick's law for the boundary conditions most commonly met in diffusing systems.

(a) Non-stationary diffusion in zeolites

One of the most extensive studies of non-stationary diffusion has been carried out by Tiselius (29). Tiselius observed the diffusion of water into the heulandite lattice. The boundary conditions for this diffusion were:

$$\begin{array}{lll} C = C_1 \text{ at } x = 0 & \text{for all } t \\ C = C_o \text{ at } x > 0 & \text{at } t = 0 \\ C = C_o \text{ at } x = \infty & \text{for all } t. \end{array}$$

For these conditions the solution of Fick's equation (19) is:

$$\frac{C_1 - C_x}{C_1 - C_o} = \operatorname{erf} \frac{x}{2\sqrt{Dt}} \qquad \ldots\ldots\ldots (20)$$

By sectioning the heulandite block Tiselius was able to determine the concentration at any point along the length of the block at any time t. From equation (20) Tiselius was able to determine the diffusion constant of water in heulandite.

(b) Non-stationary flow in capillaries

Clausing (40) has measured the non-stationary state of gas flow in a glass capillary. Working at gas pressures where Knudsen molecular streaming occurred, he observed a time lag between the instant the flow conditions were established and the time when steady state flow occurred in the capillary. This phenomenon was observed experimentally by maintaining a gas pressure virtually constant at the influent end of a capillary and a pressure approximately equal to zero at the effluent end of the capillary. This effluent pressure was measured by means of an ionization gauge, and from the rate of change of pressure, and from the volume of the system, Clausing was able to calculate the total number of molecules that had entered the low pressure vessel at any time.

From Kinetic Theory Clausing deduced that, if surface diffusion could be neglected, the diffusion constant could be calculated from the equation:

$$D = \frac{4}{3} \times \left(\frac{R^2}{2R/\bar{\omega} + T_e} \right) \qquad \cdots\cdots \quad (\underline{21})$$

where R is the capillary radius,

$\bar{\omega}$ is the root mean square velocity of the gas molecules,

and T_e is the mean life of an adsorbed molecule.

Clausing considers the flow in a capillary to take place according to the diffusion equation in the form:

$$\frac{\partial N}{\partial t} = D \frac{\partial^2 N}{\partial x^2} \qquad \ldots\ldots \quad (\underline{22})$$

where $N = N_a + N_g$ is the total number of molecules per unit length of capillary including those adsorbed on the wall.

The boundary conditions for Clausing's experiment were:

$N = N_1$ at $x = 0$ for all t

$N = 0$ at $x > 0$ at $t = 0$

$N \triangleq 0$ at $x = L$ for all t,

where L is the length of the capillary.

For which conditions it may be shown that the concentration gradient at the effluent end of the capillary is given by the equation:

$$\left(\frac{\partial N}{\partial x}\right)_{x=L} = -\frac{N_1}{L}\left(1 + 2\sum_{1}^{n} e^{-\alpha t} \cos n\pi\right)$$

where $\alpha = \frac{n^2 \pi^2 D}{L^2}$

Hence the total number of molecules that have passed through the effluent end of the capillary in time t is given by the relation:

$$N_t = \int_0^t D\left(-\frac{\partial N}{\partial x}\right)_{x=L} dt$$

That is

$$N_t = \frac{D\,N_1}{L}\left[t + 2\int_0^t \sum_1^n e^{-\alpha t} \cos n\pi\, dt\right]$$

which may be expressed in the form of the infinite series:

$$N_t = \frac{D\,N_1}{L}\left[t - \frac{2\,L^2}{\pi^2 D}\left((1 - e^{-\frac{\pi^2 Dt}{L^2}}) - \frac{1}{4}(1 - e^{-\frac{4\pi^2 Dt}{L^2}}) + \frac{1}{9}(1 - e^{-\frac{9\pi^2 Dt}{L^2}}) \ldots\right)\right] \quad \ldots\ldots \quad (23)$$

where N_1 is the number of molecules per cc. at the influent end of the capillary.

From experimental values of N_t, Clausing was able to solve equation (23). From the value of the diffusion constant (D) obtained Clausing was also able to calculate the mean life of the adsorbed molecule from equation (21).

Frenkel (41) has shown that the mean life of an adsorbed molecule may be estimated from the equation

$$T_e = T_o\, e^{\Delta H/RT}$$

where T_o is the vibration period of the adsorbed molecule,

and ΔH is the heat of adsorption.

By evaluating T_e at various temperatures Clausing was able to calculate the heat of adsorption and the vibration period of the adsorbed molecule.

It has already been shown (see page 19) that Damköhler considers that, where adsorption occurs in a pore, diffusion into the pore will take place in accordance with the differential equation (16)

$$\frac{\partial N_g}{\partial t} = D \frac{\partial^2 N_g}{\partial x^2} \qquad \ldots\ldots\ldots \quad (\underline{16})$$

where

$$D = \frac{D_g + A'' D_a}{1 + A''} \quad \text{and} \quad A'' = \frac{N_a}{N_g}$$

When the adsorption is slight, the value of A'' is small and the Damköhler diffusion constant $D = D_g$. That is:

$$\frac{\partial N_g}{\partial t} = D_g \frac{\partial^2 N_g}{\partial x^2}$$

in which form the Damköhler equation is similar to equation (22) used by Clausing. In the charcoal pore however, where the adsorption is considerable, it is to be expected that the more general equation (16) of Damköhler is more applicable.

Damköhler considers that the charcoal pore is bounded on one end, and therefore the approach to equilibrium adsorption in that pore would be in accordance with the solution of equation (16) for the boundary conditions:

$N_g = N_o$ at $x = 0$ for all t

$N_g = 0$ at $x > 0$ at $t = 0$

$\frac{\partial N_g}{\partial t} = 0$ at $x = L'$

where L' is the pore length.

These conditions lead to the equation:

$$\delta\ (t) = \frac{\int_{0}^{L'} N_g\ dx}{N_0 L'} = 1 - \frac{8}{\pi^2} \sum_{0}^{\infty} \frac{e^{-\frac{\pi^2 (2m' \pm 1) Dt}{4L'^2}}}{(2m' + 1)^2} \qquad \ldots\ldots\ (\underline{24})$$

where δ (t) is the ratio of the number of molecules adsorbed at time t to the number adsorbed at equilibrium.

No data are available for the calculation of charcoal pore lengths by means of equation (24), but Damköhler estimates that zeolite pores are of the order of 0.3 cm.

. . . .

Whereas the subject of gas flow has been dealt with superficially in one or more chapters of many texts on Physical Chemistry, relatively few treatises have been written dealing exclusively with this subject. Of the more complete text books dealing with the flow of gases through porous solids, "Diffusion in and through Solids" (42) and "Flow of Homogeneous Fluids" (43) have been found most useful.

EXPERIMENTAL

A. The Charcoal

The most important consideration in choosing the charcoal for this research was its uniformity. It is quite apparent that, where flow rates through a solid block of charcoal are being measured, any cracks or holes would make such a large contribution to the total flow that the flow phenomena associated with the fine structure would be masked. A zinc chloride activated charcoal, prepared by the National Carbons Company appeared to be the most uniform of the commercial products.

(a) Zinc chloride activated charcoal

The zinc chloride charcoal obtained from the National Carbons Company was in the form of cylindrical rods about 10 cm. long and 0.380 cm. in diameter. The surface of the rods was slightly rough and the occasional crack was also visible. One-centimeter lengths of the charcoal rods could be obtained, however, that were free from such faults as would be visible with a low-power microscope. A cleavage surface of this charcoal was sufficiently smooth to allow specular reflection of 90^{o} incident light.

In order to interpret the flow data it was necessary to know some of the physical characteristics of the zinc chloride charcoal.

(i) Helium density of the zinc chloride activated charcoal.

The apparatus used to determine the helium density of the zinc chloride charcoal is shown in Fig. 1. The limiting factor in the design of this apparatus was the small quantity of available charcoal. Although there was an adequate supply of the zinc chloride charcoal for all other purposes required in this research, the total supply was not sufficient for determination of the helium density by usual methods which require relatively large amounts of charcoal. In principle the apparatus (Fig. 1) is similar to the apparatus of Howard and Hulett (44), but in order to make their methods applicable to small volumes of charcoal, all manifold space has been reduced to a minimum in the apparatus represented in Fig. 1.

In order to maintain the system at constant volume, the manometer A was arranged so that the mercury in the pressure arm was always at a constant height indicated by the glass pointer B. To allow for variations in pressure while maintaining constant mercury height at B, mercury was removed or added to the manometer from the reservoir C.
In order to keep the volume small, the manifold F and the pressure arm of the manometer above the glass pointer B were made from 1 mm. capillary. The volumes of the bulbs G and H were obtained before they were set into the apparatus.

The volume and evacuated weight of the empty pycnometer L were obtained prior to filling with the charcoal rods. During the helium density determinations the pycnometer was connected to the manifold F by means of the standard joint K. For outgassing the charcoal however, the pycnometer was connected to the standard joint M. The charcoal was considered free from adsorbed gases after 36 hours evacuation at 150°C.

The helium density of the zinc chloride charcoal was obtained in the following manner. Helium gas at known temperature and pressure was expanded from the bulb H into the evacuated manifold system F (including the pressure arm of the manometer A and that part of the pycnometer which extends into the standard joint K). From the pressure observed on the manometer A, the volume of the manifold system was calculated. A further expansion into the evacuated pycnometer L was accomplished by opening the stopcock Q. From the observed pressure, the void volume of the pycnometer was evaluated. The difference between the void volume of the pycnometer when filled with charcoal and the volume of the empty pycnometer gives the volume of the charcoal. The ratio of the weight of the charcoal to the volume the charcoal displaces in helium is the helium density. The helium density is also the density of the solid material in the charcoal if it is assumed that the helium penetrates into all the pores but is not adsorbed.

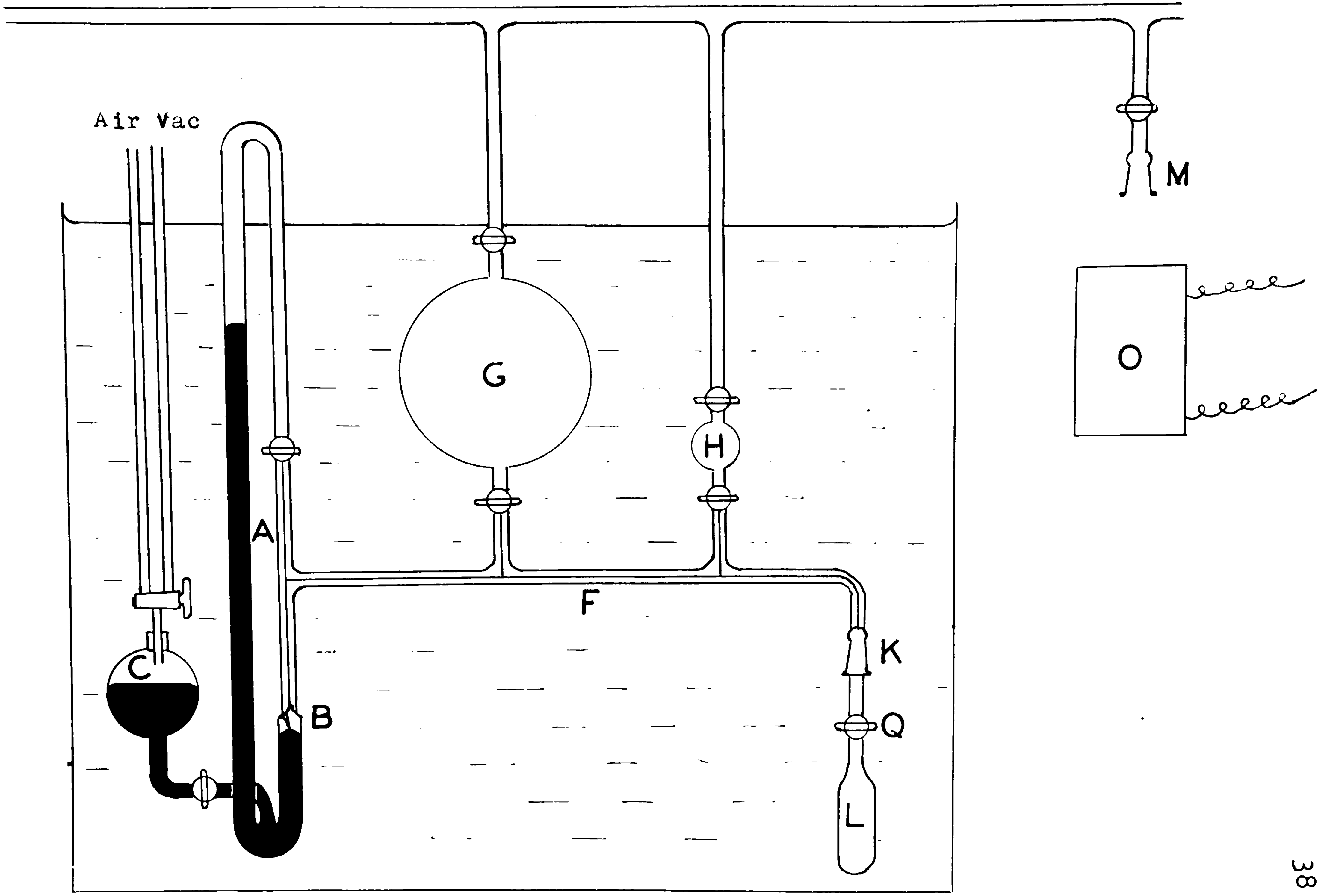

Fig. 1: Apparatus for determining helium density and nitrogen surface area.

Although the apparatus was designed to measure the helium density of a small quantity of charcoal, there was sufficient charcoal available for only one complete determination. The error involved, however, in the determination of the weight of the charcoal was relatively smaller than the error in the determination of the volume, so that two volume determinations on the same sample were, effectively, almost equivalent to two completely separate measurements.

Weight of pycnometer plus degassed charcoal		58.808 gm.
Weight of evacuated pycnometer		49.474
Therefore, Weight of Charcoal		9.334
Volume of empty pycnometer (calculated from weight of water it contained at 25°C.)		33.054 cc.
Void volume of pycnometer when filled with charcoal (calculated from helium expansions into the pycnometer. Two determinations	28.82,	28.87
Therefore, Helium volume of charcoal	4.23	4.18 cc.

But

$$\text{Helium density} = \frac{\text{Weight of charcoal}}{\text{Helium volume of charcoal}} =$$

$$\frac{9.334}{4.23} = 2.21 \text{ gm./cc.} \quad \text{(first determination)}$$

$$\frac{9.334}{4.18} = 2.23 \text{ gm./cc.} \quad \text{(second determination)}$$

The accuracy of this helium density determination was limited by the small available quantity of charcoal. A mean value of 2.22 gm. per cc. is considered sufficiently accurate for the required purposes.

(ii) Nitrogen surface area of the zinc chloride activated charcoal

The nitrogen surface area was determined by the method of Brunauer, Emmett and Teller (45). These authors have shown theoretically that adsorption should occur in accordance with the isotherm equation:

$$\frac{1}{V_o} \cdot \left(\frac{P}{P_o - P}\right) = \frac{1}{V_m c} + \left(\frac{c - 1}{V_m c}\right) \cdot \frac{P}{P_o} \qquad \ldots (\underline{25})$$

where V_o is the volume of gas adsorbed in cc. at S.T.P. per gm. of charcoal at the pressure P,

P_o is the vapour saturation pressure at the temperature of the isotherm,

V_m is the volume in cc. of gas at S.T.P. adsorbed on one gram of charcoal that just completes the formation of a monolayer on the adsorbing surface,

and c is a dimensionless constant that is dependent on the heat of adsorption and the heat of liquifaction of the gas.

It may be seen from equation (25) that a plot of $\frac{P}{P_o}$ against $\frac{1}{V_o}\left(\frac{P}{P_o - P}\right)$ gives a straight line whose slope is $\frac{c - 1}{V_m c}$ and whose intercept is $\frac{1}{V_m c}$. Thus from the experimental values of the slope and the intercept, the two constants V_m and c may be evaluated.

The surface area per gram of charcoal may be estimated from the value of V_m if it is assumed that each molecule of

The apparatus used to determine the nitrogen adsorption isotherm at 90.1° K is shown diagrammatically in Fig. 1. (The same apparatus was used to determine the helium density.) The pycnometer L containing the degassed charcoal was cooled in liquid oxygen (90.1° K) and exposed to nitrogen until adsorption equilibrium was reached. The approach to equilibrium could be observed by the change in the pressure of the system with time. After about two hours the pressure became constant and the adsorption was considered complete. The adsorption pressure was then recorded, the stopcock Q closed and the system evacuated. The adsorbed gas and the gas held in the pycnometer at the adsorption pressure was then expanded into the manifold and the calibrated flask G. The pycnometer was warmed to 25°C. in a constant temperature bath, thus causing the nitrogen held on the charcoal to desorb. Since the amount of nitrogen adsorbed on charcoal at room temperature is small in relation to that held at 90.1° K, the desorption may be considered complete (47). The amount of desorbed nitrogen is equal to the total amount of gas in the system less the amount that was held in the void volume of the pycnometer at 90.1° K and the adsorption pressure.

The experimental data for the adsorption of nitrogen on the zinc chloride activated charcoal are given in Table 1 and shown graphically by means of the Brunauer, Emmett and Teller plot in Fig. 2.

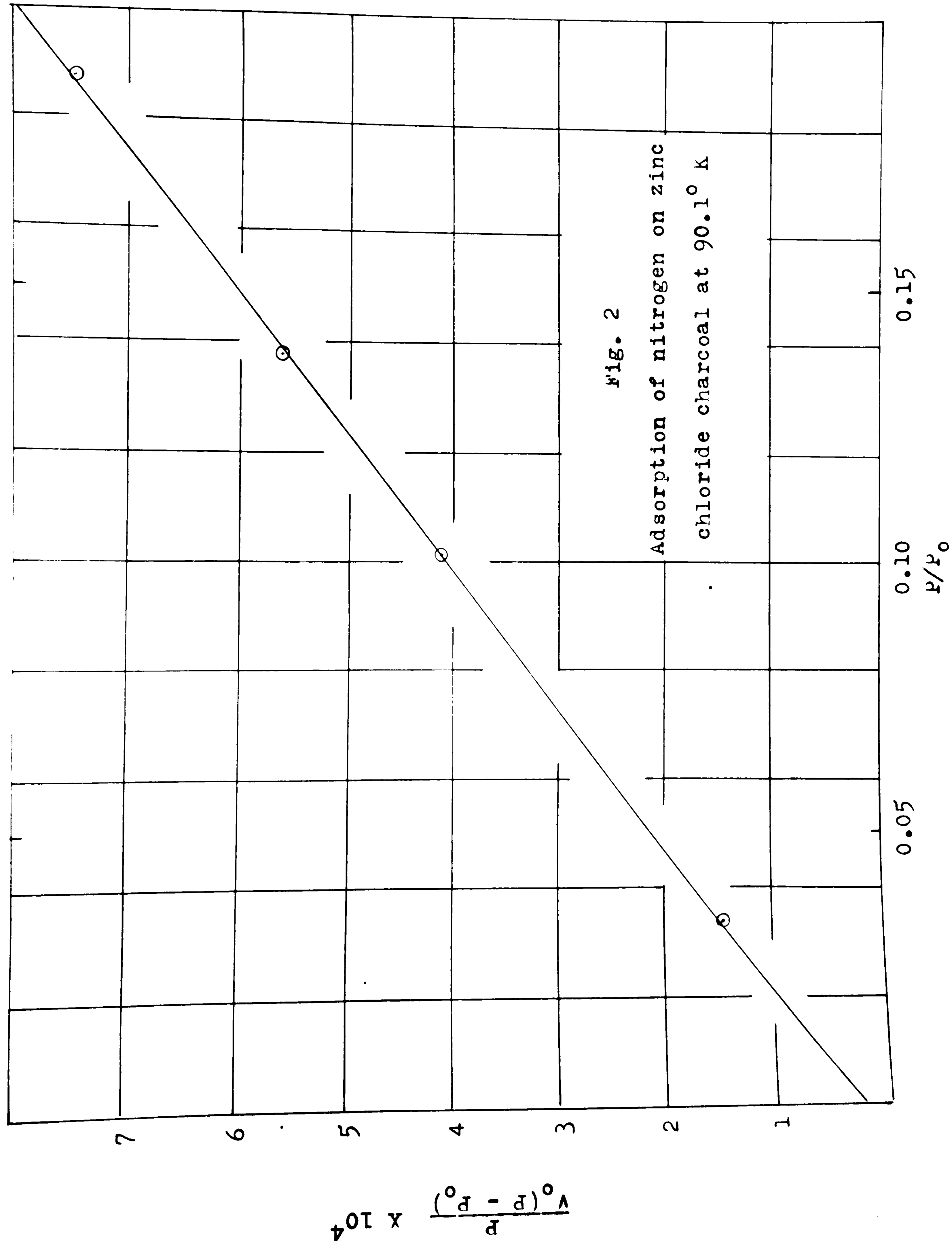

Fig. 2

Adsorption of nitrogen on zinc chloride charcoal at 90.1° K

TABLE I

Adsorption of nitrogen on zinc chloride activated charcoal at 90.1°K.

Pressure mm. Hg.	Volume adsorbed cc./gm.	$\frac{P}{P_o}$	$\frac{1}{V}\frac{P}{P_o - P}$
467.0	304	0.187	0.752×10^{-3}
345.4	284	0.137	0.560×10^{-3}
252.1	267	0.101	0.418×10^{-3}
83.3	224	0.033	0.153×10^{-3}

(P_o = 2680 mm. (48))

From Fig. 2 the experimental values of the slope and intercept are obtained.

$$\text{Slope} = 3.90 \times 10^{-3} = \frac{c-1}{V_m c}$$

$$\text{Intercept} = 0.03 \times 10^{-3} = \frac{1}{V_m c}$$

whence V_m = 250 cc. nitrogen at S.T.P./gm. charcoal.

The surface area covered by a single molecule of nitrogen at 90.1° K was evaluated from equation (27).

$$A_m = 4 \times .866 \left[\frac{28.01}{4\sqrt{2} \times 6.06 \times 10^{23} \times .751}\right]^{2/3} = 17.0 \times 10^{-20} \text{ sq. m.}$$

Substituting this value of A_m and the value of V_m calculated above in equation (26):

$$S_w = \frac{250}{22400} \times 6.06 \times 10^{23} \times 17.0 \times 10^{-20} = 1140 \text{ sq.m./gm.}$$

To obtain this value it was assumed that the amount of nitrogen held on the charcoal at room temperature was small compared to the amount held at the temperature of the liquid oxygen. In view, however, of the theoretical assumptions involved in the calculation of the nitrogen surface area such experimental errors appear insignificant. The nitrogen surface area is therefore recorded as 1.1×10^3 sq.m./gm.

(iii) Mercury density and void fraction of the zinc chloride activated charcoal

Fig. 3 shows the apparatus used for the determination of the mercury density of the zinc chloride activated charcoal. The pycnometer A contained the same charcoal that was used for the helium density and nitrogen surface area. The pycnometer was evacuated and connected to the flask B as shown in Fig. 3(a). The flask B was filled with mercury and the stopcock C opened to allow the mercury to flow into the pycnometer. The pycnometer was brought to a known temperature in a water bath and the stopcock C closed. The flask B was then detached and the excess mercury removed from the pycnometer connection. The difference between the weight of the pycnometer filled with charcoal and mercury, and the weight of the pycnometer containing the charcoal alone, gives the weight of the contained mer-

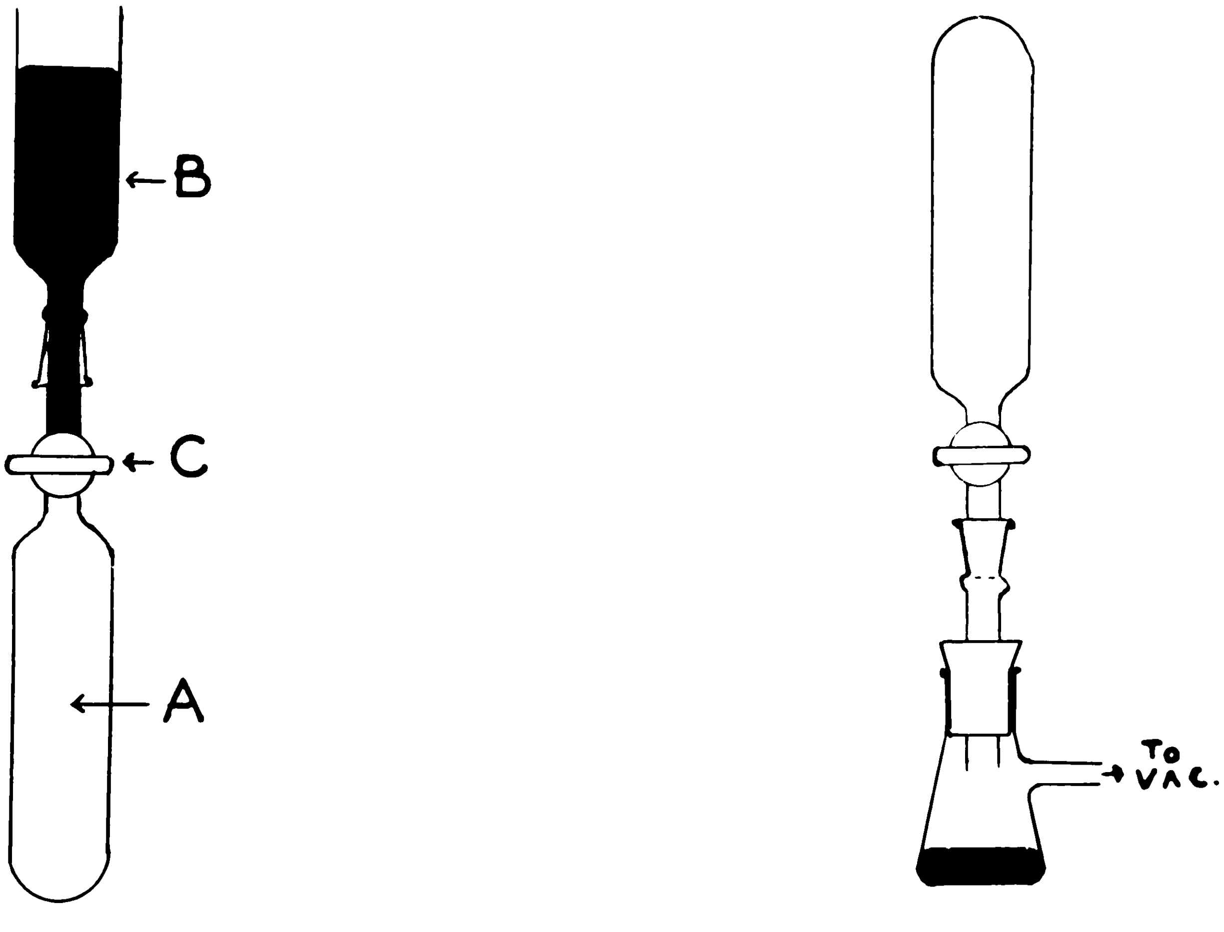

(a) (b)

Fig. 3

Apparatus for determining mercury density of charcoal cury. From the weight of the mercury and its known density the volume of the mercury may be calculated. The difference between the volume of the empty pycnometer and the calculated volume of mercury gives the apparent volume of the charcoal. The ratio of the weight of the charcoal to the apparent volume in mercury is the mercury density.

Weight of charcoal 9.334 gm. (page 39)

Volume of pycnometer 33.054 cc. (page 39)

Volume of mercury used to fill the void space in the pycnometer 19.862 cc.

But volume of pycnometer less the volume of mercury is the apparent volume of the charcoal

13.192 cc.

$$\text{Mercury density} = \frac{\text{weight of charcoal}}{\text{apparent volume of charcoal}} =$$

$$\frac{9.334}{13.192} = 0.707 \text{ gm./cc.}$$

The void fraction of the charcoal, which is defined by the ratio of the volume of the voids to the total volume of the voids and solids, may be calculated from the experimentally obtained values of the helium and mercury densities.

The helium density of the zinc chloride charcoal is 2.22 gm./cc. (see page 39) and therefore 0.707 gm. of solid charcoal would fill $\frac{0.707}{2.22} = 0.320$ cc.

But 0.707 gm. of charcoal (including voids) fill 1 cc. (from the mercury density).

Therefore 0.680 cc. (1 - 0.320) of the charcoal must be void.

That is the void fraction of the charcoal is 0.680 or in other words the charcoal is 68.0% void.

The calculation of the void fraction from the helium and mercury densities is valid only if the helium density is the true density of the solid material in the charcoal, and the mercury density is the average density of the solids and voids. That is it is necessary to assume that the helium penetrates all the pores without being adsorbed, whereas the mercury does not penetrate the pores at all.

The mercury was removed from the pycnometer by means of the apparatus shown in Fig. 3(b).

(iv) Adsorption of diethyl ether and ethyl chloride on zinc chloride activated charcoal

The pycnometer and sample of charcoal that were used for the determination of the helium density, mercury density and nitrogen surface area, were again used for the determination of the diethyl ether and ethyl chloride isotherms at 35.0°C. The evacuated pycnometer was maintained in a thermostated bath at 35.0°C. and the charcoal exposed to the adsorbable gases until pressure equilibrium was reached. The pycnometer was then weighed and the increase in weight less the calculated weight of the free gas in the pycnometer, represented the weight of the gas adsorbed.

It was necessary to have an empirical relation between the mass of gas adsorbed per unit mass of charcoal and the pressure. One of the simplest adsorption equations is the Freundlich relation (49) which may be stated in the form:

$$\frac{x}{m} = K' P^{1/n'}$$

where $\frac{x}{m}$ is the mass adsorbed per gram of adsorbent,

P is the adsorption pressure,

and K' and $1/n'$ are constants.

If experimental data conform with the Freundlich equation it may be seen that a plot of log (x/m) against log P should give a straight line of slope 1/n' and intercept K'.

The experimentally determined values for ethyl chloride and diethyl ether are presented in Table II and represented graphically in Figs. 4 and 5.

The values of the Freundlich constants K' and 1/n' were obtained from the slope and intercept values of Fig. 4.

Diethyl ether	Ethyl chloride
$K' = 0.165$	$K' = 0.0876$
$1/n' = 0.162$	$1/n' = 0.274$
$(x/m) = 0.165P^{0.162}$	$(x/m) = 0.0876P^{0.274}$

(It is to be noted from Fig. 4 that the experimental results do not give a straight line Freundlich plot over the whole pressure range. The Freundlich constants have therefore been

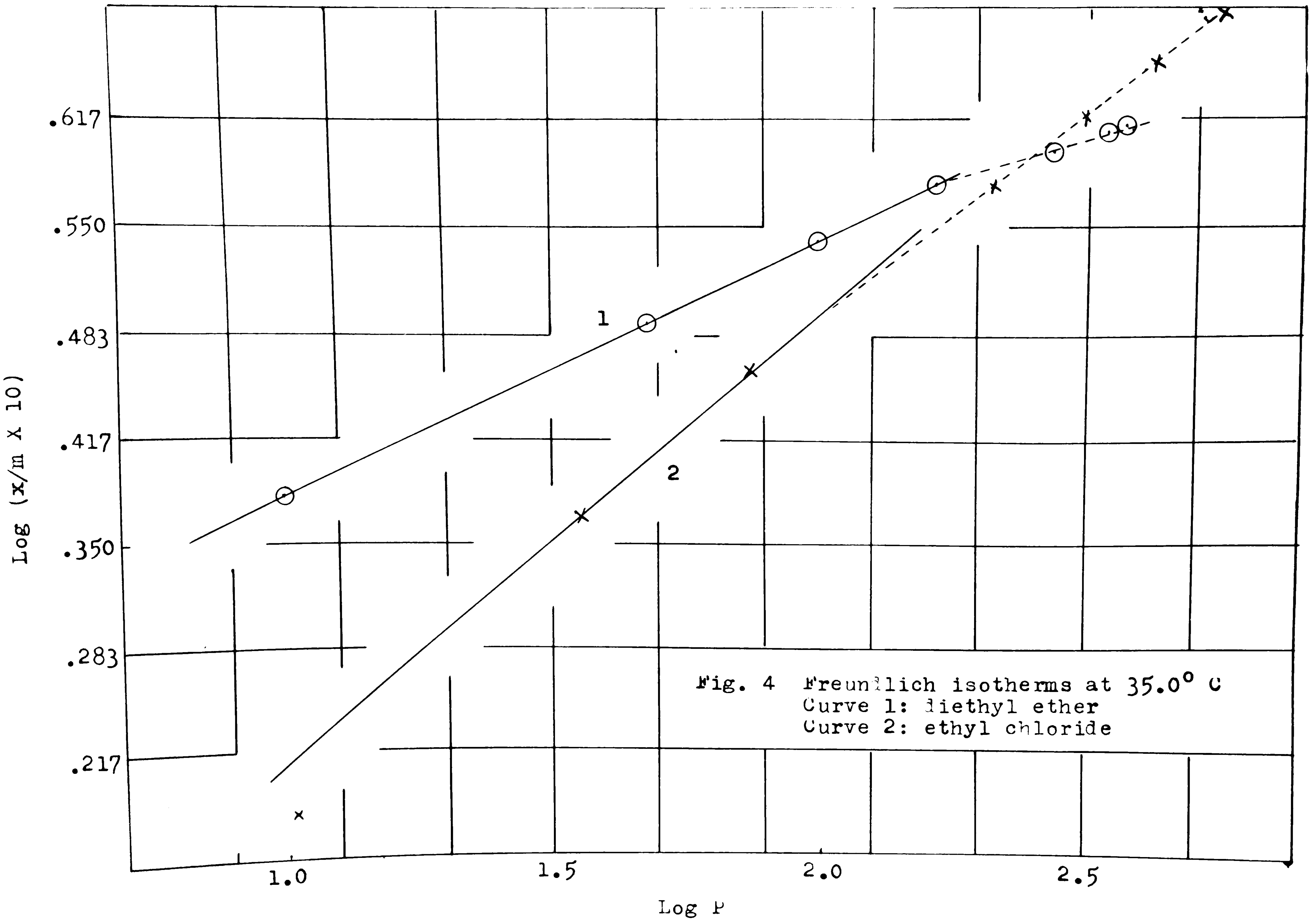

Fig. 4 Freundlich isotherms at 35.0° C
Curve 1: diethyl ether
Curve 2: ethyl chloride

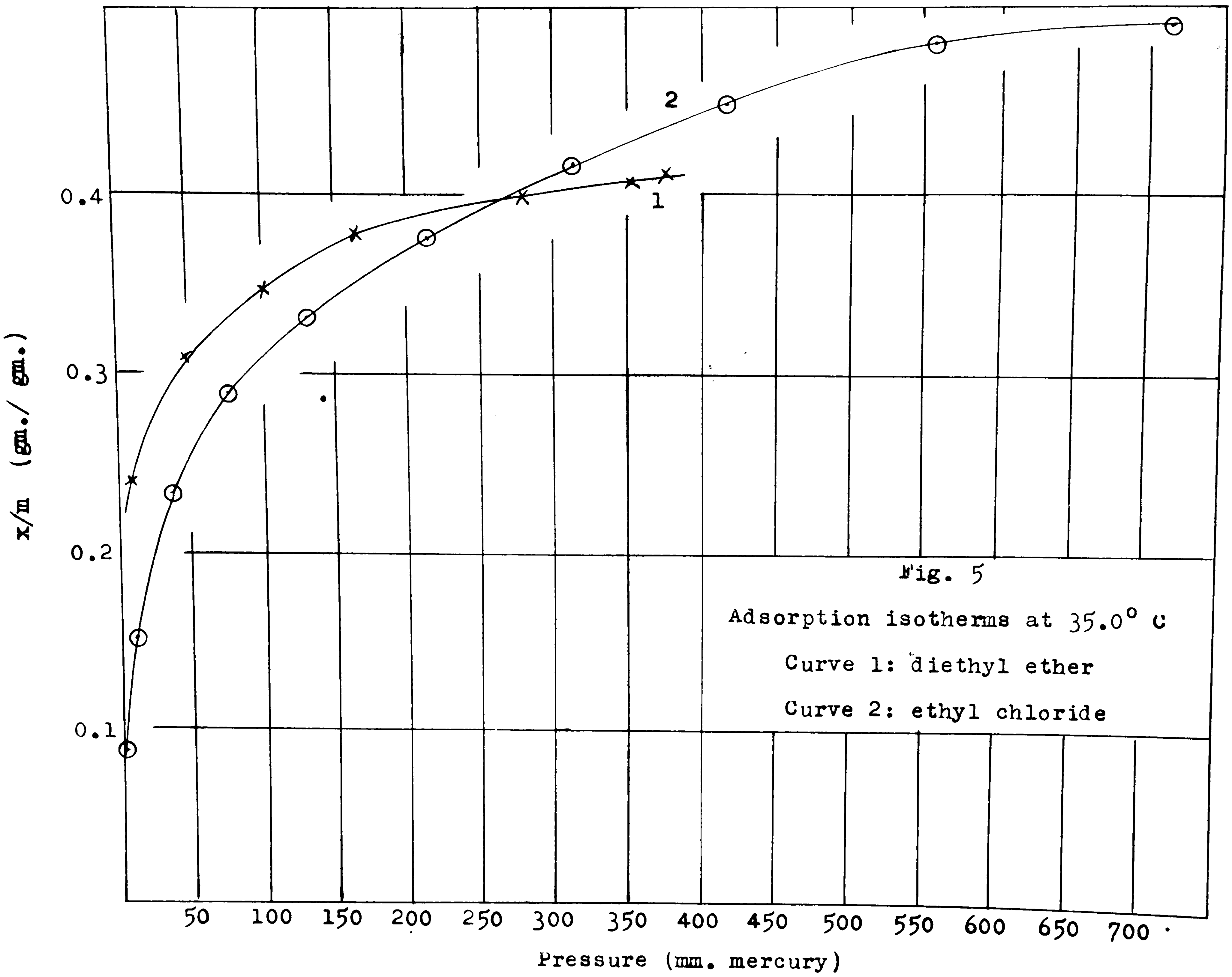

Fig. 5

Adsorption isotherms at 35.0° C

Curve 1: diethyl ether

Curve 2: ethyl chloride

obtained to give the best correlation with experimental data for the pressure range up to 100 mm.)

TABLE II

Adsorption of diethyl ether and ethyl chloride on zinc chloride activated charcoal at 35.0°C.

Diethyl Ether		Ethyl Chloride	
Mass adsorbed (gm./gm.)	Pressure (mm. Hg.)	Mass adsorbed (gm./gm.)	Pressure (mm. Hg.)
0.2398	10.1	0.0316	0.45
0.3107	48.8	0.0864	2.85
0.348	102.8	0.1507	10.55
0.378	166.6	0.234	36.15
0.395	280.3	0.290	75.35
0.405	352.4	0.332	129.9
0.410	376.0	0.375	214.1
		0.414	313.9
		0.447	417.4
		0.478	558.3
		0.490	715.5

(b) Saran charcoal

During the course of the research on the flow of gases through zinc chloride charcoal, it was brought to the attention of the candidate# that charcoal even more uniform

---

\# Private discussion with personnel of the Chemical Warfare Division of the National Research Council, Ottawa.

in appearance than the zinc chloride charcoal could be prepared. This uniform type of charcoal is prepared from moulded Saran plastic, a copolymer of vinyl chloride and vinylidene chloride (50).

While there is no published literature on the formation of Saran charcoal it is apparent that the properties of the charcoal formed from Saran would depend to a large extent on the method of preparation. The uniformity was the limiting requirement of the charcoal, and it was therefore necessary to determine what conditions would yield an active charcoal free from cracks and holes. No attempt has been made in this investigation to determine the variation in the activity of Saran charcoal with varying methods of preparation.

(i) Preparation of Saran charcoal

Saran moulding powder (S-548) was moulded in a compression type mould under a wide variety of pressure and temperature conditions. When the moulding was conducted at pressures over 4000 lb. per sq. inch, it was found that the Saran tended to blow itself apart in the subsequent activation process. It was also found that unless the steel mould were thoroughly clean and the heating cycle completed in less than one hour, the Saran tended to undergo a catalytic decomposition in the mould (51). Allowing for these conditions, a satisfactory Saran moulding could be obtained between moulding pressures of 2000 - 4000 lb. per sq. inch at a temperature of 140°C. The density of the Saran produced in this way was about 1.74 gm. per cc.

The preparation of charcoal from Saran depends on the fact that Saran, when heated, decomposes into carbon and gaseous hydrochloric acid. Experimentally the decomposition process was accomplished in two stages. In the first stage the Saran was heated at 150° C. in a vacuum oven until it lost about 30% of its total weight. This process required between 24 and 36 hours. A further decomposition and activation was carried out in an atmosphere of nitrogen. The temperature of the Saran during the activation was gradually raised over a 6 - 8 hour period from 150°C. to 500°C., and was then maintained at 500°C. for about 3 hours.

Using the method described above, Saran charcoal was prepared both in the form of rods and discs. Saran rods 7.6 mm. in diameter and about 15 mm. in length had sufficient rigidity to undergo the conversion into charcoal without warping in any way. The discs, however, which were 50.8 mm. in diameter and 1 mm. thick required support in order to be maintained flat. This support was accomplished by holding the disc between two pieces of plate glass during the complete process of converting the Saran into charcoal.

The final activation of the charcoal rods was carried out in a combustion tube through which a stream of nitrogen was flowing. The Saran discs were activated in the apparatus illustrated in Fig. 6. The disc is represented by A, and the

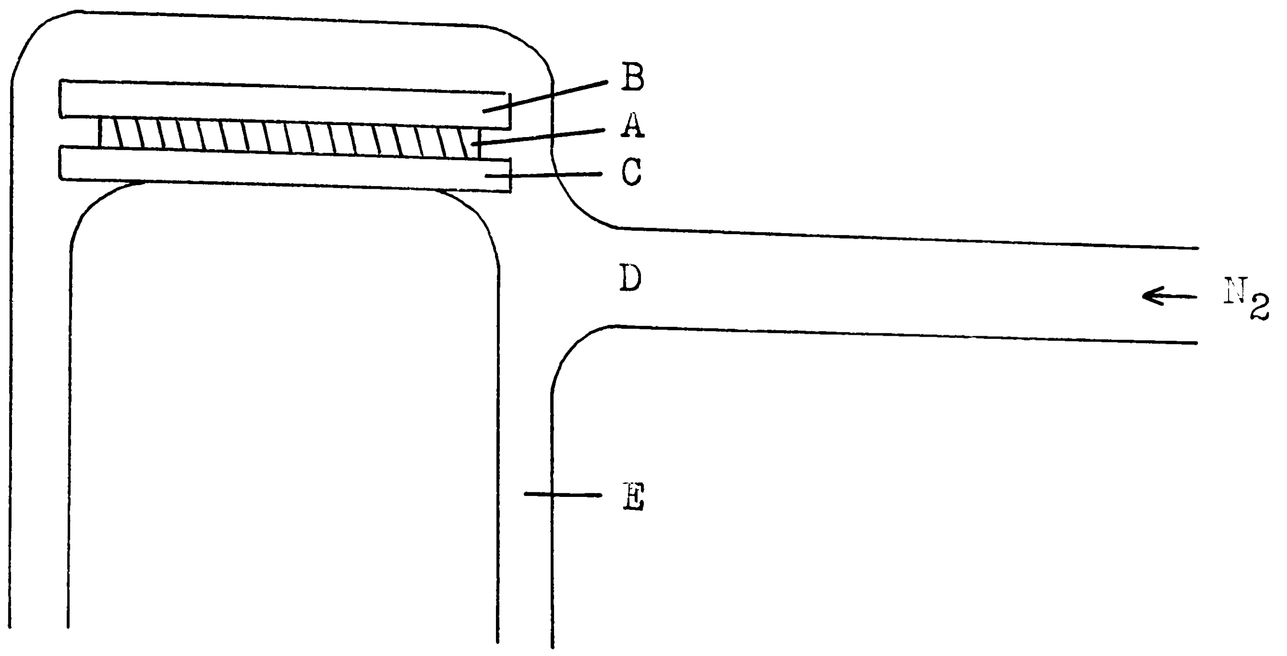

Fig. 6

Apparatus for Activation of Saran discs

supporting pieces of glass plate are represented by B and C. Nitrogen enters the activating cell through inlet D and glass wool was packed in the annular space E to prevent convection currents of air from attacking the hot charcoal.

(ii) The properties of Saran charcoal

The charcoal prepared by the method described above weighs approximately 24% of the weight of Saran used. The 76% loss in weight represents a quantitative loss of hydrochloric acid from the original Saran. A shrinkage occurs as the hydrochloric acid is given off, so that the final charcoal product including voids fills only about 37% of the volume of the moulded Saran. The density of the Saran charcoal obtained in this way is about 1.1 gm./cc. (as estimated from the physical dimensions and weight).

A detailed study of the flow through Saran charcoal would certainly require a more complete knowledge of the charcoal properties. However, no fundamental conclusions have been drawn from the work carried out with the Saran charcoal, and therefore information relative to Saran charcoal is to be considered only as supplemental to the main research, which was conducted with the zinc chloride charcoal.

B. The Flow Rate Apparatus

The quantity of gas adsorbed on charcoal is dependent on the gas pressure, and therefore any method of measuring the gas flow through charcoal which is based on continuously changing pressure conditions can not yield a steady state of flow. The limiting factor in designing an apparatus for measuring the gaseous flow rates through a charcoal rod is therefore the maintainance of constant influent and effluent pressure conditions.

The apparatus which was used for measuring the gas flow rate through a charcoal rod is illustrated in Fig. 7. This apparatus consists of five main parts:

1) The cell H in which the charcoal is mounted.
2) The manometer J which indicates the pressure differential which is driving the gas through the charcoal rod.
3) The burette K in which the mercury rise indicates the gas flow through the charcoal.

4) The control M which regulates the rise of mercury in burette K.

5) The bulb C whose volume is sufficiently large that small quantities of gas flowing into it cause little change in the gas pressure within the bulb.

To measure the gas flow rate through a charcoal sample mounted in cell H, the pure gas is allowed to enter the whole system through the manifold Q until the desired pressure for the low pressure end of the sample is gauged on the manometer A. Stopcock D is then closed and further gas is admitted to the apparatus connected to burette K until the manometer J shows the desired pressure gradient. The amount of mercury in manometer J is then adjusted from reservoir S until the contact I just touches the meniscus of the mercury. The mercury cut-off N is then closed and the rate of mercury rise in the burette K that is required to maintain constant pressure on the manometer J is observed.

The rise of mercury that maintains the constant pressure on the manometer J is controlled automatically in the following manner: when the rate of mercury rise in burette K is more rapid than the disappearance of gas into the charcoal, the gas pressure in the burette K increases. When the pressure in burette K increases, the mercury in manometer J breaks contact with the wire contact I. An electronic relay O is arranged so that when the mercury in the manometer J is not touching the contact I, the solenoid P closes the pinch cock M.

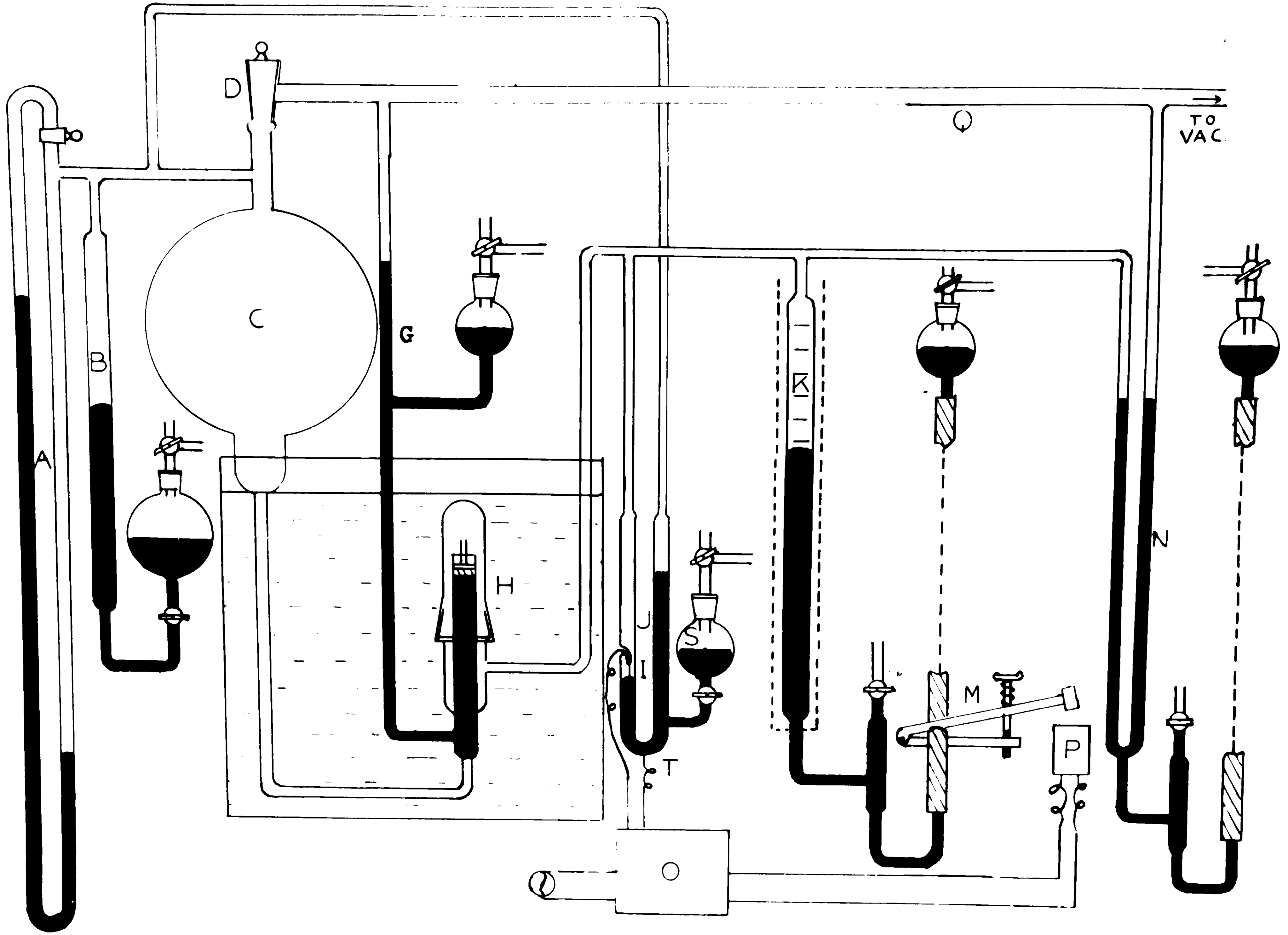

Fig. 7 Apparatus for measuring the flow rate of gases through a charcoal rod

When the pinch cock M is closed the flow of mercury into the burette K is stopped until sufficient gas has disappeared into the charcoal to reduce the gas pressure, and thus close the contact I. When the mercury in manometer J touches the contact I, the pinch cock M is released and hence the mercury may flow once again into the burette K. The rise of mercury in burette K is therefore a measure of the gas flow rate into the charcoal rod. The use of the pinch cock and solenoid for controlling mercury flow into a burette was originated by Hodgins, Flood and Dacey (52).

The contact I was made of tungsten filament wire to ensure a sensitive make and break with the mercury in the manometer J. Tungsten was found suitable because it is less easily wetted by mercury than other possible metallic contacts. To further increase the sensitivity of the flow measurement from the rise of mercury in the burette K, the volume of the manifold between the burette and the inlet side of the charcoal plug was kept to a minimum. It was found that when the apparatus was constructed in this way, as little as 0.1 ml. change in the mercury volume in burette K was sufficient to make or break contact of the mercury in manometer J with the contact I. For the highly sorbable vapours as much as six or eight hours were required before the flow rate into the charcoal became constant. For steady state flow, the recorded data have been observed for at least two hours or for a measured volume change of 50 ml.

The gas passing through the charcoal tended to change the pressure in the bulb C. This pressure was maintained constant during a run by small manual adjustments of the mercury in the burette B. The pressure in bulb C was obtained from manometer A which was observed by means of a cathetometer. The pressure of the gas flowing into the charcoal is obtained by the addition of the pressure of the gas in manometer A and the pressure obtained from the differential manometer J.

It is to be noted that all stopcocks have been eliminated from the section of the apparatus where the gas flow rates are observed. In this way it is assured that disappearance of gas from the burette K could only represent flow into the charcoal rather than such extraneous effects as gas sorption by stop cock grease.

(a) The plug holder for the zinc chloride charcoal

Various methods for mounting the charcoal have been tried. In the original system the charcoal plug was sealed into a glass tube with Wood's metal. This method of holding the charcoal rod did not give reproducible results. In Fig. 8 curve 1 represents a series of consecutive observations of the flow rate of nitrogen through plug No. 5 at various mean pressures. Curve 2 represents another series of consecutive observations of the flow rate of nitrogen through plug No. 5 after it had been exposed to diethyl ether. Curve 3 represents a third series of nitrogen flow rate measurements after a second exposure of the charcoal to the diethyl ether. The charcoal was carefully outgassed before each set of nitrogen flow measurements. It was concluded that the lack of reproducibility was caused by the formation of an annular channel between the charcoal and the Wood's metal. This crack was considered to result from a deformation of the charcoal as it attempted to expand on adsorption, followed by a shrinkage of the charcoal from the Wood's metal on desorption.

Wicke (33) has not reported any difficulty arising from adsorptive expansion of the charcoal, but he did observe an analogous lack of reproducibility caused by the thermal expansion of the charcoal (page 27). It is notable, however, that Wicke confined all his experiments with adsorbable gases to carbon dioxide, although it is clearly indicated that in his research the more strongly adsorbed gases would have given more positive results. Wicke may have avoided the use of the strongly adsorbed gases in order to avoid the further lack of reproducibility encountered in the present research. It is apparent that Wicke's conclusions regarding surface mobility would have been quite untenable had it been necessary to allow for a lack of reproducibility caused by adsorptive expansion as well as thermal expansion.

An attempt was made to allow for the expansion and contraction of the charcoal by placing a thin rubber coating between the charcoal and the Wood's metal seal. Lack of reproducibility was again observed, and it therefore appeared

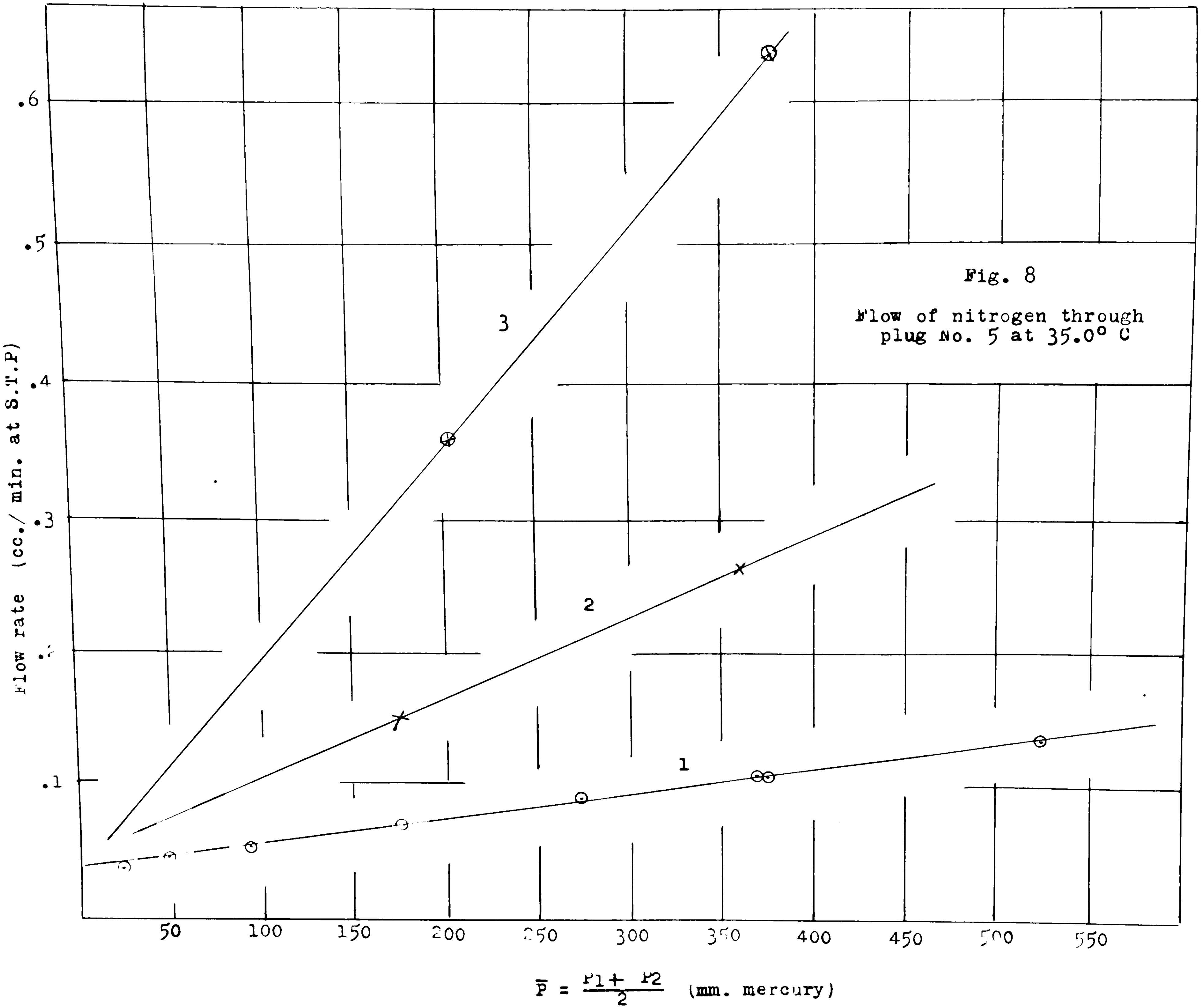

Fig. 8

Flow of nitrogen through plug No. 5 at 35.0° C that the rubber, although displaceable, is not sufficiently compressible to take up the expansion of the charcoal.

Special rubber tubing was made which fitted tightly to the wall of the charcoal and joined it to glass tubing through which the gas could be brought up to the ends of the charcoal rod. To prevent gas from by-passing the charcoal by diffusing through the wall of the tubing, the whole exterior was surrounded by mercury. This system allowed a gas flow almost ten times that expected from measurements made using a Wood's metal holder. It was concluded that the flow between the rubber and the wall of the charcoal rod was greater than through the charcoal itself.

To prevent gas from by-passing the charcoal, a mercury seal was utilized. This was accomplished by leading the gas to and from the ends of the charcoal plug by means of flanged glass tubes lined with a thin film of rubber. These flanges grasped the rim of the charcoal rod and prevented the mercury surrounding the charcoal from leaking into the gas leads. Using the mercury seal it was found that the flow varied greatly from sample to sample until it was observed that the flow was reduced on increasing the pressure of the mercury surrounding the charcoal.

Fig. 9 shows the variation in the flow rate of nitrogen through plugs Nos. 9, 10 and 11 with increasing mercury pressure on the walls of the charcoal plugs. Plug No. 9 (curve 3) was subjected to a high mercury pressure at the

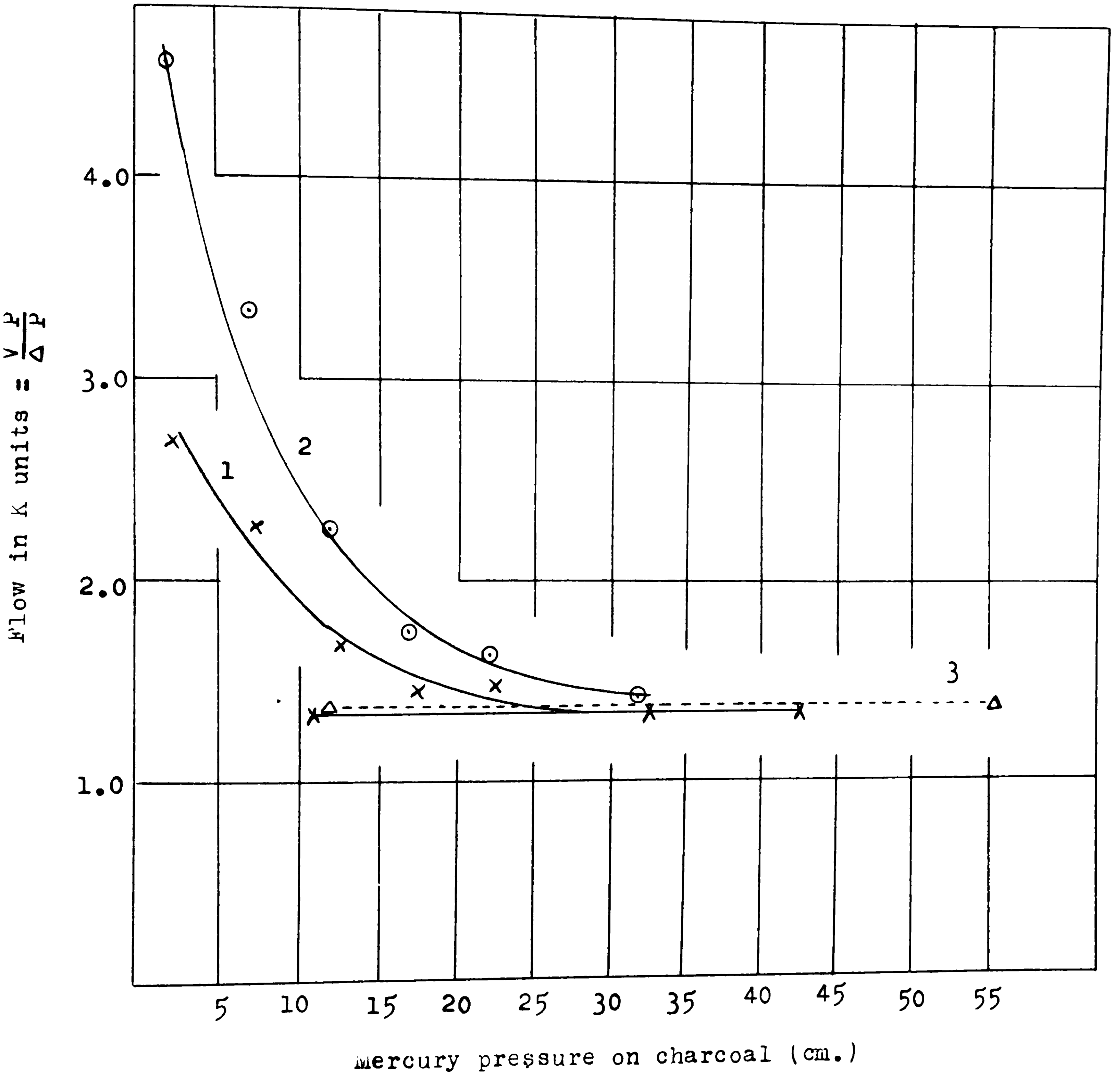

Fig. 9
Variation in flow rate of nitrogen through charcoal rods with change in mercury pressure on the wall of the sample

start and there was no increase in the flow rate as the pressure was reduced. With plug No. 10 (curve 1) and Plug No. 11 (curve 2) the pressure was increased by increments, and the flow was observed to decrease as the mercury pressure was increased. Above 35 cm. mercury pressure there was very little reduction in the flow rate with further increase in mercury pressure and it was concluded that the contribution of the flow between the charcoal and the mercury was eliminated. All subsequent flow measurements were obtained using a minimum of 40 cm. mercury pressure on the wall of the charcoal. It was also concluded from the fact that the flow rate did not increase as the mercury pressure was reduced that the mercury did not readily pull away from the irregularities of the charcoal surface once it had penetrated them. Examination of a charcoal rod after subjection to mercury pressure shows traces of mercury held on its surface, which fact tends to uphold this theory.

Considerable difficulty was caused by the tendency of the mercury surrounding the charcoal to force an entry into the glass tubing which leads the gas to and from the ends of the charcoal rod. This problem was further complicated by the longitudinal expansion and contraction of the charcoal rod. The cell, Fig. 7 H, whose detail is shown in Fig. 10, has been found satisfactory for holding a charcoal rod for flow measurements.

The charcoal rod, Fig. 10 A, is held between the

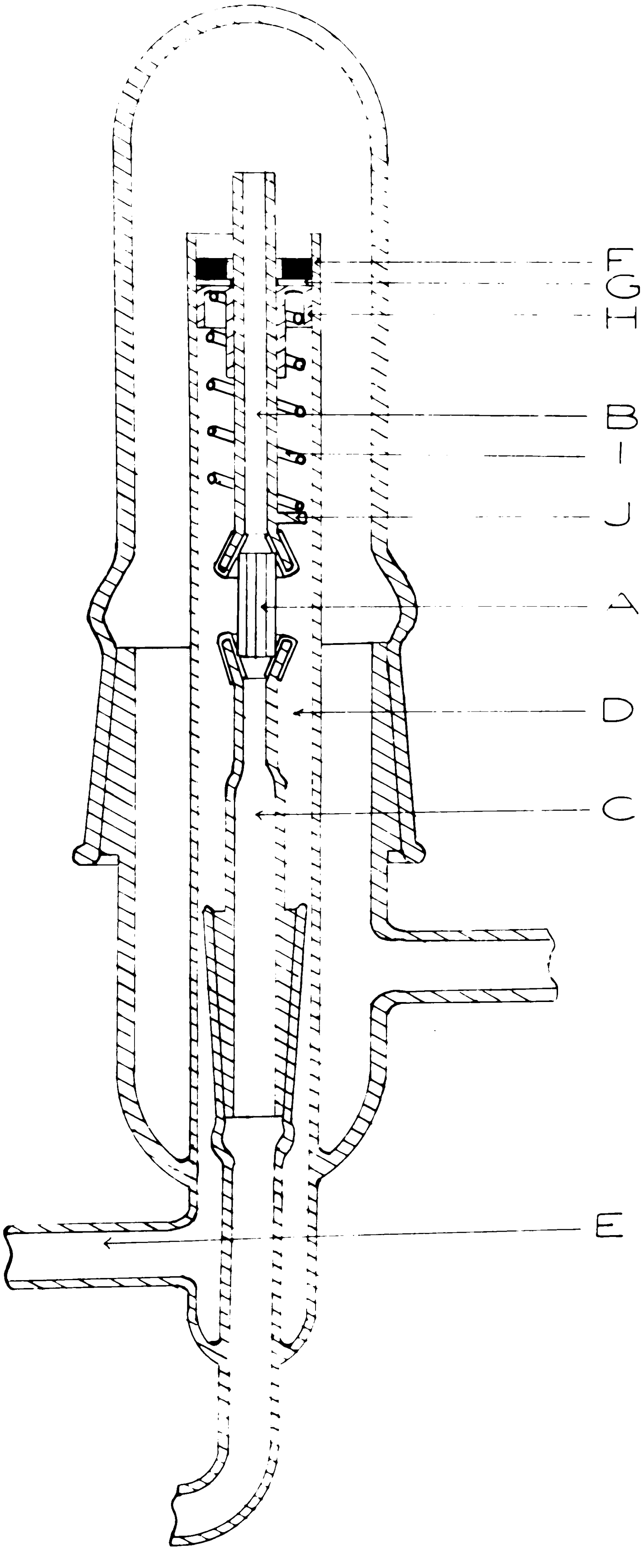

Fig. 10
Apparatus for holding zinc chloride
charcoal rods

two gas leads B and C which have funnel shaped ends lined with a thin coat of rubber (about 3/1000 inch) to ensure both a minimum contact and a tight seal between the glass and the charcoal rod. Compartment D is filled with mercury. The mercury in compartment D is under pressure which is applied through the pressure arm (Fig. 10 E, Fig. 7 G) so that there is always a minimum of 40 cm. of mercury pressure surrounding the wall of the charcoal rod. Since the pressure arm is connected to the system (Fig. 7 G), the 40 cm. mercury pressure on the charcoal wall is always in excess of the pressure of the gas in the system. The mercury in compartment D is confined by Wood's metal F (Fig. 10), metal washer G and hollow-stemmed mushroom-shaped rubber washer H. This method of retaining the mercury in compartment D allows for a short gas lead B, for otherwise the mercury would seek the level of the mercury in the pressure arm (Fig. 7 G). The Wood's metal is sealed to the wall of compartment D but not to that of the gas lead B. In this way the gas lead B is free to move up and down through the metal washer G. The rubber washer H forms a tighter seal with both the wall of compartment D and the gas lead B as the mercury pressure is increased. The gas lead B is therefore allowed freedom of motion, and at the same time the rubber washer prevents the mercury from attacking the Wood's metal. A steel spring I thrusts down on lug J attached to the gas lead B ensuring a tight fit between the gas lead B and the end of the charcoal rod.

(b) Cells used for holding Saran charcoal

Another type of cell that has been found satisfactory for holding a charcoal rod is shown in Fig. 11. In this type of cell the volume of the gas leading to the charcoal plug is reduced, and therefore the manometer J (Fig. 8) has a greater sensitivity to mercury volume changes in burette K. This cell has been found useful in measuring the flow rate through Saran charcoal where the gas flow rate was found to be about 1/50 the flow rate through the zinc chloride activated charcoal. With the increased sensitivity allowed by the use of this cell (Fig. 11) and the use of a microburette in place of burette K (Fig. 7), it is possible to obtain a flow rate accurately (within 1%) when the total measured volume is only 0.5 ml.

Mechanically the cell shown in Fig. 11 is similar to that shown in Fig. 10 with the exception that the Wood's metal backing to the rubber washer (Fig. 10) has been eliminated from the cell (Fig. 11), and a stronger type of hollow-stemmed mushroom-shaped rubber washer has been used (Fig. 11). The free space in the cell (Fig. 11) is filled with mercury from a reservoir A and the gas enters the cell through a capillary B.

A third type of cell (Fig. 12) has also been found useful for measuring the flow rates through Saran charcoal. The charcoal disc A (about 3.75 cm. in diameter) is held between two glass cups B and C. To prevent mercury from en-

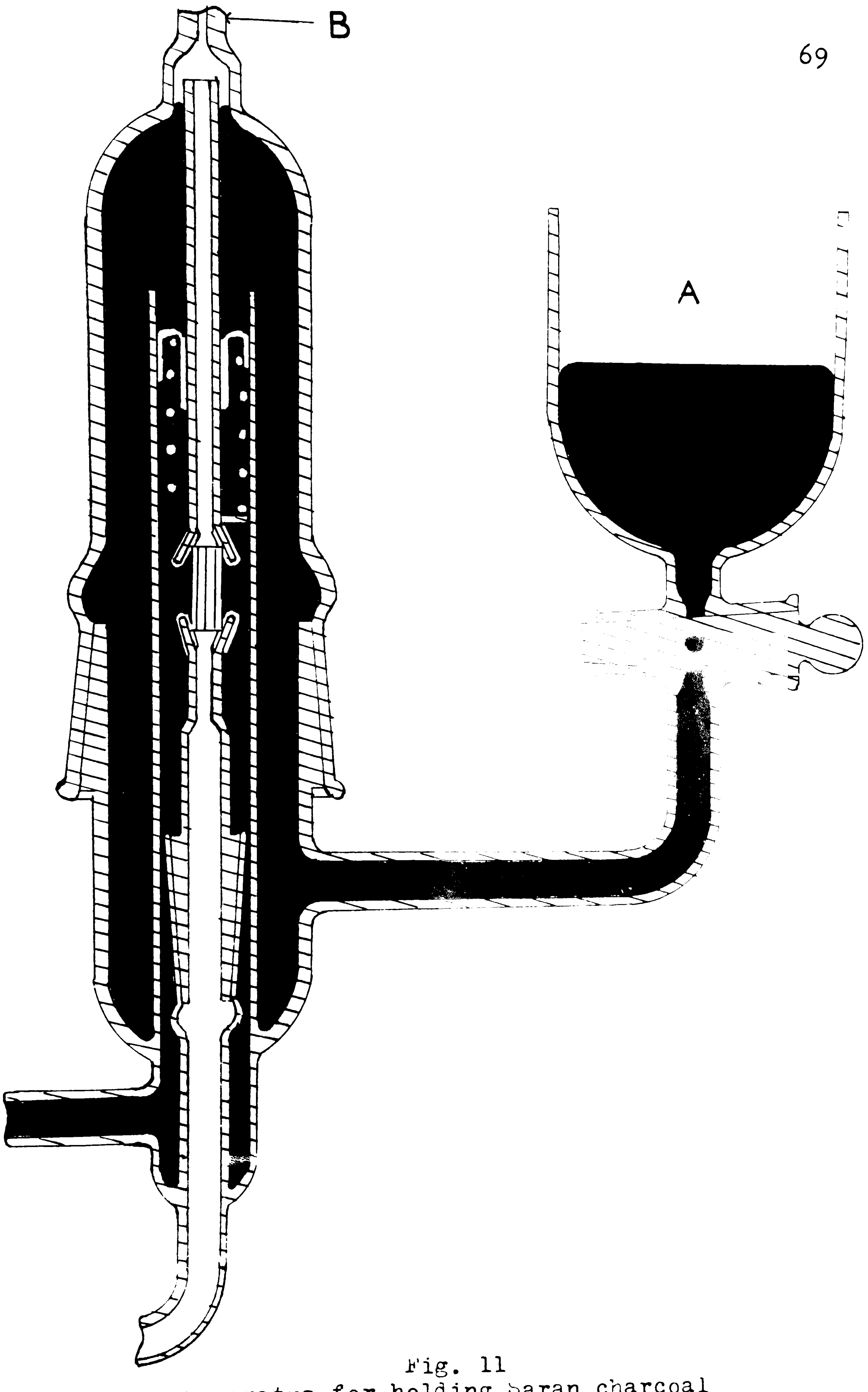

Fig. 11
Apparatus for holding Saran charcoal rods

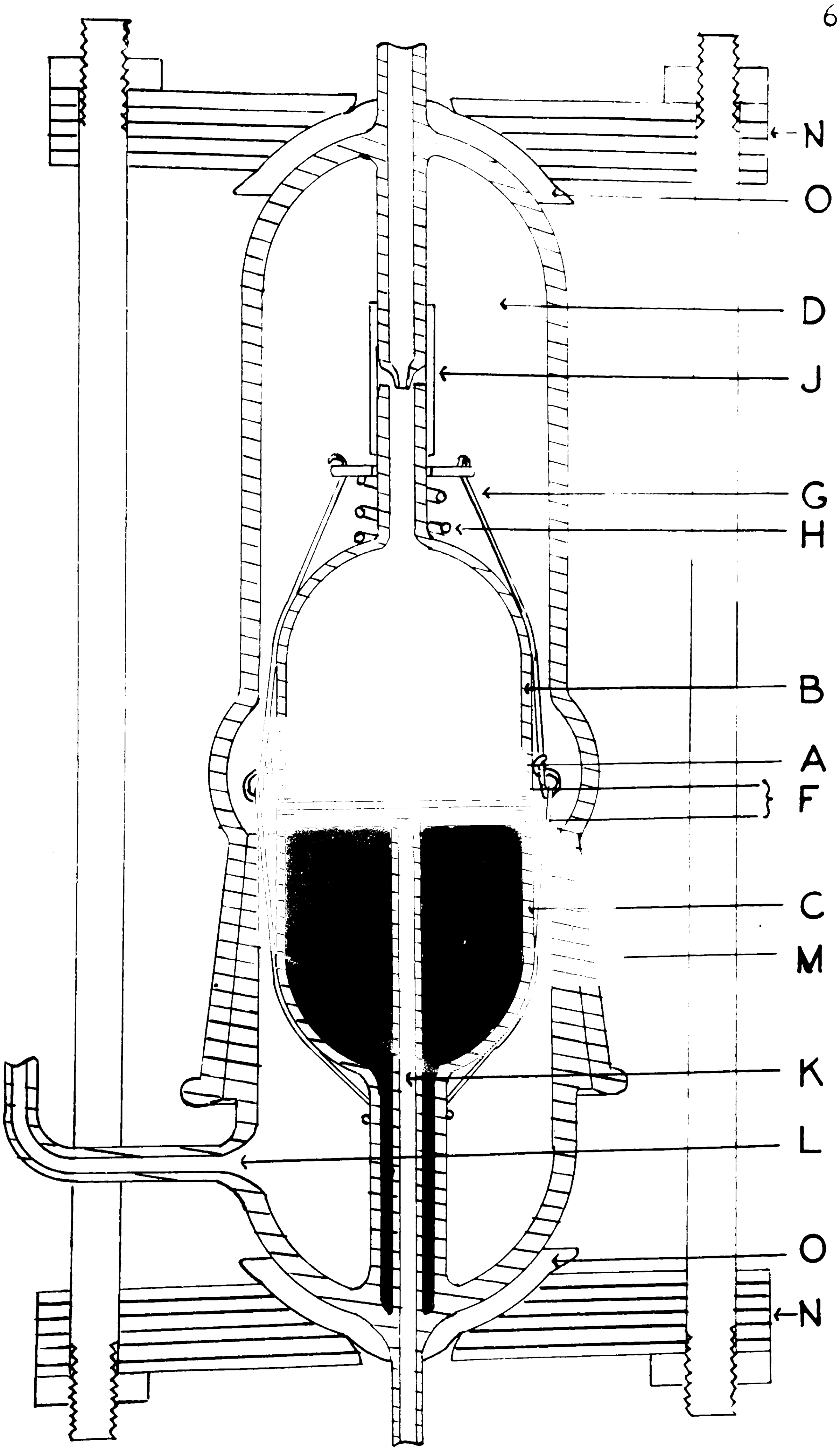

Fig. 12
Apparatus for holding Saran charcoal discs

tering into the cups B and C from compartment D, soft rubber washers F (about .75 mm. thick) are placed between the glass cups and the charcoal. Cup B is held tightly in place by steel wire stays G, which are kept taut by steel spring H. Cup B is connected to the gas outlet of the cell by means of rubber connection J. In order to keep the inlet volume of the cell to a minimum, cup C is filled with mercury and the gas inlet is through tube K. The compartment D is filled with mercury through pressure arm L. The supports N prevent the standard joint M from opening under the mercury pressure in compartment D. Thick sponge rubber O protects the glass from the strain of supports N.

It may be seen that the charcoal cells, Figs. 10, 11 and 12, not only allow for the longitudinal and radial expansion of the charcoal, but ensure that the gas flow can not by-pass the charcoal.

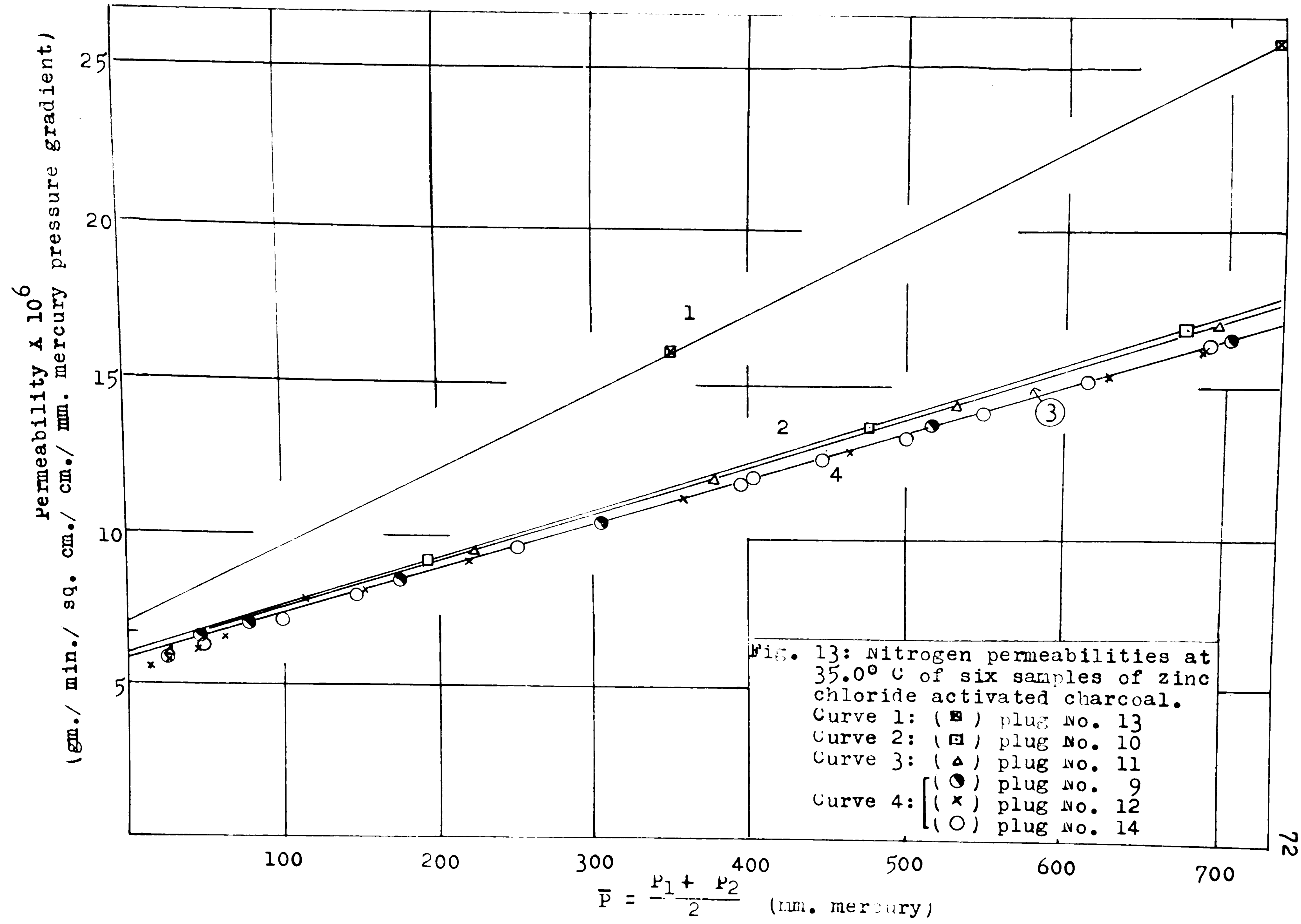

Fig. 13: Nitrogen permeabilities at 35.0° C of six samples of zinc chloride activated charcoal.

Curve 1: (☒) plug No. 13
Curve 2: (⊡) plug No. 10
Curve 3: (△) plug No. 11
Curve 4: (◐) plug No. 9
(×) plug No. 12
(○) plug No. 14

The variation in the permeability from sample to sample cannot be entirely accounted for by errors in experimental measurement. Some of this variation may, however, be ascribed to slight variations in the contact between the charcoal and the rubber gaskets which seal it to the glass flanges (see Fig. 10). Plug No. 13 was considered to have had a real fissure or hole in it, but no such defect was visible to the eye or low power lens.

The data appear to give satisfactory evidence that, with the exception of plug No. 13, the charcoal is quite uniform and therefore the experimental flow data are characteristic of the zinc chloride charcoal.

B. Mechanism of Non-Sorbable Gas[#] Flow through Zinc Chloride Charcoal

(a) Variation in flow rate with temperature and mean pressure

Flow rates of nitrogen were measured through plug No. 12[##] at the temperatures 2.5° C., 35.0° C., and 55.0° C. at various mean pressures. The experimental data obtained are represented graphically in Fig. 14 by means of the Adzumi plot (see page 17). The equations of best fit relating the flow

---

[#] The term 'non-sorbable gases' will refer to those gases only slightly adsorbad as contrasted with such gases as diethyl ether.

[##] cross sectional area 0.113 sq. cm.; length 0.99 cm.

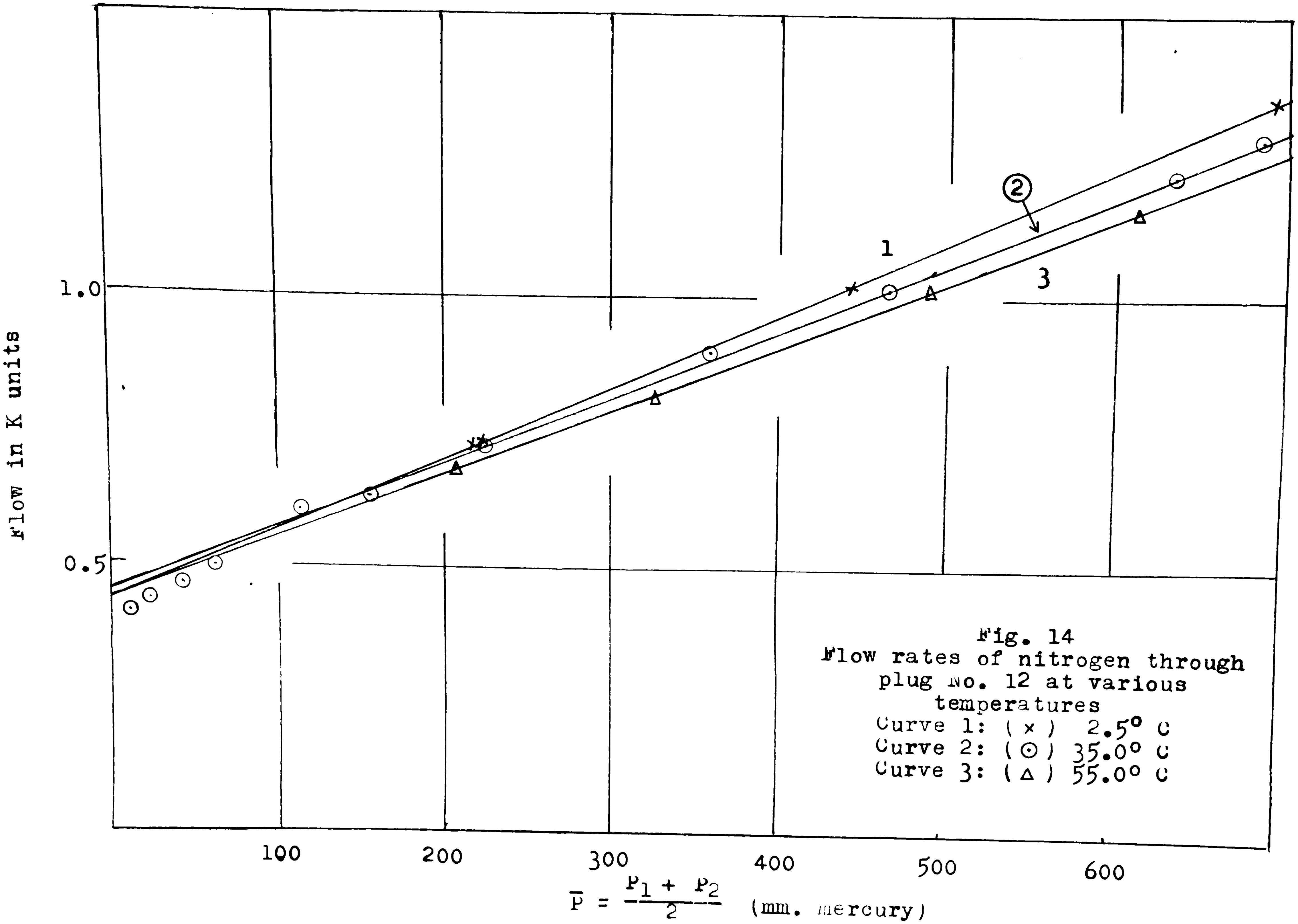

Fig. 14
Flow rates of nitrogen through plug No. 12 at various temperatures
Curve 1: (×) 2.5° C
Curve 2: (⊙) 35.0° C
Curve 3: (Δ) 55.0° C

(in the K units of Adzumi) with the mean pressure (mm. mercury) are presented in Table IV.

TABLE IV

Flow of nitrogen through plug No. 12 at various temperatures as a function of the mean pressure

Temperature	Flow in K units (experimental)	Flow in K units (calculated relative to nitrogen at 35.0°C#)
2.5°C.	$.00131\ \bar{P} + .44$	$.00131\ \bar{P} + .43$
35.0°C.	$.00121\ \bar{P} + .45$	
55.0°C.	$.00117\ \bar{P} + .45$	$.00116\ \bar{P} + .46$

Flow measured in K units $\frac{V P}{\Delta P}$, V = cc. per min.

The mean pressure $\bar{P}$ is expressed in mm. mercury

Where Adzumi type flow occurs (page 17) the slope of the flow-pressure plot should be inversely proportional to the

---

\# The viscosities of nitrogen were taken from the Chemical Rubber Handbook.

Temperature	Viscosity (poise)
2.5°C.	167.0×10^{-6}
35.0°C.	181.5×10^{-6}
55.0°C.	190.3×10^{-6}

viscosity of the gas, and the intercept of the flow - pressure plot on the flow axis should be directly proportional to the square root of the absolute temperature (see page 17). The equations of flow at 2.5°C. and 55.0°C. were calculated from the experimental equation of nitrogen flow at 35.0°C. These calculated equations are presented with the experimental equations in Table IV.

The calculated and experimental values of the slopes of the flow-pressure equations in Table IV, show a satisfactory agreement. There is no indication, however, that the experimental values of the intercepts of the flow equations are directly proportional to the square root of the absolute temperature. On the other hand the relative contribution of the intercept to the total flow rate (at the pressures where the observations were obtained) is so small that no conclusions may be drawn from the discrepancies.

It may therefore be concluded that, within the temperature range used, the flow rates are consistent with the Adzumi equation.

(b) Relative flow rates of the non-sorbable gases through zinc chloride charcoal

At 35.0°C. the flow rates of the gases nitrogen, hydrogen, helium and carbon dioxide were measured through plug No. 12 at various mean pressures. The experimental results are presented in Table V and shown graphically by means of the Adzumi plot in Fig. 15.

TABLE V

Flow rates of non-sorbable gases through plug No. 12 at 35.0° C.

Flow rate (in K units)	Mean pressure (mm. mercury)	Flow rate (in K units)	Mean pressure (mm. mercury)
Nitrogen		Carbon dioxide	
1.29	685.2	1.30	679.0
1.23	632.4	1.08	515.6
1.03	466.9	0.93	412.0
0.905	360.4	0.79	306.5
0.733	226.9	0.65	202.0
0.642	153.3	0.58	154.7
0.613	117.3	0.53	114.0
0.504	63.7	0.44	66.4
0.476	43.2		
0.440	24.0		
0.420	11.9#		
Helium		Hydrogen	
1.94	706.0	3.30	636.0
1.81	588.4	3.02	530.2
1.72	487.8	2.76	476.5
1.58	372.5	2.54	376.8
1.47	279.8	2.26	268.7
1.33	182.0	2.00	160.0
1.22	109.6	1.82	103.0
1.10	25.0	1.57	25.0

(ΔP = 50 mm. mercury except where indicated.
Flow rate measured in K units

$$\frac{V\ P}{\Delta\ P}$$

where V = cc. per min.)

\# ΔP = 23.8 mm.

Where Adzumi type flow occurs, (see page 17), the slope of the flow - pressure plot should be inversely proportional to the viscosity of the gas, and the intercept of the flow - pressure plot on the flow axis should be inversely proportional to the square root of the molecular weight of the gas. From the statistical straight line of best fit drawn through the nitrogen points (curve 5, Fig. 15), the flow rates of hydrogen, helium and carbon dioxide were calculated by means of the Adzumi equation (11) using the best available data for viscosity and molecular weight (Table VI).

TABLE VI

Viscosities and molecular weights of the non-sorbable gases

Gas	Molecular weight	Viscosity at 35.0°C. (micropoises)
Nitrogen	28.0	181.5
Hydrogen	2.02	90.3
Helium	4.0	202.5
Carbon dioxide	44.0	156.0

Viscosities taken from Chemical Rubber Handbook

In Fig. 15 the broken lines are drawn to give the best fit to the experimental data, and unbroken lines are calculated from the nitrogen curve 5 by means of the Adzumi equation. It is apparent that the straight line plot expected from the Adzumi equation when K is plotted

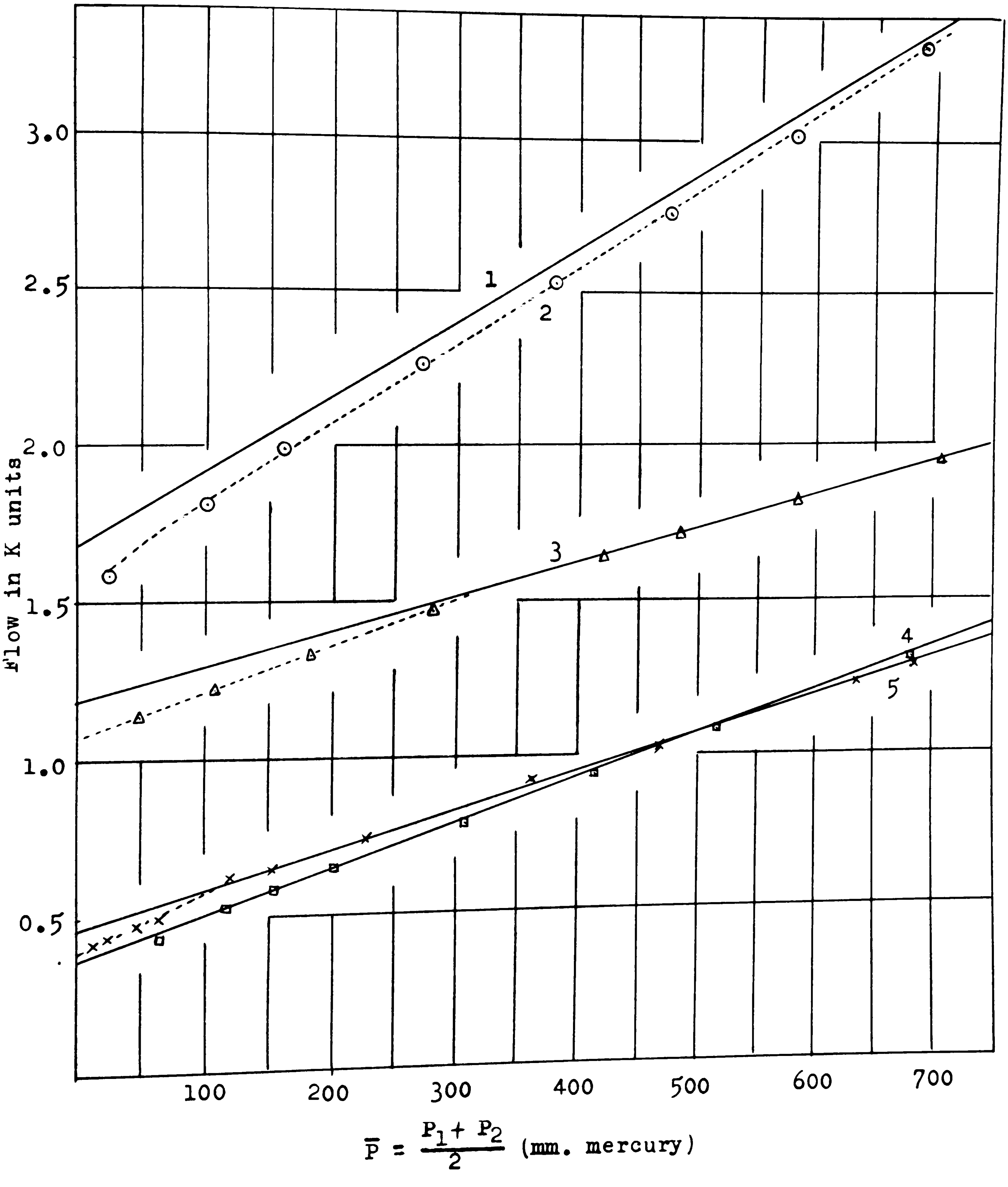

Fig. 15
Flow rates of non-sorbable gases through
plug No.12 at 35.0° C

against $\bar{P}$ does not hold exactly throughout the whole pressure range observed. In the cases of nitrogen (curve 5) and helium, (curve 3), the flow at low mean pressures is less than would be expected if it considered that the flow at higher pressures is on the straight line plot. In the case of hydrogen (curve 2) the flow is less than that predicted (curve 1) throughout the whole pressure range where flow measurements were observed, but at higher pressures the deviation is not great.

The low pressure divergence of the experimental data from the Adzumi plot has not been observed with other porous substances, and it would therefore appear likely that the phenomenon might result from either:

1) the activity of the charcoal,
2) the pore structure of the charcoal.

However, since the variation from the Adzumi straight line plot is greatest with the gases that are least adsorbed (hydrogen and helium), it is concluded that this particular phenomenon bears no relation to the sorbability of the gases. Furthermore, although little is known about the pore structure of the charcoal, the form of the Adzumi equation is such that the actual shape of the flow vs. mean pressure plot is in no way dependent on the pore structure. It would therefore appear that the low pressure deviation of the experimental flow rates from the Adzumi plot does not result from specific properties of the charcoal.

It would therefore appear desirable to consider the derivation of the Adzumi equation with reference to the present results. Various assumptions were included in the derivation of the Adzumi equation from the semi-empirical Knudsen equation (6). Only one of these assumptions however, could alter the form of the flow vs. mean pressure plot. Adzumi introduced a constant term δ to replace the pressure dependent term $\left(\frac{1 + 0.81\,{}^{5R}/\lambda}{1 + {}^{5R}/\lambda}\right)$ used by Knudsen. It may be seen however, that the Knudsen expression attains the limiting value of 1.0 at low pressures and 0.81 at high pressures (since λ varies inversely as the pressure). In other words the introduction of a pressure dependent term in the Adzumi equation (corresponding to the Knudsen expression) would cause the flow vs. mean pressure plot to curve in the opposite direction from that required by the experimental results. The low-pressure failure of the Adzumi equation does not therefore result from the assumptions required in applying the equation of flow for a single capillary to a porous system.

To describe the flow of gases through a capillary, Knudsen did not consider the kinetic energy correction# of

---

\# Where viscous flow of a gas occurs in a capillary, the gas has translational kinetic energy in addition to its thermal energy. If the flow is isothermal, the kinetic energy is gained at the expense of the potential energy (i.e. the pressure gradient). If the kinetic energy of the gas becomes significant, the gas flow rate through a system is less than would be expected from the measured pressure gradient.

of Brillouin (9). The Adzumi equation (11) which was derived from the Knudsen equation (6), has therefore, also introduced the assumption that the kinetic energy correction is negligible. It has not yet been possible to obtain a useful flow equation which would allow for the kinetic energy correction in a porous substance, but examination of the Brillouin equation for the flow through a single capillary gives an indication of what factors make the kinetic energy correction significant. The Brillouin equation was originally stated in the form:

$$P_1^2 - P_2^2 = \frac{P}{\rho g}\left(\frac{16\,\eta\,L\,G}{\pi\,R^4(1+4\zeta/R)} + \frac{2\,G^2}{\pi^2 R^4}\right) \quad \ldots\ldots \quad (\underline{28})$$

where ζ is the coefficient of "slip".

Substituting in equation (28) the Maxwell value for the coefficient of "slip" (as in equation (3)) the following relation for the flow in K units may be obtained:#

$$K = \frac{\pi\,R^4\,\bar{P}}{8\,L\,\eta} + \left(\frac{\pi}{2}\right)^{3/2}\frac{R^3}{L}\sqrt{\frac{R_0\,T}{M}}\left(\frac{2-f}{f}\right)$$

$$- G^2\left[\frac{R_0 T}{8\eta L M \Delta P} + \frac{1}{\pi^2 L R \Delta P \bar{P}}\left(\frac{\pi R_0 T}{2M}\right)^{3/2}\left(\frac{2-f}{f}\right)\right] \quad (\underline{29})$$

\# The equation obtained is not a true solution to the flow in K units, since G^2 is a flow term. When G^2 is expressed in K units, the resulting quadratic may be solved, but the equation obtained is difficult to handle. Since the terms in G^2 are considered to be relatively small, it is convenient for the purpose of the present discussion to leave the equation in the stated form.

The Brillouin equation in the form of equation (29) corresponds to the Knudsen equation (6), except that the total flow is reduced by two terms in G^2 which correct the Knudsen equation for the gas kinetic energy. Without a knowledge of the mass flow rate (G) in a single capillary of the charcoal, and a knowledge of the pore radius (R), it is difficult to state what conditions would make the terms in G^2 become significant. However, examination of the Knudsen equation in the form given on page 11 shows that in the low pressure region, the value of G is independent of the pressure (i.e. it depends primarily on the term in R^3) and therefore the second term of the kinetic energy correction in equation (29) would vary inversely as the pressure in this low pressure region. In other words the contribution of the second kinetic energy correction term would be greatest at low mean pressures. Furthermore, in this low pressure region, the value of this second kinetic energy correction term would be greatest for gases with low molecular weights (since the kinetic energy term varies inversely as the molecular weight to the three halves power and G^2 varies only as the first power of the molecular weight).

From these superficial considerations it would appear that the experimental deviation of the flow rates of the non-sorbable gases from the Aazumi plot are consistent with the deviations that would be expected if the translational kinetic energy of the gas were to become large. The magnitude of the kinetic energy correction is small however, and it appears to become negligible with all gases except those having very small molecular weights.

. . . .

In spite of the deviation observed, the foregoing experimental results indicate that the Adzumi equation adequately accounts for the pressure and temperature dependence of gas flow through charcoal, as well as the relative flow of the non-sorbable gases through charcoal. It may therefore be concluded that the non-sorbable gases pass through the zinc chloride charcoal by a mechanism that involves both viscous flow and molecular streaming (i.e. Poiseuille flow with "slip").

C. Mechanism of Sorbable Gas Flow through Zinc Chloride Charcoal

At 35.0°C. the flow rates of nitrogen, diethyl ether and ethyl chloride were measured through charcoal plug No. 14[#] at various mean pressures. The experimental results are presented in Table VII and shown graphically by means of the Adzumi plot in Fig. 16. From the Adzumi equation (11), the

---

[#] cross sectional area 0.113 sq. cm.
length 0.995 cm.

TABLE VII

Flow rates of various gases through plug No. 14 at 35.0°C.

Nitrogen

Flow rate (in K units)	Mean pressure (mm. mercury)
1.29	711.1
1.25	689.0
1.18	615.0
1.09	549.2
1.03	502.9
0.980	448.7
0.930	405.4
0.915	394.4
0.750	255.4
0.607	147.5[a]
0.543	103.0
0.475	49.9
0.427	25.0[a]

Diethyl ether

Flow rate (in K units)	Mean pressure (mm. mercury)
1.57	421.2
1.35	359.7[a]
1.23	306.6[a]
0.995	225.4[a]
0.755	134.6[a]
0.658	71.5[a]
0.645	50.0
0.630	25.0[a]
0.673	25.0[a]
0.665	12.5[b]

Ethyl chloride

Flow rate (in K units)	Mean pressure (mm. mercury)
1.91	724.0
1.80	665.0
1.78	656.1
1.62	680.5
1.63	578.4[a]
1.58	559.5
1.56	554.8
1.45	449.0
1.42	480.6
1.40	480.4[a]
1.33	446.7
1.30	432.7
1.27	405.3
1.17	355.0
1.14	340.0
1.09	325.3
1.08	308.4
1.07	305.7[a]
1.04	235.6
0.970	251.0
0.899	214.2[a]
0.866	213.0[a]
0.889	204.0
0.815	171.0
0.747	125.6
0.724	117.2[a]
0.723	114.8[a]
0.720	101.5

....

TABLE VII (Cont'd.)

Flow rates of various gases through plug No. 14 at 35.0° C.

Flow rate (in K units)	Mean pressure (mm. mercury)	Flow rate (in K units)	Mean pressure (mm. mercury)
Diethyl ether		Ethyl chloride	
......	....	0.633	58.0
....	....	0.651	58.2[a]
....	....	0.625	51.0
....	....	0.591	25.0[a]

P 100 mm. mercury except where indicated with a superscript ' a ' where P = 50 mm. mercury.

Flow rates measured in K units $\frac{V\ P}{\Delta\ P}$, where V = cc. per min.

[b] 25 mm. gradient

---

flow rates of diethyl ether and ethyl chloride were calculated from the nitrogen data using the viscosities and molecular weights shown in Table VIII. Curve 5 in Fig. 16 shows the data for nitrogen, the broken line indicating the range in which the experimental values deviate from the straight line.

In Fig. 16 the unbroken lines (curves 2 and 4) show the predicted flow rates, and the broken lines (curves 1 and 3) show the experimental flow rates of diethyl ether and ethyl chloride respectively. At low mean pressures the flow of the

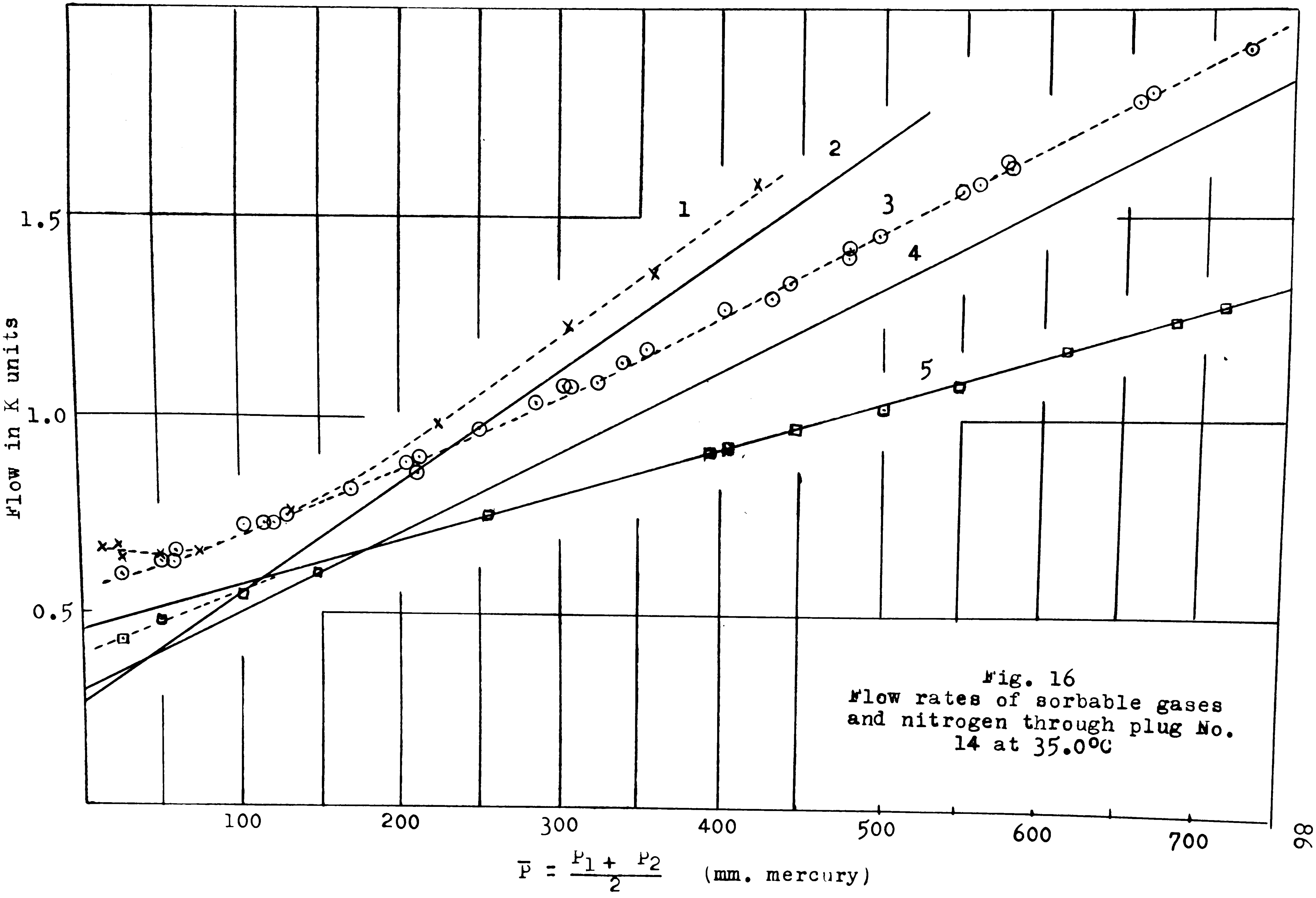

Fig. 16
Flow rates of sorbable gases and nitrogen through plug No. 14 at 35.0°C

vapours diethyl ether and ethyl chloride are approximately twice as great as the predicted flow, and in the case of the diethyl ether, the flow appears to increase as the mean pressure is reduced. At higher mean pressures the flow of ethyl chloride and diethyl ether are greater, by a small and almost constant amount, than that predicted. It is notable that if the experimental curves for the adsorbable gases are extrapolated to the flow axis, the intercepts of both the diethyl ether and the ethyl chloride are much greater than that of nitrogen. Obviously the intercepts of the highly sorbable gases are not even approximately related by the inverse square root of the molecular weight as predicted by the Adzumi equation.

TABLE VIII

Gas viscosities and molecular weights

Gas	Molecular weight	Viscosity at 35.0° C. (micropoises)
Nitrogen	28.0	181.5
Diethyl ether	74.1	77.4
Ethyl chloride	64.5	105.

Viscosities taken from Chemical Rubber Handbook.

The increased flow rate of the sorbable gases in even more surprising when it is realized that, in the process of adsorption, the amount of vapour held within the charcoal, if considered as being in the liquid phase, is sufficient to fill most of the space available for flow. For example, the charcoal is 68% voids as calculated from the helium and mercury densities (see page 47). If it is considered that the diethyl ether is in the liquid state when it is adsorbed, only 24% of the void space remains available for flow at saturation (calculated from V_m, page 44, and the liquid density). At pressures below the saturation however, a greater fraction of the void space would be available.

Because the flow of adsorbable gas at the higher pressures used is not greatly different from that predicted from the flow of a gas that is not highly adsorbed, it would seem that, in this pressure region, the mechanism of flow of the sorbable gas is essentially similar to that prevailing for the non-sorbable gases. Provided that the charcoal structure is unchanged by adsorption, it is therefore necessary to assume that the greater part of the adsorbed gas is condensed into a void region of the charcoal that does not materially contribute to the flow path. While in the high pressure region it might be considered that most of the gas is transported through the charcoal by relatively large pores, such an explanation would obviously fail to account for the very considerable increase in flow rate at the lower pressures. It is to be emphasized that most of the factors readily visualized, such as blocking of capillaries etc., should make the deviation from the predicted flow less at the lower pressures.

Since the increased flow rate is apparent only with the adsorbed gases, it would seem reasonable to conclude that this increase is the result of a surface phenomenon. If the Maxwell picture of the flow through a capillary is accepted (see page 7), the relatively high flow rates of the adsorbed gases might be considered as being due to an increase in "slip". It is reasonable to suppose that, if for some reason the density of a fluid flowing through a capillary were very much greater in the immediate neighborhood of the capillary wall, the contribution of the "slip" term would become more important than in the case of a gas whose density does not vary in this manner.

If "surface flow" or flow of adsorbed material contributes appreciably to the total flow, it is to be expected that there must be some relation between the adsorption isotherm and the surface flow. For a constant pressure difference the value of the mean pressure will determine the quantity of material adsorbed as well as the difference in the quantities adsorbed at the two ends of the charcoal rod. The isotherms of diethyl ether and ethyl chloride (Fig. 5) show that, for a constant pressure difference, the difference between the quantities adsorbed at the two ends of a charcoal rod is much more marked at low mean pressures than is the difference at high mean pressures (cf. slope of the isotherm). The marked surface concentration gradients that must exist when adsorbable gases are flowing through a charcoal rod at low mean pressures suggest that a rapid surface diffusion process would provide the most probable explanation of the experimental results. This explanation of the relative magnitude of the surface diffusion at various mean pressures is more clearly understood from the following mathematical considerations:

If the surface flow in the adsorbed layer is a diffusion process governed by Fick's law (page 28), then the contribution of surface flow at equilibrium would be given by the relation:

$$G = \theta \frac{dc}{dx}$$

where θ is a constant which depends on the shape and size of the available surface as well as the mobility of the adsorbed gas on the surface.

If the concentration at any pressure can be represented by a Freundlich equation (see page 49), then:

$$G = \frac{\theta \, d(K' P^{1/n'})}{dx} = \frac{\theta \, K'}{n'} P^{\frac{1-n'}{n'}} \frac{dP}{dx}$$

That is:

$$K = \frac{G \, R_0 \, T}{M \Delta P} = \frac{\theta \, K' R_0 \, T}{n' M \Delta P} P^{\frac{1-n'}{n'}} \frac{dP}{dx} \quad \ldots\ldots \; (\underline{30})$$

Unless the exact relation between x and P is known, the solution of equation (30) is not possible. For small pressure gradients, however, it may be assumed that, as a first order approximation, the pressure gradient is linear and hence

$$\frac{dP}{dx} = \frac{\Delta\ P}{L} \quad .$$

That is equation (30) becomes:

$$K = \frac{\theta\ K'R_0\ T}{n'\ ML}\ P^{\frac{1-n'}{n'}} \quad \ldots\ldots\ldots \quad (31)$$

Equation (31) represents the approximate contribution of the surface flow (in K units) to the total flow through an adsorbent at equilibrium conditions. For the highly sorbable gases diethyl ether and ethyl chloride, n' is greater than 1 (see page 49), so that the contribution of the surface diffusion to the total gas flow through charcoal decreases as the pressure is increased (provided that the pressure gradient is approximately linear). It may be seen from Fig. 16 that this evaluation of the contribution of the surface diffusion would qualitatively account for the difference between the experimental flow rates and those calculated by means of the Adzumi equation.

The mobility of adsorbed gases on the surface of charcoal has already been considered by other observers, but only Wicke (see page 25) has provided direct evidence of surface diffusion. From Wicke's experiments however, it was difficult to estimate the relative contribution of the surface flow, not only because of a lack of reproducibility of the results, but because the surface flow was masked by other diffusion effects. The experiments described in this research have not only provided further and independent proof of the phenomenon established by Wicke, but also allow a quantitative estimate of the surface diffusion for given experimental conditions.

D. Gas Flow through Saran Charcoal

The phenomenon of surface flow was considered of such interest that various methods of increasing the relative contribution of the surface flow to the total flow were considered. It is apparent that the larger the surface area of the charcoal, the greater would be the contribution of the surface flow. Furthermore, it is to be expected that surface flow would be more significant in a charcoal of small pore size, where the contribution of gaseous state flow would be at a minimum.

From these considerations it appeared probable that the contribution of surface flow would be greater in Saran charcoal than in the zinc chloride charcoal. Although Saran charcoal appears to have promising possibilities for demonstrating surface flow, no fundamental conclusions can be drawn from the limited data available. This section is therefore to be considered only as a supplement to the work conducted with the zinc chloride charcoal, and is offered as the basis for further research in this field.

At 35.0° C. the flow rates of nitrogen were measured through Saran charcoal plug No. 16# at various mean pressures.

#		
	Cross sectional area	0.219 sq. cm.
	Length	1.12 cm.

The experimental results are shown graphically by means of the Adzumi plot in Fig. 17 (curve 1). One measurement of the flow rate of diethyl ether was obtained at a mean pressure of 50 mm. (point 1 Fig. 17) and then a further nitrogen point was obtained at a mean pressure of 200 mm. (point 2 Fig. 17). The flow rate of diethyl ether calculated from the nitrogen data by means of the Adzumi equation (11) is represented by curve 2 Fig. 17.

It may be seen (Fig. 17) that the nitrogen flow rate was increased as a result of the exposure of the Saran charcoal to the ether, and it must be concluded that the charcoal was permanently changed or damaged as a result of this exposure. In view of the changes that occurred within the charcoal, it is difficult to draw conclusions from the relative flow rates of the nitrogen and the ether. It would appear however, that the ether flow rate is very considerably greater than could be expected on the basis of the Adzumi equation.

It is of interest to note that the nitrogen flow rate through the Saran plug No. 16 is about 1/50 the flow rate observed through the zinc chloride charcoal plug No. 14 (after allowance has been made for the dimensional differences between these two samples). This would indicate that the Saran charcoal has a smaller pore size than the zinc chloride charcoal.

At 35.0° C. the nitrogen flow rates at various mean

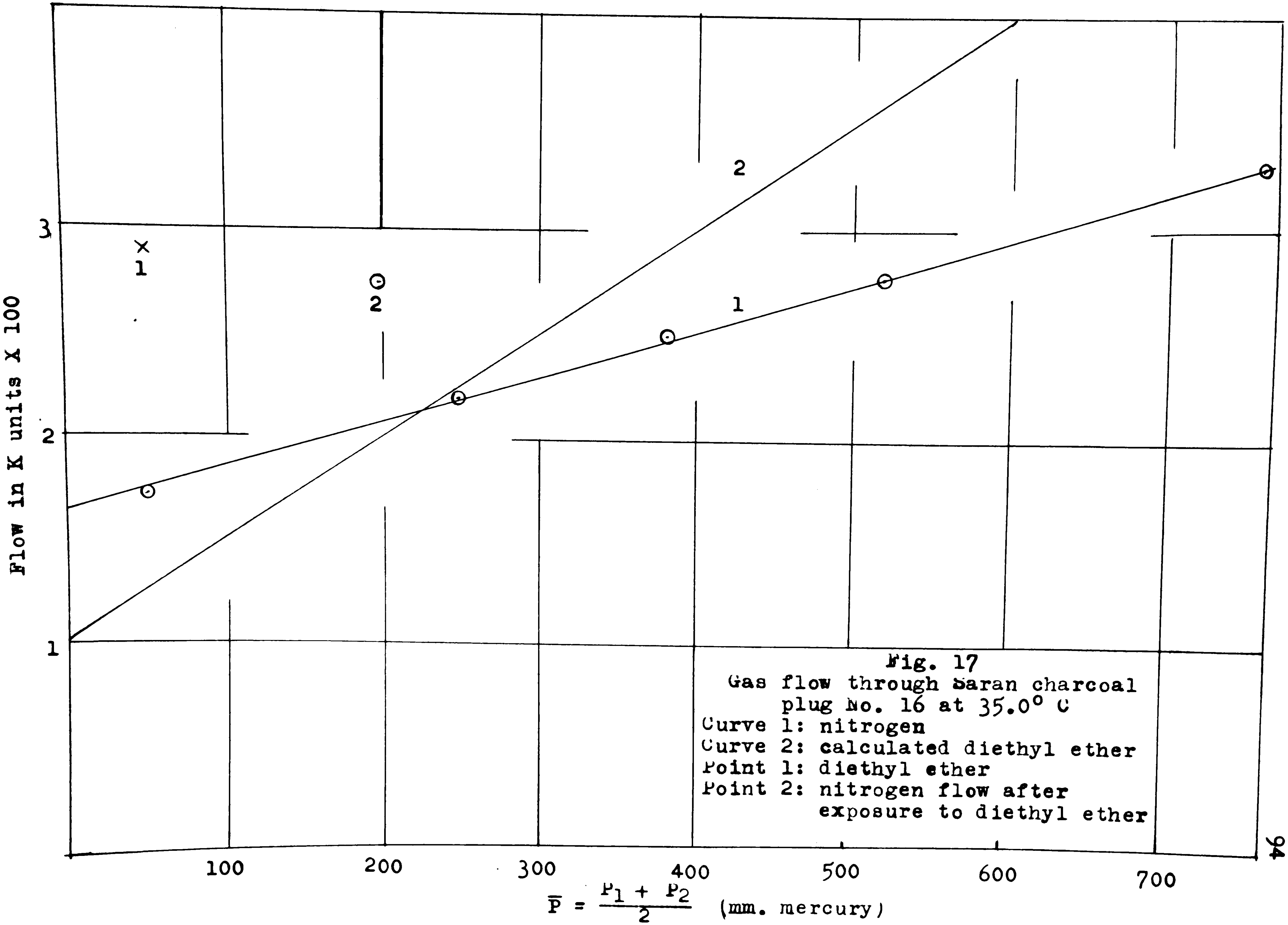

Fig. 17
Gas flow through Saran charcoal plug No. 16 at 35.0° C

Curve 1: nitrogen
Curve 2: calculated diethyl ether
Point 1: diethyl ether
Point 2: nitrogen flow after exposure to diethyl ether

pressures were measured through Saran charcoal disc No. 17#. The experimental data are shown graphically by means of the Adzumi plot in Fig. 18. In order to measure the flow of an adsorbable vapour through the charcoal disc, one face of the sample was exposed to a one centimeter pressure of diethyl ether. Within five minutes the charcoal disc shattered. Since the disc had been shown capable of withstanding much greater pressure differentials with nitrogen, it must be concluded that the stresses set up in the charcoal by the adsorption of the diethyl ether caused the Saran charcoal to fracture.

From these experiments it is indicated that great caution must be exercised in equilibrating the Saran charcoal to sorbable vapours. It may be that flow measurements through Saran charcoal are possible only for gases less highly adsorbed than diethyl ether.

E. The Non-Stationary State of Flow in Charcoal

From steady state flow data it has been concluded that gas adsorbed on charcoal, under the influence of a concentration gradient, tends to move along the surface in the direction of decreasing concentration. Analysis of the non-stationary state of flow for the highly adsorbed gases has provided an independent

---

Cross sectional area 11.0 sq. cm.
Thickness 0.135 - 0.145 cm.

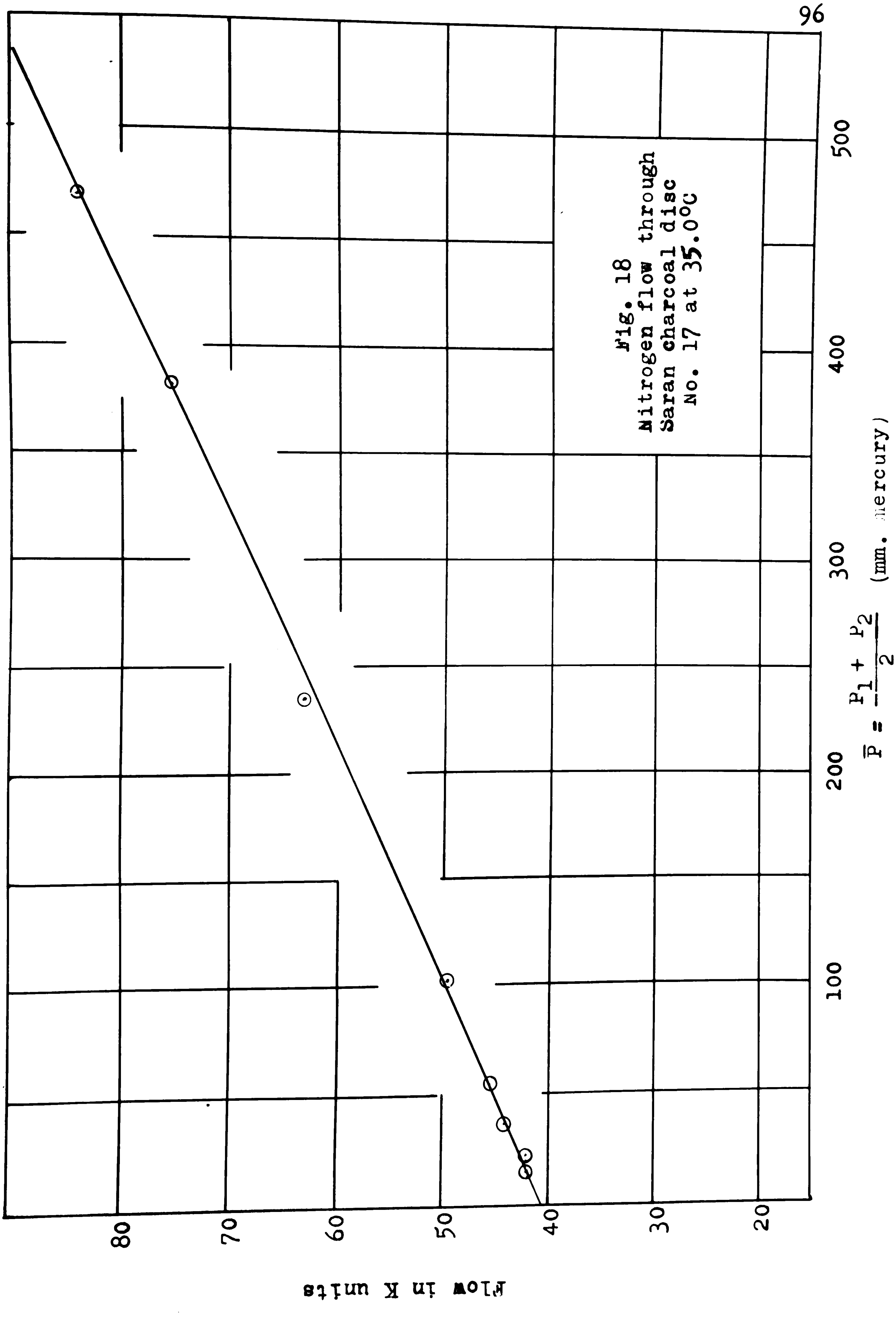

Fig. 18
Nitrogen flow through
Saran charcoal disc
No. 17 at 35.0°C

method for establishing the phenomenon of surface flow. During the course of the experimental work the possibilities of mathematical analysis of non-stationary flow were not clearly realized, and no specific attempt was made to obtain non-stationary flow data. Furthermore, the non-stationary flow equations derived can only be justified for very specialized experimental conditions. In spite of these limitations a discussion of the non-stationary state of flow has been included in this thesis not only because it provides supplementary evidence of surface diffusion, but also because, by its own merit, it contributes to the knowledge of flow phenomenon in charcoal.

Many of the equations used in this Section are original in form, but since their derivations are both lengthy and complex they have been treated separately in the Appendix "Theoretical Flow Equations".

Mathematical treatment of the non-stationary state of flow has been possible only for the conditions:

1) That there is no gas adsorbed on the charcoal at the start.
2) That the influent pressure is maintained constant and small.
3) That the effluent pressure is maintained at approximately zero.

For these conditions the following flow rate equations have been obtained (see Appendix, section A.).

$$\left(\frac{m}{t}\right)_{\substack{x=o\\ p_2=o}} = A_o(B^o + C')\left[\frac{P_1}{L} + \frac{2\,P_1}{L}\sum_{1}^{\infty} e^{-\frac{n^2\pi^2 D't}{L^2}}\right] \quad \ldots\ldots \; (51)$$

$$\left(\frac{m}{t}\right)_{\substack{x=L\\ p_2=o}} = A_o(B^o + C')\left[\frac{P_1}{L} + \frac{2\,P_1}{L}\sum_{1}^{\infty} \cos n\pi \; e^{-\frac{n^2\pi^2 D't}{L^2}}\right] \quad \ldots\ldots \; (52)$$

$$\left(\frac{m}{t}\right)_{\substack{x=o\\ p_2=o\\ L=\infty}} = \frac{A_o(B^o + C')P_1}{\sqrt{\pi\, D't}} \quad \ldots\ldots \; (53)$$

where B^o, is a constant of molecular effusion,
C' is a constant of surface mobility
and D' is a diffusion constant defined in terms of the gas permeability and adsorbability.

Equation (51) gives the isothermal flow rate of a gas into a charcoal rod of length L at any time t. If the rod is of infinite length, equation (51) reduces to equation (53). Equation (52) is the relation for the effluent flow rate from a rod of finite length L. These equations are only valid if the following conditions are fulfilled:

1) The influent pressure P_1 is sufficiently small that the contribution of viscous flow is negligible.

2) The adsorption isotherm is linear between the pressures P_1 and zero.

The mass of gas adsorbed on a charcoal rod at equilibrium flow conditions is given by the following relations (see Appendix, Section B.).

$$M' = \frac{A_o \rho_s K'L P_1^{1/n'}}{2} \qquad \ldots\ldots\ldots \quad (56)$$

$$M' = 2A_o \rho_s K'L \left[\frac{\frac{n'}{1 + 2n'} P_1^{\frac{1 + 2n'}{n'}} + \left(\frac{B^o}{A^o}\right) \frac{n'}{n' + 1} P_1^{\frac{1 + n'}{n'}}}{P_1^2 + 2 P_1 \left(\frac{B^o}{A^o}\right)} \right]$$

$$\ldots\ldots\ldots \quad (60)$$

Equation (56) was obtained from equations (51) and (52) for the influent and effluent flow rates, and is therefore limited in its application by the conditions required by the flow equations. Equation (60) is an exact relation for the mass adsorbed on a charcoal rod at equilibrium flow conditions provided that:

1) There is no contribution to the total flow from surface flow, and therefore that:
2) The amount adsorbed on the charcoal rod at any point is in equilibrium with the pressure at that point when steady state flow conditions are reached.

Both equation (56) and equation (60) are limited in accuracy by the validity of the Freundlich isotherm relation in the required pressure range[#] .

[#] If the Freundlich isotherm equation is not valid, equations (56) and (60) may be obtained in similar forms using other empirical isotherm relations.

Experimentally, conditions approximating those required by the flow equations (51), (52) and (53) were obtained in the following manner: the charcoal was evacuated for approximately two days. At t = 0, the gas burette K (Fig. 7, page 58) was filled with gas to a pressure P_1 from a gas reservoir, and the mercury seal N was closed. As soon as possible the rate of mercury rise in burette K (while maintaining constant pressure in manometer J) was recorded. At the start the flow rate was changing rapidly with time, so that measurements represented only an average flow rate over the period of the observation. This average flow rate was recorded as occurring at the mean time of the observation. The rapidly changing flow rates made it necessary to measure both small volume changes and small time intervals at the start. The accuracy at the start therefore, was not as good as at equilibrium flow conditions. The effluent end of the charcoal rod was maintained at the lowest pressure possible by means of a diffusion pump, and this effluent pressure was measured by means of a McLeod gauge. An attempt was made to correlate the McLeod gauge pressure at any given time, to the capacity of the diffusion pump at any given pressure, in order to evaluate the effluent flow rate. It is apparent however that, in a system which is continuously evacuated by means of a diffusion pump, mercury will be distilled from the McLeod gauge. This efflux of mercury vapour from the McLeod gauge prevents the influx of other vapours into the gauge until the partial pressure of the gases other than mercury approaches in magnitude the vapour pressure of the mercury at the temperature of the gauge. The effluent flow rate therefore, was not measured.

The experimental data for the non-stationary flow of diethyl ether and ethyl chloride into zinc chloride charcoal are given in Tables IX, X and XI. The experimental data from Table IX are shown graphically in Fig. 19 (curve 1). Included in Tables IX, X and XI are the theoretical flow rates based on the equations indicated in the Tables. In the case of diethyl ether at 50 mm. influent pressure, the calculated influent and effluent flow rates are represented graphically in Fig. 19 (curves 2 and 3 respectively).

Column 3 in Tables IX, X and XI gives the product of the experimental flow rates and the square root of the times at which the flow rates occurred. It was the observation of the constant flow rate - root time product that led to the entire theoretical analysis of the non-stationary flow. It may be seen from equation (53) that the flow rate - root time product should be constant as long as the charcoal behaves as though it were infinitely long (i.e. until appreciable quantities of gas are passing through the effluent end). It is to be noted that the flow rate - root time product in Tables IX, X and XI is constant for about fifty minutes, and therefore 1 cm. lengths of zinc chloride charcoal behave as rods of infinite length to the gases diethyl ether and ethyl chloride for about fifty minutes (for the conditions indicated).

TABLE IX

Non-stationary flow of diethyl ether into plug No. 14 at 35.0° C.

1	2	3	4	5	6
Time (min.)	Influent rate gm./min. $\times 10^{-4}$	Flow rate $X\sqrt{t}$ $\times 10^{-4}$	Calc.[a] influent rate $\times 10^{-4}$	Calc.[b] influent rate $\times 10^{-4}$	Calc.[c] effluent rate $\times 10^{-4}$
3	6.8	12.3	5.9	5.9	0.00
4	6.0	12.6	5.1[d]	5.1[d]	0.00[d]
7	4.4	12.2	3.9	3.9	0.00
10	3.6	12.0	3.2	3.2	0.05
14	3.4	13.4	2.7	2.7	0.18
17	3.0	13.1	2.5	2.5	0.32
23	2.6	12.9	2.2	2.2	0.53
29	2.2	12.4	1.9	1.9	0.73
36	2.0	12.6	1.7	1.71	0.91
50	1.75	13.1	1.5	1.50	1.12
77	1.49	13.8	1.2	1.36	1.26
93	1.43	14.6	1.1	1.33	1.29
660 - ∞	1.31	35.5 - ∞	0.45 - 0	1.31	1.31

Influent pressure P_1 = 50 mm. for all values of t
Effluent pressure P_2 = 0 mm. for all values of t
No gas adsorbed on charcoal at start.

a) From equation (53) (see Appendix Section A.)
b) From equation (51) (see Appendix Section A.)
c) From equation (52) (see Appendix Section A.)
Calculated in Appendix Section C.

Note. These equations assume the existence of surface flow. Since the contribution of this surface flow can not be evaluated theoretically, the calculations require a knowledge of the steady state flow for the given conditions.

TABLE X

Non-stationary flow of diethyl ether into plug No. 14 at 35.0° C.

1	2	3	4	5	6
Time (min.)	Influent rate gm./min. x 10^{-4}	Flow rate X $\sqrt{t}$ x 10^{-4}	Calc.[a] influent rate x 10^{-4}	Calc.[b] influent rate x 10^{-4}	Calc.[c] effluent rate x 10^{-4}
1.3	15.8	18	13.0	13.0	0.00
2	14.2	20	10.5	10.5	0.00
3	11.0	19	8.6	8.6	0.02
5	8.7	19	6.6	6.6	0.04
21	4.3	20	3.2	3.2	1.70
33	3.3	19	2.6	2.75	2.21
46	2.9	20	2.2	2.58	2.38
59	2.7	21	1.9	2.51	2.45
74	2.60	22	1.7	2.49	2.47
95	2.56	25	1.5	2.48	2.48
160 - ∞	2.48	31 - ∞	1.2 - 0	2.48	2.48

Influent pressure P_1 = 100 mm. for all values of t
Effluent pressure P_2 = 0 mm. for all values of t
No gas adsorbed on charcoal at start.

a) From equation (53) (see Appendix Section A.)
b) From equation (51) (see Appendix Section A.)
c) From equation (52) (see Appendix Section A.)

Note. These equations assume the existence of surface flow. Since the contribution of this surface flow can not be evaluated theoretically, the calculations require a knowledge of the steady state flow for the given conditions. Sample calculations appear in Appendix Section C.

TABLE XI

Non-stationary flow of ethyl chloride into plug No. 14 at 35.0° C.

1	2	3	4	5	6
Time (min.)	Influent rate gm./min. $\times 10^{-4}$	Flow rate $X\sqrt{t}$ rate $\times 10^{-4}$	Calc.[a] influent rate $\times 10^{-4}$	Calc.[b] influent rate $\times 10^{-4}$	Calc.[c] effluent rate $\times 10^{-4}$
2	9.5	13.5	9.2	9.2	0.00
4.5	7.7	16.3	6.1	6.1	0.02
9	6.3	15.8	4.3	4.3	0.35
11	4.9	16.2	3.9	3.9	0.56
12	4.6	15.9	3.8	3.8	0.67
21.5	3.3	15.3	2.8	2.8	1.45
25	3.2	16.0	2.7	2.7	1.63
29	2.9	15.6	2.5	2.5	1.78
33	2.7	15.5	2.3	2.4	1.88
37	2.6	15.8	2.2	2.32	1.96
44	2.4	15.9	2.0	2.24	2.04
52	2.3	16.6	1.8	2.19	2.09
73	2.25	19.2	1.5	2.15	2.13
150 - ∞	2.14	26.3 - ∞	1.1 - 0	2.14	2.14

Influent pressure P_1 = 102 mm. for all values of t.
Effluent pressure P_2 = 0 mm. for all values of t.
No gas adsorbed on charcoal at start.

a) From equation (53) (see Appendix Section A.)
b) From equation (51) (see Appendix Section A.)
c) From equation (52) (see Appendix Section A.)

Note. These equations assume the existence of surface flow. Since the contributions of this surface flow can not be evaluated theoretically, the calculations require a knowledge of the steady state flow for the given conditions. Sample calculations appear in Appendix Section C.

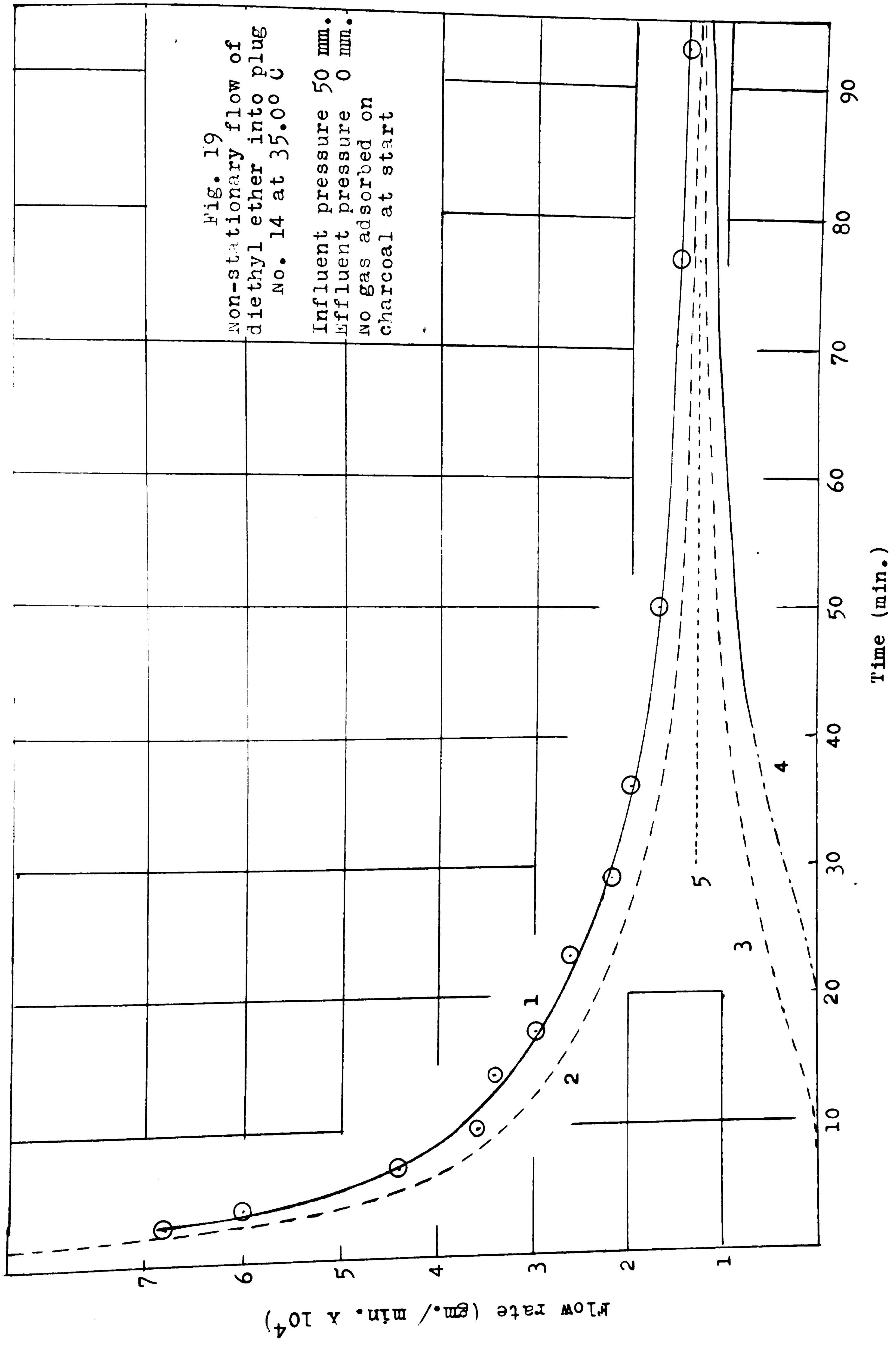

Fig. 19
Non-stationary flow of diethyl ether into plug No. 14 at 35.00° C

Influent pressure 50 mm.
Effluent pressure 0 mm.
No gas adsorbed on charcoal at start

The calculated flow rates given in Tables IX, X and XI are based on theoretical equations that are exact only if the following conditions are fulfilled:

1) The influent pressure is sufficiently small that the contribution of viscous flow is negligible.

2) The adsorption isotherm is linear between the pressures P_1 and zero.

Neither of these conditions have been exactly fulfilled in the experiments recorded in Tables IX, X and XI. The error, however, that results from a failure of the experimental conditions to conform with condition 1) is relatively small. (In Fig. 16, it may be seen that for mean pressures up to 50 mm. the contribution of the pressure dependent or viscous flow is small.) The main source of the difference between the calculated and experimental flow rates in Tables IX, X and XI would appear to be accounted for by a failure of the experimental conditions to be consistent with condition 2). Examination of the adsorption isotherms for diethyl ether and ethyl chloride (Fig. 5 page 51) show that between the limits of 0 - 50 mm. or 0 - 100 mm. the adsorption isotherms are not linear. The assumption of the linear isotherm is more nearly correct, however, between the limits of 0 - 50 mm. than 0 - 100 mm. It is notable therefore that the correlation between the theoretical and experimental flow rates is better for the influent pressure of 50 mm. (Table IX) than for the influent pressure of 100 mm.

(Table X). Examination of Fig. 5 shows that the adsorption isotherm of ethyl chloride is more nearly linear than that of diethyl ether between the pressure limits of 0 - 100 mm. It is therefore notable that the correlation between the experimental and theoretical flow rates in Table XI (columns 2 and 5 respectively) for ethyl chloride is better than the correlation in the case of diethyl ether (Table X).

From these considerations it would appear that the small deviations of the theoretical values from the experimental values are caused by the failure of the experimental conditions to conform to the boundary conditions for which the theoretical equations are valid. If the flow rates had been measured for gases showing linear adsorption isotherms, or if the gas flow rates into the charcoal had been measured at lower mean pressures, the theoretical flow rates would probably have shown even better agreement with experimental flow rates than is shown by the data represented in Tables IX, X and XI.

Unfortunately, as explained above, the effluent flow rate has not been measured. It would appear however, that the effluent flow rate may be estimated with a fair degree of certainty. The form of the influent and effluent flow rate equations ((51) and (52) respectively) are such that, after a certain time, they tend to give "mirror image" flow rate values about the line of equilibrium flow (Fig. 19 curve 5) on the flow rate vs. time plot. (i.e. the flow into the charcoal is as much greater than equilibrium flow as the effluent flow is less than the equilibrium value). The theoretical equations (51) and (52) show that "mirror image" flow rates occur after thirty minutes, for the flow of ether into charcoal at 50 mm. pressure (compare columns 5 and 6 in Table IX with the equilibrium value of 1.31×10^{-4} gm./min.). By analogy, the actual effluent flow must correspond to the experimental influent flow rate in a similar manner. If, corresponding to the experimental influent flow rate (curve 1), a "mirror image" be drawn about the line of equilibrium flow for times greater than forty minutes (curve 4), very little extrapolation is required to complete the effluent flow rate curve. This extrapolation (dotted section curve 4) has been carried out by analogy with the theoretical effluent flow rate curve 3.

In Fig. 19, the area between the influent flow rate curve 1 and the effluent flow rate curve 4 represents the mass of gas adsorbed on the charcoal rod at equilibrium flow conditions. By graphical integration methods the mass adsorbed was evaluated as:

$$M' = 0.018 \text{ gm.}$$

This value represents the experimental mass of ether adsorbed on charcoal plug No. 14 at equilibrium flow conditions, when the influent pressure is 50 mm. (The accuracy of this value is, of course, limited by the accuracy of the extrapolation in curve 4 Fig. 19).

as the flowing gas, adsorption would be continuously occurring at the influent end of the charcoal and desorption continuously occurring at the effluent end of the charcoal, even at equilibrium flow conditions. That is, at equilibrium flow, the mass adsorbed at any point along the length of the charcoal rod would not be in equilibrium with the gas pressure at each point.

From these considerations it may be seen that surface flow might account for the difference between the experimental and theoretical values of the mass adsorbed at equilibrium flow conditions. The conditions involved however, are complex, and further experimentation must be carried out before definite conclusions may be drawn.

Before an adequate analysis of the non-stationary flow may be carried out, it is necessary to measure the effluent flow rate. This could be accomplished by the method used by Clausing (page 30). It would be to further advantage to use gases showing a linear isotherm within the working pressure ranges, and to use smaller pressure gradients across the charcoal sample.

F. Properties and Structure of Charcoal from Flow Considerations

When a porous substance is composed of particles, an estimate of the pore size and surface area may be obtained from a knowledge of the size and packing of the particles. Arnell (19) has shown that for such agglomerations of particles the surface area and pore size obtained by direct measurement compare favourably with the values of these properties calculated from flow data. The solid charcoal rods, however are not agglomerations of particles in the same sense as the porous substances used by Arnell, so that there is no evidence that the Adzumi equation (11) or the Arnell equation (9) are directly applicable to the calculation of pore size and surface area of charcoal. Since however, the Adzumi equation (and hence the Arnell equation) have been found adequate for relating the flow rates of the non-sorbable gases through charcoal (page 73 - 83), it would appear reasonable to use these equations to calculate the pore size and surface area of charcoal.

Using the method of Arnell (16), it may be seen that the surface area of the charcoal may be calculated from equation (9). When K (i.e. $\frac{V' \bar{P}}{\Delta P} = \frac{VP}{\Delta P}$) is plotted against $\bar{P}$ the value of the intercept on the flow axis is given by the relation:

$$\text{Intercept} = \delta \, \frac{8}{3} \sqrt{\frac{2 R_0 T}{\pi M}} \; \frac{A_0}{L \, S_v} \; \frac{\varphi \varepsilon}{(1 - \varepsilon)} \qquad \ldots\ldots\ldots \quad (32)$$

For the flow of nitrogen through plug No. 14 at 35.0° C. (see page 83).

$M = 28.0$
$A_0 = 0.113$ sq. cm.
$L = 0.995$ cm.

Also $\varepsilon = 0.68$ (see page 48)
$\delta = 0.9$ (see page 16)
Assuming $\varphi = \varepsilon$

Whence from equation (32):

$$S_v = \frac{1.055 \times 10^4}{\text{Intercept}}$$

If the volume flow rate of the nitrogen is measured in cc. per min.

$$S_v = \frac{1.055 \times 10^4 \times 60}{\text{Intercept}}$$

The value of the intercept for the flow of nitrogen through plug No. 14 at 35.0° C . (taken from (Fig. 16 curve 5) is 0.45. Whence S_v equals 141 sq. m. per cc. of solid charcoal. That is the surface area per unit mass of charcoal equals $\frac{141}{2.22}$ equals 64 sq. m. per gm. (2.22 is the density of the solids in the zinc chloride charcoal, taken from page 39).

It is of interest to compare the surface area of the zinc chloride charcoal calculated from the nitrogen flow data (64 sq.m. per gm.) with the nitrogen surface area (page 45) calculated from nitrogen adsorption data (1100 sq. m. per gm.). In view of the assumptions involved in the calculation of either of these two surface areas however, conclusions based on their comparison are to be treated with caution.

The surface area of the Saran charcoal can not be evaluated from the Arnell equation without a knowledge of the void fraction. It is worthy of note however, that assuming a void fraction of 0.5, the surface area calculated for the Saran charcoal plug would be 2000 sq. m. per cc. of solids.

Using the method of Adzumi (11) the pore radius may be calculated for both the zinc chloride charcoal and the Saran charcoal. It may be seen from equations (11) and (12), that:

$$\frac{A}{B} = \frac{\pi\, n''\bar{r}^{\,4}}{8\, L\, \eta} \times \frac{3L}{4\, \delta\, n''\, r^3} \sqrt{\frac{M}{2\pi R_0\, T}}$$

Whence $$\bar{r} = \frac{A}{B}\; \frac{32\, \eta\, \delta}{3\, \pi} \sqrt{\frac{2\, \pi\, R_0\, T}{M}}$$

For nitrogen at 35.0° C.

$\eta = 181.5 \times 10^{-6}$ (see Table VI)
$M = 28.0$
$\delta = 0.9$ (see page 16)

Whence $$\bar{r} = 42\, \frac{A}{B}$$

If the pressure is measured in mm. mercury.

$$\bar{r} = \frac{42}{1.33 \times 10^3}\; \frac{A}{B} \qquad \ldots\ldots\ldots \quad (33)$$

For the zinc chloride charcoal, the values of the slope A and intercept B for the flow of nitrogen through plug No. 14 may be taken from Fig. 16 (curve 5).

That is: $$\bar{r} = \frac{42 \times 0.00120}{1.33 \times 10^3 \times 0.45} = 8.4 \times 10^{-5} \text{ cm.}$$

For the Saran charcoal rod, the values of A and B for the solution of equation (33) may be taken from Fig. 17 curve 1.

$$\bar{r} = \frac{42 \times 0.0000214}{1.33 \times 10^3 \times 0.0165} = 4.1 \times 10^{-5} \text{ cm.}$$

The pore radius in the Saran charcoal disc may be evaluated by substitution of the values of A and B obtained from Fig. 18 in equation (<u>33</u>)

$$\bar{r} = \frac{42 \times 0.0816}{1.33 \times 10^3 \times 41} = 6.3 \times 10^{-5} \text{ cm.}$$

From these calculations it is indicated that the pore radius of either the Saran charcoal or the zinc chloride charcoal is of the order of 10^{-5} cm. Although this value is considerably larger than the pore size usually attributed to activated charcoals, it is to be emphasized that a value of the pore radius, calculated from flow measurements, would tend to favour the large pores in the event that there was a distribution in the pore size. This is clearly realized when it is considered that capillary flow occurs according to the third and fourth power of the capillary radius. (see equation (<u>11</u>)).

On page 87 it was pointed out that a considerable portion of the space available for flow could be filled with adsorbable material without restricting the rate of flow. To explain this it was necessary to consider that the adsorption occurred in a region within the charcoal, where it did not block the flow path. In view of the uniformity of the charcoal (see page 72) and the calculated value of the pore size (10^{-5} cm.), it would appear reasonable to exclude the possibility of material faults in the zinc chloride charcoal. It is therefore necessary to consider that the gas flow through charcoal occurs in a continuous macropore system, whereas the adsorption occurs elsewhere within the charcoal. This conclusion supports the essential points of Wicke's theory on the structure of charcoal (see page 23), but in itself is not sufficient evidence to establish Wicke's concept of the "ball-like particles". It is apparent that any theory for the structure of charcoal, that included both a continuous and independent macropore system and a micropore system, would be consistent with the present data.

It is difficult to state from the information available whether or not the macropore system is essential to the structure of charcoal. This problem can be answered only after further research, and it appears that a study of Saran charcoal would provide the most fruitful approach.

SUMMARY AND CONCLUSIONS

An apparatus has been devised and constructed for measuring the flow rates of gases and vapours through solid charcoal. This apparatus is capable of measuring the gas flow rates into a charcoal sample while maintaining constant pressure conditions throughout the system.

Various cells have been devised for holding the charcoal specimens. These holders make allowance for the small volume changes that the charcoal undergoes during adsorption and desorption, while at the same time they ensure that no gas can by-pass the charcoal.

Gas flow rates have been measured through two types of charcoal:

1) A commercial zinc chloride activated charcoal.
2) A charcoal obtained from Saran plastic.

The results obtained indicate that the zinc chloride charcoal is highly uniform, and that the flow data are characteristic of its structure. In order to interpret the flow data for the zinc chloride charcoal, the following properties have been measured:

1) The adsorption isotherms at 35.0° C. for the gases diethyl ether and ethyl chloride.
2) The nitrogen surface area.

3) The charcoal density to displaced helium.
4) The charcoal density to displaced mercury.

In an effort to obtain a charcoal even more uniform than the zinc chloride charcoal, the potentialities of a new type of charcoal prepared from Saran plastic have been investigated. It has been found that charcoal may be prepared from Saran in any size and shape, and this Saran charcoal has a pore size smaller than that of the zinc chloride charcoal. It is indicated that further work might be carried out to advantage with the Saran charcoal.

It has been shown that the Adzumi type equation adequately accounts for the relative flow rates, as well as the variation in flow rate with temperature and pressure, of the non-sorbable gases. It is therefore concluded that both molecular streaming and viscous flow contribute to the total flow of non-sorbable gases through zinc chloride charcoal (i.e. Poiseuille flow with "slip"). The permanent gases, however, show small deviations from the Adzumi type flow particularly at low pressures. It has been shown that these small deviations may be accounted for in a qualitative manner, if a kinetic energy correction term is introduced into the Adzumi type equation.

Non-stationary flow equations have been derived which adequately account for the time-dependent flow of the sorbable gases into the zinc chloride charcoal under the following conditions:

1) That no gas is adsorbed on the charcoal at start.
2) That the influent pressure is small and constant.
3) That the effluent pressure is approximately zero.

Equations for calculating the mass of gas adsorbed on charcoal at equilibrium flow conditions have also been deduced. The values calculated with these equations do not accurately check with experimental values, but the deviations are considered reasonable when the assumptions involved in the theoretical equations are considered. The only assumption involved in one of these equations is that surface flow does not contribute to the total flow, and therefore the failure of this equation indicates that surface flow may exist. These theories are not substantiated with sufficient experimental evidence, and therefore further work must be conducted before definite conclusions can be drawn.

The pore size and surface area of the charcoals have been calculated from flow data. The surface area calculated from flow data is only about 1/17 the value obtained from adsorption data. The pore size (10^{-5} cm.) calculated from the flow data is larger than the value that might be expected for an activated charcoal, but it is sufficiently small that the pores can not be considered as faults or cracks in the usual sense.

The flow rates of the sorbable gases at high pressures indicate that the flow paths are in no way blocked by the adsorbed gases. In view of the uniformity of the charcoal and the small calculated pore size, it is necessary to consider that the adsorption occurs in a micropore system, whereas the gas flow occurs in an independent and continuous macropore system.

At low pressures, the flow rates of the sorbable gases are about twice as large as would be expected from the normal application of Kinetic Theory to flow through porous diaphragms. From normal considerations it would be expected that, at low pressures (where the contribution of viscous flow is small), the flow rates of gases through a porous diaphragm would be related by the inverse square roots of their molecular weights. The experimental results show that the flow rates of the highly adsorbed gases through zinc chloride charcoal are not related in this manner. For example, the flow rate of diethyl ether (M.W. 74) is greater than the flow rate of nitrogen (M.W. 28) in this low pressure region. To explain the experimental results it has been necessary to consider that surface flow of the adsorbed gases contribute to the total apparent flow, and in a qualitative manner it has been shown that such a concept would explain the data obtained.

CLAIMS TO ORIGINAL RESEARCH

1. Original methods have been developed by which it is possible to measure accurately the flow rates of gases through solid charcoal.

2. It has been established that the zinc chloride activated charcoal used in this research is highly uniform. Consequently, the experimental flow data are not only characteristic of the individual samples, but are also characteristic of the structure of this type of charcoal.

3. A new and highly uniform charcoal has been prepared from Saran plastic.

4. It has been shown for the first time that, in the pressure ranges investigated, both viscous flow and molecular streaming contribute to the gas flow through zinc chloride activated charcoal.

5. A gas flow phenomenon, not observed in other porous systems, has been shown to exist in zinc chloride activated charcoal. This phenomenon does not appear to result from either the structure or activity of the charcoal. It is suggested that the gas translational kinetic energy which is usually considered negligible, does influence the gas flow rates through charcoal.

6. Equations for the non-stationary state of flow have been derived which quantitatively account for the time dependent flow rates of the highly sorbable gases into zinc chloride charcoal.

7. New methods, both theoretical and experimental, have been used for estimating the quantity of gas adsorbed on a charcoal rod at equilibrium flow conditions.

8. The pore size and surface area of the zinc chloride activated charcoal have been calculated by means of established flow equations. The values obtained are the first estimates of pore size and surface area of any charcoal ever obtained from flow data.

9. The experimental data are consistent with the theory that a continuous macropore system occurs within charcoal. This macropore system has been found to be independent of the system in which adsorption occurs.

10. New methods for establishing the existence of surface diffusion have been developed. For the first time a quantitative estimate of the surface flow on charcoal for given conditions has been obtained experimentally.

APPENDIX

Theoretical Flow Equations

A. Derivation of Non-Stationary Flow Equations

Observation of the steady state flow of nitrogen, helium, hydrogen and carbon dioxide through charcoal have established the validity of the Adzumi, Arnell, or similar types of equations for estimating relative flow rates through charcoal. That is the gas flow through charcoal may be represented by the Arnell equation (9)

$$V' = A_o \left[\frac{1}{5 \eta S_V^2} \frac{\varepsilon^3}{(1-\varepsilon)^2} + \frac{8}{3}\sqrt{\frac{2 R_o T}{\pi M}} \frac{\delta}{\bar{P} S_v} \frac{\varphi \varepsilon}{(1-\varepsilon)} \right] \frac{\Delta P}{L}$$

whence $\frac{m}{t} = V' \quad g =$

$$A_o \left[\frac{1}{5 \eta S_V^2} \frac{\varepsilon^3}{(1-\varepsilon)^2} \frac{\bar{P} M}{R_o T} + \frac{8}{3}\sqrt{\frac{2 M}{\pi R_o T}} \frac{\delta}{S_V} \frac{\varphi \varepsilon}{(1-\varepsilon)} \right] \frac{\Delta P}{L}$$

where $\frac{m}{t}$ is the mass flow per unit time

and ρ_g is the gas density. At the pressure $\bar{P}$,

$$\rho_g = \frac{\bar{P} M}{R_o T}$$

That is:

$$\frac{m}{t} = A_o \left(A^o \bar{P} + B^o \right) \frac{\Delta P}{L} \qquad \ldots\ldots \quad (34)$$

where
$$A^{o} = \frac{M}{5\, R_o\, T\, \eta\, S_v^{2}} \cdot \frac{\varepsilon^{3}}{(1 - \varepsilon)^{2}}$$

$$B^{o} = \frac{8}{3} \sqrt{\frac{2\, M}{\pi\, R_o\, T}}\; \frac{\delta}{S_v}\; \frac{\varphi\, \varepsilon}{(1 - \varepsilon)}$$

Equation (34) may be expressed in the differential form:

$$\frac{m}{t} = - A_o \, (A^{o} P + B^{o}) \, \frac{dP}{dx} \qquad \ldots\ldots\ldots \qquad (35)$$

where x is the distance into the charcoal rod.

The equation (35) has considered only the contribution of the gas flow through the charcoal pores. If in addition to the gas flow there is a surface flow of an adsorbed phase, then the steady state flow equation (35) may be represented in the form:

$$\frac{m}{t} = - A_o \, (A^{o} P + B^{o}) \, \frac{dP}{dx} - A_o \, C'' \, \frac{d(x/m)}{dx} \qquad \ldots\ldots \qquad (36)$$

where (x/m) is the concentration of the adsorbed material in grams of gas per gram of charcoal,

and C'' is a constant depending on the kinetics of surface flow.

The value of (x/m) is usually dependent on the pressure in some non linear form. The Freundlich relation is one of the simplest relations between the mass adsorbed on unit mass of charcoal and the pressure.

That is:

$$(x/m) = K' p^{1/n'}$$

where K' and n' are constants.

The introduction of a Freundlich function for (x/m) into equation (36) leads to a differential equation for which a solution has not been found possible. If however, within the experimental limits of pressure, (x/m) is a linear function of the pressure. That is:

$$(x/m) = K'' P$$

equation (36) becomes:

$$\frac{m}{t} = - A_o \left(A^o P + B^o + C' \right) \frac{dP}{dx} \qquad \cdots\cdots\cdots \quad (\underline{37})$$

where $C' = K'' C''$

If equation (37) represents the mass flow rate at equilibrium, then the mass stored per unit time in an element of area A_o and thickness dx is given by the equation:

$$d\left(\frac{m}{t}\right) = A_o \left[A^o \left[P \frac{d^2P}{dx^2} + \left(\frac{dP}{dx}\right)^2 \right] + (B^o + C') \frac{d^2P}{dx^2} \right] dx \qquad \cdots\cdots\cdots \quad (\underline{38})$$

But the mass dm of a charcoal element of area A_o and thickness dx is given in the relation:

$$dm = A_o \, dx \, \rho_s$$

where ρ_s is the bulk density of the charcoal (mercury density).

$$(x/m) = K' \, p^{1/n'}$$

where K' and n' are constants.

The introduction of a Freundlich function for (x/m) into equation (36) leads to a differential equation for which a solution has not been found possible. If however, within the experimental limits of pressure, (x/m) is a linear function of the pressure. That is:

$$(x/m) = K'' P$$

equation (36) becomes:

$$\frac{m}{t} = - A_o \, (A^o P + B^o + C') \, \frac{dP}{dx} \qquad \ldots\ldots\ldots \quad (37)$$

where $C' = K'' \, C''$

If equation (37) represents the mass flow rate at equilibrium, then the mass stored per unit time in an element of area A_o and thickness dx is given by the equation:

$$d\left(\frac{m}{t}\right) = A_o \left[A^o \left[P \frac{d^2P}{dx^2} + \left(\frac{dP}{dx}\right)^2 \right] + (B^o + C') \frac{d^2P}{dx^2} \right] dx \qquad \ldots\ldots\ldots \quad (38)$$

But the mass dm of a charcoal element of area A_o and thickness dx is given in the relation:

$$dm = A_o \, dx \, \rho_s$$

where ρ_s is the bulk density of the charcoal (mercury density).

Also if Q is the mass adsorbed on unit mass of the charcoal for unit increase in pressure, then:

$$d\left(\frac{m}{t}\right) = A_o\, dx\, \rho_s \quad Q \quad \frac{dP}{dt} \qquad \cdots\cdots\cdots \quad (\underline{39})$$

Equating equations ($\underline{38}$) and ($\underline{39}$)

$$A_o dx \rho_s Q \frac{\partial P}{\partial t} = A_o \left[A^o \left[P \frac{\partial^2 P}{\partial x^2} + \left(\frac{\partial P}{\partial x} \right)^2 \right] + (B^o + C') \frac{\partial^2 P}{\partial x^2} \right] dx$$

Whence

$$\frac{\partial P}{\partial t} = \frac{A^o}{\rho_s Q} \left[P \frac{\partial^2 P}{\partial x^2} + \left(\frac{\partial P}{\partial x} \right)^2 \right] + \frac{(B^o + C')}{\rho_s Q} \frac{\partial^2 P}{\partial x^2}$$

$$\cdots\cdots\cdots \quad (\underline{40})$$

Equation ($\underline{40}$) represents, in the general differential form, the relation between the pressure P, at any point x, at any time t. The general solution of equation ($\underline{40}$) has not been established, but it is possible to obtain solutions for particular experimental conditions. It may be seen that when the pressure is low, equation ($\underline{37}$) reduces to the form:

$$\frac{m}{t} = - A_o(B^o + C')\frac{dP}{dx} \qquad \cdots\cdots\cdots\cdots \quad (\underline{41})$$

Thus if terms arising from A^o are neglected, equation ($\underline{40}$) becomes:

$$\frac{\partial P}{\partial t} = \frac{(B^o + C')}{\rho_s Q} \frac{\partial^2 P}{\partial x^2} = D' \frac{\partial^2 P}{\partial x^2} \qquad \cdots\cdots \quad (\underline{42})$$

Where:

$$D' = \frac{(B^o + C')}{\rho_s Q} \qquad \ldots\ldots\ldots \quad (\underline{43})$$

Equation ($\underline{43}$) defines a diffusion constant D' in terms of the adsorptive capacity, permeability and density of the charcoal.# By dimensional analysis it may be seen that D' has the units $\text{cm.}^2 \times \text{min.}^1$ when

B^o gm./min./cm.^{2}/cm./mm. mercury pressure

C' gm./min./cm.^{2}/cm./mm. mercury pressure

ρ_s gm./cm.^{3}

Q gm./gm./mm. mercury pressure.

An entirely theoretical evaluation of the diffusion constant D' from equation ($\underline{43}$) is not possible until the

---

The diffusion constant D' is analogous to the "diffusivity constant" used in heat flow equations. The "diffusivity constant" is defined in terms of the heat capacity, heat conductivity and density of the material. Barrer ($\underline{53}$) has also defined a diffusion constant in terms of the solubility and permeability of a gas in a solid. Barrer has shown that

$$D = \frac{P'_o L}{S \Delta P}$$

where D is the diffusion constant in $\text{cm.}^2 \text{ x}_2\text{sec.}^{-1}$,
P is the permeability in cc./sec./cm.^{2}/mm./atm. pressure,
S is the solubility in cc./cc./atm. pressure
and $\Delta P/L$ is the pressure gradient in mm. mercury/cm.

kinetics of surface diffusion are established. If however, the steady state permeability of the gas is known (that is B^o and C' in equation (<u>43</u>)), the value of the diffusion constant may be evaluated (see this Appendix, Section <u>C</u>.)

Equation (<u>42</u>) is similar in mathematical form to the Damköhler equation (<u>16</u>) (see page 21), except that equation (<u>42</u>) uses pressure where the Damkhöler equation uses concentration. Damköhler, however, only considers the diffusion into a single pore, whereas equation (<u>42</u>) represents the flow into a porous system. The Damköhler diffusion constant has moreover, neglected the fact that during the approach to equilibrium adsorption, considerable quantities of the gas diffusing into the capillary are adsorbed and thereby permanently removed from the gas phase system. It is only when adsorption equilibrium is reached that the number of molecules striking the surface of the pore is equal to the number leaving the wall of the pore. The Damköhler diffusion constant D_g (see page 21) has therefore no theoretical significance until equilibrium adsorption is reached.

To obtain equation (<u>42</u>), the following assumptions were made:

1) The flow occurring in the gaseous state may be represented by an Arnell type equation.
2) The rate of surface diffusion is proportional to the concentration gradient.

3) The adsorption isotherm is linear within the experimental pressure limits.

4) The contribution of viscous flow may be neglected (terms arising from A^o).

The validity of assumption (1) has been established in this thesis (provided that the structure of the charcoal is not materially changed by the sorbable gases). Although the mechanism of surface diffusion has not been determined, the concept introduced by assumption (2) should receive general recognition. Since adsorption isotherms are generally non-linear, an error is introduced by assumption (3). If however, the pressure limits applied to the solution of equation (42) are small, the error caused by assumption (3) should also be small. The extent of the contribution of viscous flow at any pressure may be estimated from the flow-pressure plot. For example, in Fig. 16, the relative contribution of viscous flow at any pressure may be evaluated by subtracting the value of the intercept from the total flow at that pressure. It may be seen that if the pressure is sufficiently small, the error introduced by assumption (4) becomes negligible.

Experimentally it is possible to approach the conditions which would allow the application of equation (42). Agreement between experiment and equation (42) should occur for the following boundary conditions.

$P = P_1$ is small at $x = 0$ for all t

$P = P_2 = 0$ at $x = L$ for all t

$P = 0$ at $x > 0$ at $t = 0$

Where the flow occurs into a rod of finite length L.

The solution to equation (42) for these boundary conditions may be obtained thus:

Let $$P = X \cdot T$$

where $X = f\ (x)$ and $T = f_{\prime}\ (t)$

then $$X \frac{dT}{dt} = T\, D' \frac{d^2X}{dx^2}$$

That is $$\frac{d^2X}{dx^2} + \alpha^2 X = 0 \quad \text{and} \quad \frac{dT}{dt} = -\alpha^2 D'\, T$$

Whence $$X = Y' \sin \alpha x + Z' \cos \alpha x, \quad \text{and} \quad T = Fe^{-\alpha^2 D' t}$$

Therefore $$P = (Y \sin \alpha x + Z \cos \alpha x)\, e^{-\alpha^2 D' t} \qquad \ldots\ldots (44)$$

Equation (44) is a solution to the differential equation (42), but the sum of any number of solutions is also a solution, and therefore a more general form of equation (44) is:

$$P = \sum_{0}^{\infty} (Y_\alpha \sin \alpha x + Z_\alpha \cos \alpha x)\, e^{-\alpha^2 D' t} \qquad \ldots (45)$$

But $P = P_1$ when $x = 0$ and $t = 0$

In order that the summation of equation (46) equal zero at $x = 0$ and $t = 0$, the coefficients of $\cos \alpha x$ must also equal zero. Equation (46) therefore becomes:

$$P = P_1 - \frac{P_1 x}{L} + \sum_{1}^{\infty} (Y_\alpha \sin \alpha x)\, e^{-\alpha^2 D' t} \quad \ldots\ldots \quad (47)$$

But $P = 0$ at $x = L$ for all t.

Therefore $\sin \alpha L = 0$ or $\alpha L = n\pi$

Whence

$$P = P_1 - \frac{P_1 x}{L} + \sum_{1}^{\infty} \left(Y_\alpha \sin \frac{n\pi x}{L}\right) e^{-\frac{n^2 \pi^2 D' t}{L^2}}$$

Y_α are the Fourier coefficients, and may be evaluated by the general equation:

$$Y_\alpha = \frac{2}{L} \int_0^L \left[f(x') - \left(P_1 - \frac{P_1 x'}{L}\right)\right] \sin \frac{n\pi x'}{L}\, dx'$$

so that

$$P = P_1 - \frac{P_1 x}{L} - \frac{2}{\pi} \sum_{1}^{\infty} \frac{P_1}{n} \sin \frac{n\pi x}{L}\, e^{-\frac{n^2 \pi^2 D' t}{L^2}}$$

$$+ \frac{2}{L} \sum_{1}^{\infty} \sin \frac{n\pi x}{L}\, e^{-\frac{n^2 \pi^2 D' t}{L^2}} \int_0^L f(x') \sin \frac{n\pi x'}{L}\, dx'$$

But at $t = 0$, $P = 0$ at $x > 0$ therefore:

$$P = P_1 - \frac{P_1 x}{L} - \frac{2}{\pi} \sum_{1}^{\infty} \frac{P_1}{n} \sin \frac{n\pi x}{L} e^{-\frac{n^2 \pi^2 D' t}{L^2}} \quad \ldots\ldots \quad (\underline{48})$$

Differentiating the equation (48) with respect to x, the value of the pressure gradient is obtained for any time t and at any distance x along the length of the rod.

$$\frac{dP}{dx} = -\frac{P_1}{L} - \frac{2\,P_1}{L} \sum_{1}^{\infty} \cos \frac{n\pi x}{L} e^{-\frac{n^2 \pi^2 D' t}{L^2}} \quad \ldots\ldots \quad (\underline{49})$$

But the steady state flow is given by the equation (41) assuming a linear isotherm and that the contribution of viscous flow is negligible. That is:

$$\frac{m}{t} = -A_o(B^o + C')\frac{dP}{dx} \quad \ldots\ldots \quad (\underline{41})$$

Substituting the value of the pressure gradient from equation (49) in equation (41)

$$\left(\frac{m}{t}\right)_{P_2=o} = A_o(B^o + C')\left[\frac{P_1}{L} + \frac{2P_1}{L} \sum_{1}^{\infty} \cos \frac{n\pi x}{L} e^{-\frac{n^2 \pi^2 D' t}{L^2}}\right]$$

$$\ldots\ldots \quad (\underline{50})$$

The flow into the charcoal at $x = 0$ is then given by:

$$\left(\frac{m}{t}\right)_{\substack{x=o \\ P_2=o}} = A_o(B^o + C')\left[\frac{P_1}{L} + \frac{2P_1}{L} \sum_{1}^{\infty} e^{-\frac{n^2 \pi^2 D' t}{L^2}}\right] \quad \ldots\ldots \quad (\underline{51})$$

Also from equation (50) by putting $x = L$ the equation for the effluent flow is obtained.

$$\left(\frac{m}{t}\right)_{\substack{x=L\\ p_2=o}} = A_o(B^o + C')\left[\frac{P_1}{L} + \frac{2P_1}{L}\sum_{1}^{\infty} \cos n\pi \, e^{-\frac{n^2\pi^2 D't}{L^2}}\right] \quad .... \; (52)$$

From equation (51) it is possible to obtain the flow rate into a rod of infinite length:

$$\left(\frac{m}{t}\right)_{\substack{x=o\\ p_2=o\\ L=\infty}} = A_o(B^o + C')\,\frac{2\,P_1}{L}\int_o^{\infty} e^{-\frac{n^2\pi^2 D't}{L^2}}\,dn = \frac{A_o(B^o + C')\,P_1}{\sqrt{\pi\ D't}}$$

$$..... \; (53)$$

Equation (51) therefore gives the isothermal flow rate of an adsorbable gas into a charcoal rod of length L at any time t. Equation (51) is only valid if P_1 is small and the adsorption isotherm is linear between the pressures P_1 and 0. Equation (52) gives the effluent flow rate for the same conditions as equation (51). Equation (53) is equivalent to equation (51) as long as the charcoal rod behaves as though it were infinitely long. The charcoal rod is considered to behave as though it were infinitely long until appreciable quantities of gas flowing out of the low pressure end.

Equation (52) is comparable to the equation used by Clausing for the effluent flow from a single capillary (see page 32). Equation (53) is mathematically similar to that used by Tiselius for the gas flow into zeolites (see page 29). The equation used by Tiselius reduces to the form of equation (53) when the flow is considered only at the influent end.

B. The Mass Adsorbed on a Charcoal Rod when the Flow Rate has reached Equilibrium

If there is no gas adsorbed on the charcoal at the start, the mass adsorbed at equilibrium flow rate may be evaluated experimentally by a graphical integration method. When the influent and effluent flow rates are plotted against time, the area between the curves so formed represents the total mass adsorbed. The value obtained in this manner will be called the experimental mass adsorbed on the charcoal rod.

Theoretically the mass adsorbed on the charcoal rod may be obtained from equations (51) and (52). It may be seen that the mass adsorbed must equal the difference between the influent and effluent flow rates integrated between the limits of $t = 0$ and $t = \infty$. This method corresponds to the experimental method for obtaining the mass adsorbed.

From equations (51) and (52) the mass adsorbed is therefore given by the relation:

$$M' = A_o(B^o + C')\frac{2\,P_1}{L}\left[\sum_{n=1}^{\infty}\int_{t=o}^{\infty} e^{-\frac{n^2\pi^2 D't}{L^2}}\,dt - \sum_{n=1}^{\infty}\cos n\pi \int_{t=o}^{\infty} e^{-\frac{n^2\pi^2 D't}{L^2}}\,dt\right]$$

where M' is the total mass adsorbed at equilibrium.

That is:

$$M' = A_o (B^o + C') \frac{2 P_1 L}{\pi^2 D'} \left[\sum_{n=1}^{\infty} \frac{1}{n^2} - \sum_{n=1}^{\infty} \frac{\cos n\pi}{n^2} \right]$$

$$= A_o (B^o + C') \frac{2 P_1 L}{\pi^2 D'} \times 2 \sum_{n=1}^{\infty} \frac{1}{(2n-1)^2}$$

$$= \frac{A_o (B^o + C') P_1 L}{2 D'}$$

But for the experimental boundary conditions:

$$D' = \frac{(B^o + C')}{\rho_s Q} \qquad \text{(see equation (42))}$$

Therefore

$$M' = \frac{A_o \rho_s L P_1 Q}{2} \qquad \ldots\ldots\ldots \quad (54)$$

where Q has been defined as the mass adsorbed per unit mass charcoal per unit pressure difference.

That is, if the mass adsorbed at any pressure may be represented by a Freundlich relation:

$$(x/m) = K' P^{1/n'}$$

then the value of Q between the limits P_1 and 0 is given by the relation

$$Q = \frac{K' P_1^{1/n'}}{P_1} \qquad \ldots\ldots\ldots \quad (55)$$

When this value of Q is substituted in equation (54) the mass adsorbed at equilibrium flow conditions ($P = P_1$ at $x = 0$, $P = 0$ at $x = L$) is given by the relation

$$M' = \frac{A_0 \rho_s K' L P^{1/n'}}{2} \quad \dots\dots\dots \quad (56)$$

Equation (56) embodies the assumptions included in the derivation of equations (51) and (52). That is equation (56) assumes that the adsorption isotherm is linear between the pressures P_1 and 0. From this same assumption the value of M' in the same form as equation (56) may be written by inspection. It is of interest, however, that the mathematical analysis leading to equation (56) provides a check on the form of the equations (51) and (52).

The mass adsorbed on a charcoal rod at equilibrium flow conditions may be calculated by an exact method, if it is assumed that surface mobility does not occur. The equilibrium flow rate for gases not adsorbed to a great extent is given by equation (35).

$$\frac{m}{t} = - A_0 (A^o P + B^o) \frac{dP}{dx}$$

Solving this equation for P when the boundary conditions are

$$P = P_1 \quad \text{at} \quad x = 0$$

$$P = P_2 \quad \text{at} \quad x = L$$

$$\frac{A^oP^2}{2} + B^oP + \left[\left(\frac{(P_1^2 - P_2^2)\,A^o}{2} + B^o\,(P_1 - P_2)\right)\frac{x}{L} - \left(\frac{A^oP_1^2}{2} + B^o\,P_1\right)\right] = 0$$

Whence $P =$

$$\frac{-B^o \pm \sqrt{(B^o)^2 - 2A^o\left[\left(\frac{(P_1^2 - P_2^2)A^o}{2} + B^o(P_1 - P_2)\right)\frac{x}{L} - \left(\frac{A^oP_1^2}{2} + B^oP_1\right)\right]}}{A^o}$$

That is

$$P = R' \pm \sqrt{S' - T'x} \qquad \ldots\ldots \quad (\underline{57})$$

where

$$R' = -\frac{B^o}{A^o} \quad \text{and} \quad S' = \left(\frac{B^o}{A^o}\right)^2 + \left(P_1^2 + \frac{2\,B^oP_1}{A^o}\right)$$

and

$$T' = \frac{2}{A^oL}\left[\frac{(P_1^2 - P_2^2)\,A^o}{2} + B^o\,(P_1 - P_2)\right]$$

If the mass of gas adsorbed for each gram of charcoal can be represented by an empirical equation such as the Freundlich equation:

That is $(x/m) = K'P^{1/n'}$

Then the mass dm adsorbed on an element of charcoal of cross sectional area A_o, thickness dx, and density ρ_s at a distance x along the length of the charcoal rod will be given by the relation:

$$dm = A_o \rho_s \, dx \, K' \, P^{1/n'} \qquad \ldots\ldots\ldots \quad (58)$$

Substituting the value of P from equation (57) in equation (58)

$$dm = A_o \rho_s \, dx \, K' \, (R' \pm \sqrt{S' - T'x})^{1/n'}$$

which when integrated between the limits of $x = 0$ and $x = L$, gives the total mass adsorbed on a rod of length L.

$$M' = A_o \rho_s K' \int_o^L (R' \pm \sqrt{S' - T'x})^{1/n'} \, dx$$

That is:

$$M' = - \frac{2 A_o \rho_s K'}{T'} \left[\frac{n'}{1 + 2n'} (R' \pm \sqrt{S' - T'L})^{\frac{1 + 2n'}{n'}} - \frac{R'n'}{1 + n'} (R' \pm \sqrt{S' - T'L})^{\frac{1 + n'}{n'}} - \frac{n'}{1 \quad 2n'} (R' \pm \sqrt{S'})^{\frac{1 + 2n'}{n'}} + \frac{R'n'}{1 + n'} (R' \pm \sqrt{S'})^{\frac{1 + n'}{n'}} \right] \qquad \ldots\ldots\ldots\ldots \quad (59)$$

where R', S' and T' were defined below equation (57).

Equation (59) is therefore an exact equation for estimating the total mass adsorbed on a charcoal rod of cross sectional area A_o, density ρ_s and length L when the influent pressure is P_1 and the effluent pressure is P_2. The only theoretical assumption involved in equation (59) is that there is no contribution from surface flow (and therefore at equilibrium flow the amount adsorbed at any point above the charcoal rod is in equilibrium with the pressure at that point).

Substitution of the values of R', S' and T' in equation (59) for the boundary condition that $P_2 = 0$, gives the solution.

$$M' = 2A_o \rho_s K'L \left[\frac{\dfrac{n'}{1 + 2n'} P_1^{\frac{1+2n'}{n'}} + \left(\dfrac{B^o}{A^o} \right) \dfrac{n'}{n' + 1} P_1^{\frac{1+n'}{n'}}}{P_1^2 + \dfrac{2 P_1 B^o}{A^o}} \right] \qquad \ldots\ldots (60)$$

C. Calculations

(a) Non-stationary flow in zinc chloride charcoal

The following are sample calculations of the data appearing in Table IX columns (4), (5) and (6). For illustrative purposes the time $t = 4$ has been chosen.

$x/m = 0.165\ P^{0.162}$ (page 49)

$\rho_s = 0.707$ gm./cc. (page 47)

$A_o = 0.113$ sq. cm.

$L = 0.995$ cm.

$m/t = 1.31 \times 10^{-4}$ gm./min. at equilibrium (Table IX)

From equation (41)[#]:

$$(B^{o} + C') = \frac{1.31 \times 10^{-4} \times 0.995}{0.113 \times 50} = 2.32 \times 10^{-5}$$

And from equation (55)

$$Q = \frac{K' P_1^{1/n'}}{P_1} = \frac{x/m}{P_1} = \frac{0.165 \times 50^{0.162}}{50}$$

Substituting the values of $(B^{o} + C')$, ρ_s, and Q in equation (43)

$$D' = \frac{2.32 \times 10^{-5} \times 50^{0.838}}{0.707 \times 0.165} = 0.00522 \text{ cm.}^2\text{/min.}$$

Substituting the values of the required constants into equation (51) for t = 4 min. gives the following series.

$$\frac{m}{t} = 0.113 \times 2.32 \times 10^{-5} \left[\frac{50}{0.995} + \frac{100}{0.995} \left(e^{-0.206} + e^{-0.824} + e^{-1.85} + e^{-3.30} + e^{-5.15} + e^{-7.42} \; \ldots\ldots \right) \right]$$

That is:

[#] Until the kinetics of surface flow are known, the value of C' can not be evaluated theoretically. The value of $(B^{o} + C')$ is therefore evaluated from the experimental steady state flow by means of equation (41).

$$\frac{m}{t} = (1.31 \times 10^{-4}) + 2.62 \times 10^{-4}(0.814 + 0.439 + 0.157$$
$$+ 0.037 + 0.006 + 0.001 \quad \ldots\ldots)$$
$$= (1.31 \times 10^{-4}) + (2.62 \times 10^{-4} \times 1.45)$$
$$= \underline{\underline{5.1 \times 10^{-4} \text{ gm./min.}}}$$

which is the solution to equation (51) for the given conditions at $t = 4$ min.

The term $\cos n\pi$ in equation (52) has the effect of changing the sign of the odd terms of the series in equation (51). That is equation (52) leads to the series:

$$\frac{m}{t} = 1.31 \times 10^{-4} + 2.62 \times 10^{-4} \quad (-0.813 + 0.439 - 0.157$$
$$+ 0.037 - 0.006 + 0.001 \quad \ldots)$$
$$= 1.31 \times 10^{-4} + (2.62 \times 10^{-4} \times - 0.500)$$
$$= \underline{\underline{0.00 \text{ gm./min.}}}$$

That is at $t = 4$ min. the effluent flow rate is less than 0.00 gm./min.

Substitution of the required constants in equation (53) yields the solution:

$$\frac{m}{t} = \frac{(0.113 \times 2.32 \times 10^{-5}) \times 50}{\times 0.00522 \times 4.0} = 5.1 \times 10^{-4} \text{ gm./min.}$$

It is to be noted that the solution to equation (53) is the same as the solution to equation (51) at $t = 4$ min. That is at $t = 4$ min., diethyl ether flows into a 1 cm. length of zinc chloride charcoal (for the given conditions) as though it were a rod of infinite length.

b) The mass adsorbed on zinc chloride charcoal at equilibrium flow conditions

The following are sample calculations to show the use of equations (56) and (60):

Calculation of the mass of diethyl ether adsorbed on plug No. 14 at equilibrium flow conditions. ($P_1 = 50$ mm., $P_2 = 0$ mm. and temperature 35.0° C.)

$K' P^{1/n'} = 0.165\ P^{0.162}$ (page 49)

$A_o = 0.113$ sq. cm.

$L = 0.995$ cm.

$\rho_s = 0.707$ gm./cc. (page 47)

Substituting the required values in equation (56) for the pressure $P_1 = 50$ mm.:

$$M' = \frac{0.113 \times 0.707 \times 0.995 \times 0.165 \times 50^{0.162}}{2}$$

$$= \underline{\underline{0.0124 \text{ gm.}}}$$

Substituting the required numerical values in equation (60):

$$M' = 2 \times 0.113 \times 0.707 \times 0.165 \times 0.995$$

$$\times \left[\frac{\frac{6.18}{13.36} \times 50^{2.162} + \frac{6.18}{7.18} \times 50^{1.162} \left(\frac{B^o}{A^o} \right)}{2500 + 100 \left(\frac{B^o}{A^o} \right)} \right]$$

$$= 0.0262 \left(\frac{2180 + 81.10\ B^o/A^o}{2500 + 100\ B^o/A^o} \right) \quad \ldots\ldots. \quad (\underline{61})$$

It may be seen that the bracketted function of equation (61) has the limiting values 0.872 and 0.811 for the limiting values of the ratio B^o/A^o (i.e. zero and infinity respectively). It is therefore apparent that the value of the ratio B^o/A^o is not critical to the solution of equation (60). The ratio B^o/A^o may be evaluated however, in the following manner: The nitrogen permeability of plug No. 14 at 35.0° C. is given by the relation:

$$1.54 \times 10^{-8}\ \bar{P} + 5.81 \times 10^{-6} \qquad \text{(Table III)}$$

That is the diethyl ether permeability at 35.0° C. is given by the relation: (assuming the slope of the flow pressure plot is inversely proportional to the viscosity, and the intercept is inversely proportional to the square root of the molecular weight)

$$1.54 \times \frac{181.5}{77.5} \times 10^{-8}\ \bar{P} + 5.81 \sqrt{\frac{28.0}{74.1}} \times 10^{-6}$$

Where the viscosities and molecular weights for converting the nitrogen permeability were obtained from Table VIII, that is the expression:

$$3.61 \times 10^{-8}\ \bar{P} + 3.56 \times 10^{-6}$$

which may be stated in the form:

$$\frac{m}{t} = A_0(H.\ 3.61 \times 10^{-8}\ P + H.\ 3.56 \times 10^{-6})\ \frac{d\bar{P}}{dx} \qquad \ldots\ldots\ (\underline{62})$$

where H is a constant which need not be evaluated since it is the ratio B^o/A^o that is required.

Comparison of equation (<u>62</u>) with equation (<u>41</u>) shows that

$$\frac{B^o}{A^o} = \frac{3.56 \times 10^{-6}}{3.61 \times 10^{-8}} = 99$$

Substitution of this value of B^o/A^o in equation (<u>61</u>) gives the value of the mass adsorbed at equilibrium.

$$M' = 0.0262 \times 0.860$$

$$= \underline{\underline{0.0226 \text{ gm.}}}$$

GLOSSARY OF SYMBOLS

(Only those symbols which occur repeatedly throughout the text are included. Other symbols are defined where they occur.)

A	is a constant of the Adzumi equation (page 16).
A''	is a constant of the Damköhler equation (page 21).
A_{o}	is the cross sectional area.
A^{o}	is a constant of viscous flow (page 123).
B	is a constant of the Adzumi equation (page 16).
B^{o}	is a constant of molecular streaming (page 123).
C	is the concentration.
C'	is a constant of surface diffusion (page 124).
D	is the diffusion constant.
D'	is a diffusion constant defined by $\frac{B^{o} + C'}{\rho_{s} Q}$ (page 125).
f	is the fraction of molecules giving non specular reflections from a surface.
G	is the mass flow per unit time.
K	is the flow rate in Adzumi's units (page 10).
K_{o}	is a composite shape and tortuosity factor which is numerically equal 5.0 (page 13).
L	is the length of a flow system.
N_{a}	is the number of molecules in the adsorbed phase per cm. of pore length.
N_{g}	is the number of molecules in the gas phase per cm. of pore length.
N_{t}	is the number of molecules that have diffused out of a capillary after a time t.

n	is an integer.
m/t	is the mass flow per unit time.
M	is the molecular weight.
P	is the pressure.
P_1	is the gas pressure at the influent end of a capillary.
P_2	is the gas pressure at the effluent end of a capillary.
$\bar{P}$	is the mean pressure defined by $\frac{P_1 + P_2}{2}$
ΔP	is the pressure differential defined by $P_1 - P_2$
Q	is the mass of gas adsorbed per unit mass of charcoal per unit pressure difference.
$\bar{r}$	is the Adzumi radius (page 15).
R	is the capillary radius.
R_o	is the gas constant.
S_v	is the surface area per unit volume of solids (page 12).
t	is the time.
V	is the volume flow per unit time measured at the pressure P_1.
V'	is the volume flow per unit time measured at the pressure $\bar{P}$.
x	is the distance along the length of a flow path.
x/m	is the mass adsorbed per unit mass of charcoal.
δ	is a constant resulting from the coefficient of "slip" and is numerically equal to 0.9 (page 16).
ρ_g	is the density of a gas.
ρ_s	is the density of a solid (the mercury density of charcoal).
ϵ	is the void fraction (page 47).
φ	is the effective fraction of void area (page 14).
∞	is infinity.

BIBLIOGRAPHY

1. Poiseuille, J.; Mém. Savants Étrangers, 9: 433 (1846)

2. Wiederman, G.; Pogg. Ann., 99; 221 (1856).

3. Maxwell, J.C.; "Scientific Papers", Cambridge Univ. Press, London, 1890, p. 708.

4. Taylor, J.B.; Phys. Review, 35: 375 (1930).

5. Blankenstein, E., Phys. Review, 22: 582 (1923).

6. Millikan, R.A., Phys. Review, 21: 217 (1923).

7. Knudsen, M.; Ann. Physik., 28: 75 (1909).

8. Knudsen, M.; Ann. Physik., 35: 389 (1911).

9. Brillouin, M.; Leçons sur la Viscosite, Paris (1907).

10. Reynolds, O.; Philos. Trans., 174: 935 (1883).

11. Kozeny, J.; Sitzber. Akad. Wiss. Wien, Math. - Naturw. Klasse, 136 A: 271 (1927).

12. Adzumi, H.; Bull. Chem. Soc. Japan, 12: 199, 285 (1937).

13. Carman, P.C.; J. Soc. Chem. Ind., 57: 225 T (1938).

14. Holmes, W.R.; Nature, 157: 694 (1946).

15. Rigden, P.J.; J. Soc. Chem. Ind., 66: 130 (1947).

16. Arnell, J.C.; Can. J. Research, A24: 103 (1946).

17. Lea, F.M. and Nurse, R.W.; Soc. Chem. Ind. Symposium on particle size analysis. Advance copy Feb. 4, 1947.

18. Arnell, J.C., and Carman, P.C.; Authors' manuscript. To be printed in Can. J. Research.

19. Arnell, J.C.; Can. J. Research, A25: 191 (1947).

20. Glasstone, S.; "Textbook of Physical Chemistry", Van Nostrand Co.; New York, second edition, 1946 p. 270.

21. Hey, M.; Phil. Mag., 22: 492 (1936).

22. Richardson, O., Nicol, J., and Parnell, T.; Phil. Mag. (6) 8: 1 (1904).

23. Damköhler, G.; Z. Phys. Chem. Abt. A 174: 222 (1935).

24. Volmer, M., and Esterman, J.; Z. Physik., 7: 13 (1921).

25. Volmer, M., and Adhikari, G.; Z. Phys. Chem., 119: 46 (1926).

26. Bangham, D.M. and Fakhoury, N.; J.C.S., 1324 (1931).

27. Evans, G.; Trans. Faraday Soc., 28: 364 (1932).

28. Damkhöler, G.; Z. Electrochem., 48; 178 (1942).

29. Wicke, E.; Kolloid Z., 86: 167 (1939).

30. Wicke, E.; Kolloid Z., 88: 295 (1939).

31. Wicke, E.; Kolloid Z., 93: 129 (1940).

32. Wicke, E.; Z. Electrochem., 44: 587 (1938).

33. Wicke, E.; and Kallenbach; Kolloid Z., 97: 1355 (1941).

34. Fick; Pogg. Ann., 94: 59 (1855).

35. Barrer, R.M.; "Diffusion in and through Solids", Cambridge Press. 1941 p. 305.

36. Carslaw, H.S.; "Mathematical Theory of the Conduction of Heat", Macmillan and Co., London 1921.

37. Boltzman, L.; Ann. Phys., Lpz. 53: 959 (1894).

38. Barrer, R.M.; "Diffusion in and through Solids", Cambridge Press, 1941 p. 1 - 51.

39. Tiselius, A.; Z. Phys. Chem., Abt A 174: 401 (1935).

40. Clausing, P.; Ann. Phys., Lpz., 7: 489, 569 (1930).

41. Frenkel, J.; Z. Phys., 26: 117 (1924).

42. Barrer, R.M.; "Diffusion in and through Solids", Cambridge Press, 1941.

43. Muskat, M.; "The Flow of Homogeneous Fluids through Porous Media", McGraw-Hill Book Co., New York, 1937.

44. Howard, H.C., and Hulett, G.A.; J. Phys. Chem., 28: 1082 (1924).

45. Brunauer, S., Emmett, P.H., and Teller, E.; J. Am. Chem. Soc., 60: 309 (1938).

46. Emmett, P.H., and Brunauer, S.; J. Am. Chem. Soc., 59: 2682 (1937).

47. International Critical Tables of Numerical Data, Physics, Chemistry and Technology, McGraw-Hill Book Co., New York, N.Y. 1928 Vol. III, p. 250.

48. International Critical Tables of Numerical Data, Physics, Chemistry and Technology, McGraw-Hill Book Co., New York, N.Y. 1928 Vol. III, p. 204.

49. Freundlich equation; see McBain, J.; "Sorption of Gases and Vapours by Solids". George Routledge and Sons Ltd. 1932, p. 5.

50. Goggin, W.C.; News Ed. (J. Am. Chem. Soc.), 18: 923 (1940).

51. Goggin, W.C., and Lowry, R.D.; J. Am. Chem. Soc. 34: 327 (1942).

52. Hodgins, J.W., Flood, E.A. and Dacey, J.R.; Can. J. Research, B24: 168 (1946).

53. Barrer, R.M.; "Diffusion in and through Solids" Cambridge Press, 1941, p. 139.